

Analysis of a Lower Limb Prosthesis

A Major Qualifying Project Report

Submitted to the Faculty of Worcester Polytechnic Institute

in partial fulfillment of the requirements for the

Degree of Bachelor of Science in

Mechanical Engineering, Biomechanics concentration

By

Victoria S. Richardson

Erin J. Vozzola

April 24, 2008

Advisors:

1. Prosthetics
2. Finite Element Analysis
3. Assistive Technology

Professor Holly K. Ault

Professor Allen H. Hoffman

Abstract

The Center for International Rehabilitation (CIR) has programs all over the world to provide people in developing countries with the training and equipment they need to supply prosthetic devices to local landmine victims. CIR has created a monolimb, which is a lower limb prosthesis where the socket and shank are molded from a single piece of thermoplastic material. The monolimb can be fabricated on-site with minimal equipment at a low-cost. The shank portion of the device, which replaces the tibial region of the leg, was investigated through a finite element analysis computer program, COSMOSWorks.

The current prosthetic device utilized by CIR uses a hollow, cylindrical shape with a rib on the posterior side as the overall shank design. This study combined varying circular outer diameters and rib lengths to determine which combination of parameters contributed to lower overall von Mises stresses and minimal displacement. Four hollow elliptical cross sectional shapes of different minor and major diameters were also modeled and compared to the results of the circular parameter study.

The models were input into COSMOSWorks to perform a static analysis on each of the models and the results were displayed through contour plots. The output for each model was analyzed and compared to determine the maximum stresses and overall stress distributions. The displacement present was examined, paying particular attention to the flexibility across the shank, as the displacement can mimic that of natural ankle movement. The ISO Test Standard 10328, which details the necessary structural testing for lower limb prostheses, was used as the basis for testing.

The final results compared the overall stress distributions and displacement of each of the models in COSMOSWorks to determine which shape would best withstand the ISO Test Standard 10328 specified load. The results determined that an increase in diameter and rib length positively influences the von Mises stress results and displacement by decreasing their values throughout the shank.

Acknowledgements

Our team would like to thank our contacts at the Center for International Rehabilitation, Kim Reisinger and Hector Casanova. They provided us with information regarding CIR's current programs, as well as specifics regarding the monolimb. They provided us with direction regarding how we could aid CIR in their research.

Special thanks are extended to our project advisors, Professor Allen Hoffman and Professor Holly Ault. Their comments, suggestions, and support throughout the entire project have been greatly appreciated. This project would not have been possible without their continued guidance and support during this learning experience.

Table of Contents

Abstract.....	i
Acknowledgements.....	ii
Table of Contents	iii
List of Figures	vi
List of Tables	viii
Executive Summary	ix
Introduction	1
Anatomy of the Knee.....	4
Low Cost Prosthetics.....	5
Trans-Tibial Prosthetic Modular Component.....	5
Simple Prosthetic Device.....	6
Low Cost Composite Prosthetic.....	8
Elliptical/Circular Shaped Low Cost Prosthetic.....	10
Jaiper Below Knee Prosthetic.....	12
Fabrication Process.....	13
Materials.....	19
Glass Fiber	19
Thermoplastics	20
Other Low Cost Materials	23
Comparison	24
Objectives	27
Parameter Study of the Circular Cross Section	29
Shank Height.....	29
Test Plates	30
Shank Diameter	30
Length of the Rib	31
Thickness of Material.....	31
Parameter Combinations	32
Elliptical Cross Section	32

ISO Standard.....	33
Testing Level.....	34
Type of Testing	34
Coordinate System.....	35
Alignment.....	36
Reference Planes	36
Forces.....	39
Shank Models.....	40
Force Application.....	41
Finite Element Analysis Testing.....	42
Finite Element Analysis.....	43
Failure Criteria.....	43
Von Mises Stress.....	43
Displacement.....	45
Results	50
Von Mises Stresses	50
Loading Condition I.....	50
Circular Shanks	50
Loading Condition II.....	53
Circular Shanks	53
Displacement	59
Loading Condition I.....	59
Circular Shanks	59
Circular Shank: 58.5 mm Outer Diameter	61
Circular Shanks	64
Comparisons	70
Von Mises Stresses	70
Displacement.....	76
Material Analysis.....	81
Conclusions.....	87
Recommendations	88

Works Cited.....	90
Appendix A: History of Prosthetics.....	93
Appendix C: Programs for Third World Countries.....	100
Mobility India	100
Handicap International	100
Helping Hands for Haiti.....	101
Bhagwan Mahaveer Viklang Sahayata Samiti (BMVSS)	102
Prosthetics Outreach Foundation	102
Appendix D: Circular Shank Parameter Combinations	104
Appendix E: Analytical Stress Calculations Procedure	105
Appendix F: Analytical Stress Calculation Results	107
Appendix G: von Mises Stress Contour Plots.....	110
Appendix H: Displacement Plots for Loading Condition I and Loading Condition II	119
Loading Condition I.....	119
Loading Condition II.....	121
Appendix I: In Plane Displacement Graphs.....	123
Appendix J: Out of Plane Displacement Graphs.....	124

List of Figures

Figure 1: Trans-Tibial Prosthetic Modular Component	6
Figure 2: Simple Prosthetic-Standing Position (G. Pearce 2007)	7
Figure 3: Simple Prosthetic-Kneeling Position (G.Pearce 2007)	7
Figure 4: Low Cost Composite Prosthetic Device (Bartkus 1994)	9
Figure 5: Circular and Elliptical Prostheses (Lee 2006).....	11
Figure 6: Fatigue Test Set Up (Lee 2006)	12
Figure 7: Jaiper Below Knee Prosthetic (BMVSS 2007).....	13
Figure 8: Standing Alignment System (CIR Manual).....	15
Figure 9: Trapezoidal Plastic Cut (CIR Manual)	17
Figure 10: "Mobility for Each One" Fiberglass Prosthetic.....	20
Figure 11: Monolimb Cross Section.....	31
Figure 12: Drawing of Elliptical Shape	33
Figure 13: ISO 10328 Coordinate System	35
Figure 14: ISO 10328 Reference Planes (ISO 10328).....	37
Figure 15: Plane for stress and displacement measurements.....	46
Figure 16: Front View of Probed Points	48
Figure 17: Scale of Displacement Values	48
Figure 18: Graph of Resultant Displacement.....	49
Figure 19: 48.5 mm OD von Mises Stress Contour Plots (Loading Condition I)	51
Figure 20: von Mises Stress Contour Plots for Elliptical Shanks (Loading Condition I)	52
Figure 21: 48.5 mm OD von Mises Stress Contour Plots (Loading Condition II)	54
Figure 22: von Mises Contour Plots for Elliptical Shanks (Loading Condition II).....	57
Figure 23: 48.5 mm OD Displacement Contour Plots (Loading Condition I).....	59
Figure 24: Resultant Displacement (48.5 mm OD).....	60
Figure 25: Resultant Displacement of 53.5 mm OD	60
Figure 26: 58.5 mm OD Resultant Displacement (Loading Condition I)	61
Figure 27: Resultant Displacement of 63.5 mm OD	61
Figure 28: Displacement Plots for Elliptical Shanks (Loading Condition I).....	62
Figure 29: Resultant Displacement Graph for Elliptical Shanks (Loading Condition I)	63
Figure 30: 48.5 mm OD Displacement Contour Plots (Loading Condition II).....	64
Figure 31: 48.5 mm OD Resultant Displacement (Loading Condition II)	65
Figure 32: Resultant Displacement (Loading Condition II, 53.5 mm OD	66
Figure 33: 58.5 mm OD Resultant Displacement Graph.....	67
Figure 34: 63.5 mm OD Resultant Displacement (Loading Condition II)	68
Figure 35: Displacement Plots for Elliptical Shanks (Loading Condition II).....	69
Figure 36: Resultant Displacement for Elliptical Shanks (Loading Condition II).....	70
Figure 37: von Mises stresses at probed point- Rib Length Comparison (Loading Condition I)	72
Figure 38: von Mises stresses at probed point- Rib Length Comparison (Loading Condition II)	72
Figure 39: von Mises Stress Values for Elliptical Shanks	74
Figure 40: Circular and Elliptical Shank von Mises Stress Comparison (Loading Condition I)	75
Figure 41: Circular and Elliptical Shank von Mises Stress Comparison (Loading Condition II)	76

Figure 42: In-Plane Displacement Trends for Loading Condition I	77
Figure 43: In-Plane Displacement Trends for Loading Condition II	78
Figure 44: Maximum Out-of-Plane Displacement Comparison (Loading Condition I)	79
Figure 45: Maximum Out-of-Plane Displacement (Loading Condition II).....	80
Figure 46: U Normal Stresses.....	109
Figure 47: 53.5 mm OD von Mises Stress Contour Plots	110
Figure 48: 58.5 mm OD von Mises Stress Contour Plots (Loading Condition I)	111
Figure 49: 63.5 mm OD von Mises Contour Plots (Loading Condition I)	113
Figure 50: 53.5 mm OD von Mises Contour Plots (Loading Condition I)	114
Figure 51:53.5 mm OD 0 mm Rib ISO Clipping (Loading Condition II).....	115
Figure 52: 58.5 mm OD von Mises Contour Plots (Loading Condition II)	116
Figure 53: 63.5 mm OD von Mises Stress Contour Plots (Loading Condition II)	117
Figure 54: 53.5 mm OD Displacement Plots (Loading Condition I)	119
Figure 55: 58.5 mm OD Displacement Contour Plots (Loading Condition I).....	120
Figure 56: 63.5 mm OD Displacement Contour Plots (Loading Condition I).....	120
Figure 57: 53.5 mm OD Displacement Contour Plots (Loading Condition II).....	121
Figure 58: 58.5 mm OD Displacement Contour Plots (Loading Condition II).....	121
Figure 59: 63.5 mm OD Displacement Contour Plots (Loading Condition II).....	122
Figure 60: In-Plane Displacement (Loading Condition I)	123
Figure 61: In-Plane Displacement (Loading Condition II)	123
Figure 62: Displacement Trends for Loading Condition I	124
Figure 63: Out-of-Plane Displacement Trends for Loading Condition I.....	124

List of Tables

Table 1: Polypropylene Material Properties	22
Table 2: Polyethylene Material Properties (MatWeb)	23
Table 3: Material Properties for Polypropylene-Polyethylene (90/10).....	23
Table 4: Vinyl Ester Material Properties (MatWeb)	24
Table 5: Properties of Low Cost Prosthetic Materials	25
Table 6: Circular Test Parameters	32
Table 7: Elliptical Parameters.....	33
Table 8: Loading Offset Locations	38
Table 9: Loading Condition Load Locations	38
Table 10: Cosine Values	40
Table 11: Force Components	40
Table 12: Polypropylene/Polyethylene Copolymer Material Properties.....	42
Table 13: von Mises Stress Values for circular models (Loading Condition I).....	51
Table 14: von Mises Stress Values for Elliptical Shanks (Loading Condition I).....	53
Table 15: 48.5 mm OD von Mises Stress Values (Loading Condition II)	54
Table 16: Probed von Mises values for elliptical shanks (Loading Condition II)	56
Table 17: von Mises Stress Values for Elliptical Shanks (Loading Condition II).....	58
Table 18: von Mises Stresses at probed point - Comparison by Loading Condition	71
Table 19: Material Length Requirements	82
Table 20: Elliptical Shank Perimeters	82
Table 21: Circular Shank Weight	83
Table 22: Elliptical Shank Weight	84
Table 23: Circular Shank Parameter Combinations.....	104
Table 24: 53.5 mm OD von Mises Stress Values (Loading Condition I)	111
Table 25: 63.5 mm OD von Mises Stress Values (Loading Condition I)	112
Table 26: 53.5 mm OD von Mises Stress Values (Loading Condition II)	115
Table 27: 58.5 mm OD von Mises Stress Values (Loading Condition II)	117
Table 28: 63.5 mm OD von Mises Stress Values (Loading Condition II)	118

Executive Summary

The Center for International Rehabilitation (CIR) is a Chicago based non-profit organization, whose mission is “to assist people with disabilities worldwide in achieving their full potential” (CIR 2007). The creation of the CIR began in 1996 when Dr. William Kennedy Smith founded the organization Physicians Against Land Mines (PALM). In 1997, one year after its inception, this organization received the Nobel Peace Prize. The CIR was opened in 1998 by Physicians Against Land Mines (PALM) to expand its facilities to include victim assistance in rehabilitation services and advocacy. The center is now present in six countries, educating over seventy students to date who treat approximately 8,600 amputees yearly.

CIR is currently supplying low-cost prosthetics to developing countries around the world. They provide the people in these countries with the training and equipment they need to supply prosthetic devices to local landmine victims. CIR has created a monolimb, which is a lower leg prosthesis where the socket and shank are molded from a single piece of thermoplastic material. The monolimb can be fabricated on-site with minimal equipment at a low-cost. The shank portion of the device, which replaces the tibial region of the leg, was investigated through a finite element analysis computer program, COSMOSWorks.

The analysis compared circular shanks with and without the addition of a rib on the posterior end of the shank with different combinations of diameters and rib lengths. These results were furthered compared to the data for elliptical shanks. The circular shank is the design currently utilized for the CIR’s outreach programs. The diameters tested were 48.5 mm, 53.5 mm, 58.5 mm, and 63.5 mm; the minor diameters of the elliptical shanks were identical to these diameters and an aspect ratio of 1.55 was applied to determine the major diameter. Rib lengths of 0 mm, 10 mm, and 20 mm were tested for each circular diameter. “Changes in shank geometry can alter the stress distribution within the monolimb and at the residual limb-socket interface and, respectively, affect the deformability and structural integrity of the prosthesis and comfort perceived by amputees” (Lee, JRRD 2004). Therefore, the overall objective was to determine which combination of parameters would allow the monolimb to withstand the loads specified by the ISO Test Standard 10328 Ultimate Static P5 test.

The parameters of this study were chosen to maximize the testing conditions. The height of the shank was chosen by applying the maximum distance between the ankle and knee planes in the ISO Test Standards, 420 mm, Based on anthropometric data, 60 mm was subtracted from this length as it is the minimum length required of a residual limb to retain a fully functioning knee. This height of 360 mm was applied to each of the models. Next, twelve circular models and four elliptical models of this height were built using the three-dimensional modeling program, Solidworks. A test plate was added to the distal end of each shank by bonding the two components to one another. This plate was added to provide a point of application for the off-set load.

The ISO Test Standard 10328 was consulted to ensure that our testing procedure complied with the guidelines set forth for lower limb prostheses. The coordinate system, load location, and force load components were all extracted from the standards and applied to our shank models. Two loading conditions were applied to each model to account for two of the main stages of the gait cycle, heel strike and toe off. Heel strike is considered Loading Condition I, while toe off is considered Loading Condition II.

The models were then analyzed through the finite element analysis program, COSMOSWorks. This program output data regarding the stress values throughout the shank as well as the displacement. The stress distributions were visible through contour plots where different stress levels corresponded to different colors, allowing for the visual depiction of stresses present throughout the shank. One point in particular was probed on each of the models to provide consistency throughout our comparisons. This point was located 25 mm below the proximal end of the shank on the plane where the highest stresses were expected to occur.

The von Mises stress failure criteria was applied by comparing the von Mises stresses at the probed point for each model to the Yield Strength of the thermoplastic material. Stress values which fell below this limit were considered to have successfully withstood the loading conditions for the ISO Test Standard 10328. Those models whose stress values were above the Yield Strength were considered to fail the test and it was recommended that prosthetic devices of this size not be used.

Next, displacement was analyzed to determine the level of flexibility within the shank. Displacement was investigated because flexibility in the shank can mimic that of natural ankle motion, which is a desirable quality in a prosthetic. This analysis demonstrated how the shank responds to the loading and which set of parameters provided sufficient rigidity. Data regarding displacement were obtained by probing equidistant points along the height of the shank and exporting these data to Excel. The data were then manipulated to determine the resultant displacement present for each shank to understand the effect the rib length had on the displacement values. Next, the in-plane displacement was found to establish the deformation caused by the bending loads and the out-of-plane displacement was calculated to better understand the effect of the torsional and transverse loads on the shank.

The analysis highlighted which set of parameters could minimize displacement and von Mises stresses in response to the specified loads. An increase in diameter was found to decrease both von Mises stress values as well as displacement. Similarly, an increase in rib length decreased stress and displacement values throughout the shank. Through a comparison of each of the models per diameter and loading condition, the models with a 0 mm rib were consistently found to have the highest stress values, while the elliptical shanks had the lowest values in both stress and displacement.

Although the von Mises stress and displacement analysis provided data which showed that the elliptical performed well under the applied loading conditions, the 53.5 mm shanks and higher all fell below the Yield Strength as well as exhibited consistent stress values between both loading condition I and II. Before recommendations were made regarding which shank is most appropriate for CIR to use in the field, a material analysis was conducted. This analysis determined the amount of material necessary to fabricate each shank model, while also considering the weight differences between the larger and smaller models. Through this analysis, the elliptical shanks were shown to have similar weights to those of the 20 mm ribbed shanks of the same diameter. In the case of the 58.5 mm and 63.5 mm, the elliptical models had more mass than those of the circular shank models, making them a less desirable option for amputees. These models also required more material, which may contribute to increased costs

for CIR when purchasing material, as they are trying to maximize the use out of their limited budget.

The recommendation has been made to CIR that they continue to use the hollow cylindrical model with a rib design within their programs. It is being recommended that at 58.5 mm shank with a 20 mm rib should be adopted as it requires a slight increase in amount of material, however this model successfully withstood the ISO Test Standard Loading Conditions.

Introduction

Prostheses have been in development since the BC era. There is a natural human desire to feel whole and complete, and providing artificial limbs has helped to satisfy this need. The advancement of technology has increased the means of providing such assistance, and injuries sustained in wars have brought about many opportunities for experimentation. It wasn't until the World War I era that inventors really began to drive forward with prosthetic advancements. Through World War II, the number of amputees and the need for prostheses increased in parallel. Numerous societies and organizations were created to support prosthetists and their designs. The Veteran's Administration (VA) has played a significant role in the progress of American prosthetics. They have provided numerous opportunities for people to learn about the field and to get involved. The growth and development of prosthetic devices has continued to flourish into the present, as the improvement of the lives of people with disabilities is a constant focus.

There are millions of individuals living in this world who have suffered from land mines or other traumatic events, which have caused amputation. The majority of these people are unable to afford the technology they need to account for their disability. To address this issue, many people have designed prosthetic devices which can be created locally at a low cost. Many of these programs exercise fabrication techniques which can be applied in developing countries and taught to people who do not have any previous technical training. These programs are being implemented all over the world by companies such as Prosthetics and Orthotics Outreach, Inc., Handicap International, Bhagwan Mahaveer Viklang Sahayata Samiti, and the Center for International Rehabilitation.

The designs developed for use in developing countries are produced at low cost and vary in shape, size, and material. In some of the designs, the shape of the shank varies from a uniform circular shape to a more elliptical shaped limb. Many of the prosthetic devices are supplied to the prosthetist in component form; the tibial length, foot, and socket are separate pieces which are assembled in the field for the patient. Many of these designs apply the

monolimb design, which is a transtibial prosthesis where the socket and the shank are molded from a single piece of thermoplastic material. CIR has applied this design to their global programs by providing the material, fabrication education, and tools.

The fabrication method used by CIR is the anatomically-based-alignment (ABA) system. This method uses a process that is easy to understand, as it needs to be translated into numerous languages. A casting and fabricating kit, which has all of the equipment and materials necessary for construction, is distributed to the prosthetist at the local clinic. There are four main processes included in this method: casting, standing alignment, alignment transfer, and monolimb fabrication. A monolimb is “a prosthesis in which the socket and pylon are formed from one piece of plastic” (CIR Manual). The cut of the plastic material is very important and exclusive to CIR. They cut a rectangular piece of thermoplastic material into three trapezoidal pieces. This shape allows the prosthetist to fit the patient while cutting less material off for waste. The alignment process is also very important as it allows the user to have correct posture and support from their device.

In order to produce prosthetics for developing countries, the material selected must be both durable, easy to fabricate, and low cost. Several of the low cost prosthetics have been made from fiber glass because it is a strong, rigid material which is fairly easy to fabricate while being affordable. One of the designs utilizes a plastic bottle and locally available wood to form a prosthetic which can easily be created from very cheap and easily accessible materials. Some of the more popular materials used for this application are thermoplastic materials. Thermoplastic materials are used because they can be remolded after their initial fabrication. This is an advantage because if there are any issues with the original fabrication, the material can be reheated and remolded. A polypropylene-polyethylene, both thermoplastic materials, co-polymer has been dedicated to this specific low cost prosthetic because it combines the rigidity of polypropylene and the flexibility of polyethylene. This combination provides a strong yet comfortable prosthetic limb.

To provide CIR with background testing for their prosthetic designs, several different shaped cross sectional shanks were tested using Finite Element Analysis (FEA). Elliptical and circular shapes were analyzed through the FEA software program, COSMOSWorks. The three-

dimensional models were created in the modeling program, Solidworks and then meshed and run in COSMOSWorks. Loads were applied to the models as detailed in the ISO Test Standard 10328. The reaction of the monolimb to specified forces was displayed in the form of contour plots. Stress and displacement contour plots was output and analyzed to better understand the reaction of the monolimb to the applied forces. The various sized cross sections were compared in order to draw conclusions regarding which shaped monolimb would be most appropriate for use in the field.

Background Research

A review of the research and literature regarding low cost prosthetics was undergone to provide background information regarding the project to be detailed throughout this report. Several areas were researched and have been included in this section, and more research has been included in the appendixes.

In this section, you will find information about the anatomy of the knee, as well as information from journal articles regarding various other low cost prosthetics devices currently being used in the field or further researched by other organizations. The fabrication techniques utilized by CIR has been briefly discussed and the material properties of low cost prosthetics, with an emphasis on thermoplastic materials has been included. The Appendixes include information regarding the history of prosthetics as well as other programs, similar to CIR, who are providing prosthetic solutions to third world countries.

Anatomy of the Knee

The knee joint is an important aspect to the human anatomy, particularly regarding movement, including walking and running. There are two main bones that are present within the knee joint, the femur and the tibia. The femur rests on the top of the tibia and when these two bones come together, the hinge joint of the knee is formed. It is covered by the patella, also known as the kneecap. The patella fits into the groove that is formed when these two bones come together.

The ends of the tibia and the femur are covered by articular cartilage, which acts as cushioning between these bones. The lateral meniscus, which is located on the outer side of the knee, and medial meniscus, which is located on the inner side of the knee, are also present in the knee joint and they are the shock absorbers between the bones.

On top of bone and cartilage, there are also ligaments in the knee which help with stabilization such as the collateral ligaments and the anterior cruciate ligament (ACL). The collateral ligament limits sideways motion and runs along the side of the knee. The ACL connects the tibia and the femur; it limits the rotation and forward motion of the tibia. Finally,

the Posterior Cruciate Ligament (PCL) is located behind the ACL and it limits the backward motion of the tibia.

The knee is a vital joint necessary for walking, running, and many other forms of movement. It is a joint which is often preserved during amputation to allow the amputee to use a lower limb prosthesis and the function of their own knee to walk again. For lower limb amputees, part of the tibia needs to be preserved. A minimum of 6 centimeters from the proximal end of the tibia must remain for a patient to keep a fully functioning knee joint.

Present within the knee are ligaments, bones, and cartilage which all contribute to the hinge motion of the knee. Through the directional restriction of the ligaments and the cushioning protection of the cartilage, both the tibia and the femur come together to form one of the most important joints in the human body.

Low Cost Prosthetics

Millions of people undergo amputations every year due to various traumas including landmine tragedies. The most applicable solution to these travesties is to fit the amputees with prosthetic devices to counteract their disability. However, artificial limbs are not easily accessible to people in lower income countries because of the high cost associated with prosthetics. Due to this fact, there are many designs being implemented by various outreach programs to provide low cost prosthetic systems to developing countries. These designs use various materials, designs, and testing procedures to validate their systems.

Trans-Tibial Prosthetic Modular Component

Mobility India developed a light weight plastic prosthesis which is comprised of several different components to provide people with a full below the knee prosthetic. This system includes a disc, socket adapter, pylon, and nuts and bolts which are used for alignment purposes as are displayed in Figure 1. The components come in separate pieces, which are easy to assemble and applied to the patient. The entire kit is provided for the prosthetist who will apply this system to patients. The separate pieces allow height to be addressed while allowing the prosthetic to be aligned properly (Mobility India 2007).

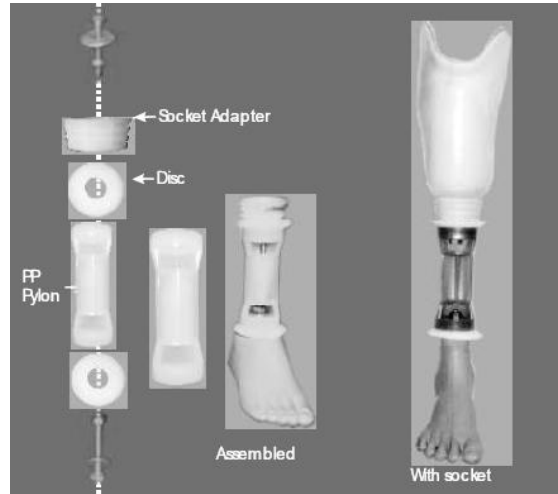


Figure 1: Trans-Tibial Prosthetic Modular Component

Polypropylene is used for the disc, socket adaptor, and pylon. Polypropylene was chosen as the material for this purpose because it is light weight and cost effective. To further improve the strength of the system, four ribs are carved into the outer diameter of the pylon. The pylon has been made in twenty different sizes, which increase in height by a centimeter with each size increase. This has been done to provide a variety of sizes which can incorporate a wider range of height differences. The fabrication process has been made very simple in order to ensure that any individual could create it after limited training has been completed (Mobility India 2007).

Mobility India has implemented these prosthetic designs in India in hopes to bring more people the tools they need to walk as normally as possible for a much lower cost as commercial prosthetics. They have successfully created a low cost and ultra-low weight prosthetic which can be fabricated by people with little experience. This system will be able to be applied in many developing areas throughout our world for an affordable price (Mobility India 2007).

Simple Prosthetic Device

The Division of Biomedical Sciences at Wolverhampton University in the United Kingdom designed and built a simple, cheap, and effective lower limb prosthesis which can be utilized by landmine victims in third world countries. Their underlying goal was to create an artificial device which can be used in developing countries to enable mobility over a short range while assisting people to stand and kneel. The kneeling portion of the design has been incorporated

into the final design because many of the users of this device work in the fields and need to kneel to properly complete their working tasks (G. Pearce). A visual depiction of both positions has been included in the pictures below, Figure 2 and Figure 3.



Figure 2: Simple Prosthetic-Standing Position (G. Pearce 2007)



Figure 3: Simple Prosthetic-Kneeling Position (G.Pearce 2007)

There are several components to this design: femoral component, knee component, foot, and cross strut. The thigh component is made using a plastic bottle which can be packed with comfortable material to protect the stump of the patient. A Velcro strap is wrapped around the thigh to keep the prosthetic in place. The tibial component of the device, the shank, is made using locally available wood. This wood is shaped into the proper height and width for the patient by the prosthetist. The cross strut is a bar which can be locked into place to allow the limb to be in a standing position or in a bent knee position for kneeling. The strut is made of locally available shaped wood also. Finally, a rubber component is added to the bottom of the wood shank to absorb the ground reaction forces and allow for easier mobility. Due to its simple design and use of available materials, it can be produced easily using basic carpentry tools and at a very low cost (G. Pearce).

In order to validate the prosthetic system created by the Biomedical Department at Wolverhampton University, several tests and analyses were performed on the device. Using “Design Space,” the forces were calculated and stress calculations were conducted. There were several stress tests run on the upper and lower knee joint. Using the computer software, axial stresses, principal stresses, and maximum deformation were all analyzed to determine whether or not the device could withstand the necessary forces to be used for a patient to walk with. After testing was completed, the device was found to be capable of withstanding the forces required for walking; the overall test results indicate that the prosthesis can support an average person involved in everyday activities for short distances. Therefore, the system can confidently be implemented in third world countries (G. Pearce).

Low Cost Composite Prosthetic

This prosthetic system was designed using low cost fiber reinforced composite materials using modern alignment methods to ensure the device was comfortable and durable while remaining affordable for less fortunate amputees. Fiber glass was utilized for this purpose in the form of Sheet Molding Components (SMC). The material is created by combining unidirectional fibers are layered on the bottom, followed by layers of randomly oriented fibers. This reinforcing of the fibers is adopted because it increases the weight reduction of the system while increasing the biofidelic response of the device. This biofidelic response is similar to the “energy storing” properties of some of the more expensive prosthetic materials. The goal of this prosthetic device is to apply the “energy storing” properties to the artificial limb without increasing the cost (Bartkus 1994).

The design of this system incorporates a flexible action foot, solid composite pylon, and a stump socket adaptor. The pylon is a cylindrical rod which supports the foot at the distal end and connects to the socket adapter at the proximal end. The socket adapter is a plastic piece which has been molded to fit the outer contour of the patients’ limb while also securing the prosthetic limb to the patient. An important aspect to this design is that the height of the limb can be adjusted by adding a screw to the distal end of the pylon. In total, an extra 1.5 inches can be added at any given time as shown in Figure 4 (Bartkus 1994).

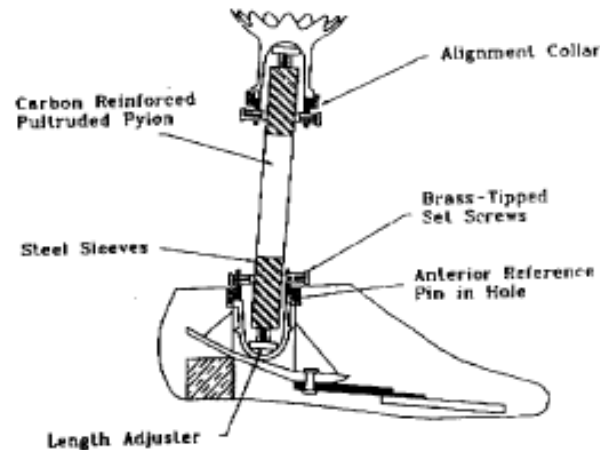


Figure 4: Low Cost Composite Prosthetic Device (Bartkus 1994)

Glass fiber, vinyl ester, and aluminum have been incorporated into the design of this device. Glass fiber was chosen because of its bending fatigue life, torsional strength, and lower cost. Aluminum was used for the screws which are applied at various points on the limb. These screws can be adjusted to provide the proper alignment for the patient. Further, alignment collars are used to ensure that the pylon is in the correct place to maximize a patient's gait. The glass fiber pylon can withstand compressive, bending, and torsional loads, which are important for a person to use the device for mobility purposes (Bartkus 1994).

In order to ensure that the proposed device could withstand the necessary loads associated with mobility, testing was completed. First, material testing was completed to compare the different types of materials available for use with prosthetics. This was done to ensure that the most appropriate and cost effective material was chosen for the prosthetic limb. E-fiber glass, carbon fiber-reinforced epoxy, vinyl ester, and polyester-pultruded/compressive molded rods were all tested to evaluate their properties. Each material was evaluated using compressive, bending fatigue, and static torsion tests.

Next, axial bending fatigue tests were performed on the pylon. The pylon was cycled at 300 lbs for 1,000 cycles and the load was increased by 50 lbs every 1,000 cycles until failure. Static torsion tests were performed by applying an axial moment to the ends of the pylon using a torque wrench. The moment was increased until the prosthetic fractured and angular deflection measurements were collected throughout the test. After the completion of these

tests, the E glass-reinforced vinyl ester was chosen because it had good fatigue life, high torsional strength, and the cost was much lower than the other materials.

Finally the assembled prosthetic was tested in a fatigue tester, which simulates walking, to ensure that each component works well together and will last for the user during everyday use. The system weighs 1.5 lbs, which is the lowest weight of any system currently on the market. After completion of the tests, many patients have used the system successfully without failure and have reported that it is lighter and smoother to walk with many other low cost prosthetic devices. In the end, low cost composite materials keep the cost down for prosthetics while also providing some of the energy storing properties. Their ability to be compression molded makes them an even more valuable asset to the low cost prosthetics industry.

Elliptical/Circular Shaped Low Cost Prosthetic

A low cost monolimb has been designed for less fortunate amputees using both circular and elliptical shaped shanks. A monolimb is a transtibial prosthesis where the socket and the shank are molded from a single piece of thermoplastic material. The specific thermoplastic material used for this prosthetic limb is polypropylene (PP). PP was chosen because of its strength, ductility, and flexibility. The flexibility of PP causes the monolimb to deflect during walking which simulates ankle joint motion (Lee 2006).

The two designs utilized for this prosthetic were an elliptical shank and a circular shank, both with uniform cross sections throughout the entire shank. Similarly, the sockets used were identical and used vacuum sealing methods (Lee 2006).

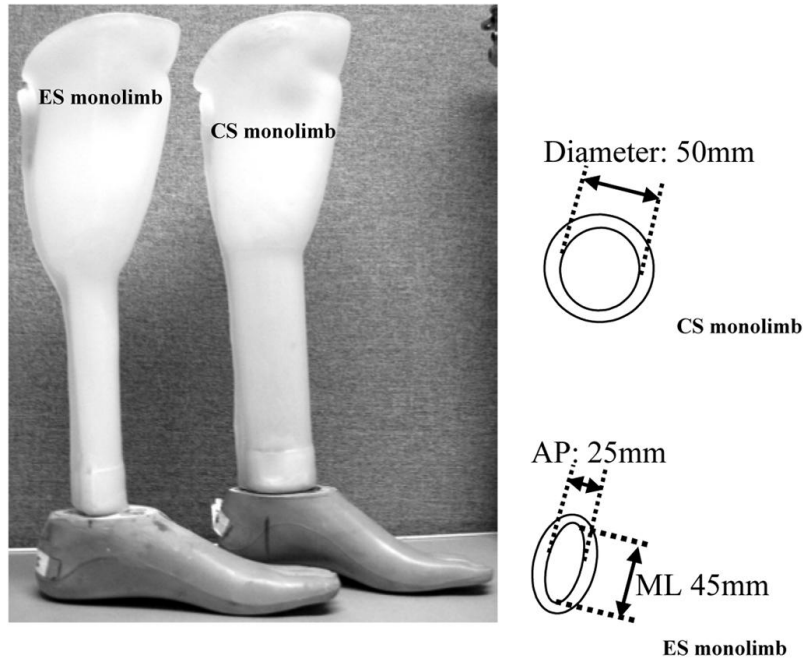


Figure 5: Circular and Elliptical Prostheses (Lee 2006)

Testing was done to determine which design provided the patient with a smoother gait while wearing the prosthetic. The testing was performed according to the ISO Standard 10328. Four male transtibial amputees were asked to walk using the prosthetic limb and the forces were analyzed, as was the gait of the individual. The subjects were blindfolded and asked to walk with each of the prostheses. After they had tested them several times, they were asked to rate them on several different properties: comfort, stability, ease of walking, flexibility, and weight. As a supplement to the real time feedback from patients, Finite Element Analysis and the Taguchi Method were both utilized as tools to measure the reliability and flexibility of the two types of monolimb cross sections (Lee 2006). Fatigue testing was also performed on the monolimb, emphasizing the “heel on” and “toe off” portion of the gait cycle. The test set up is shown below as Figure 6.

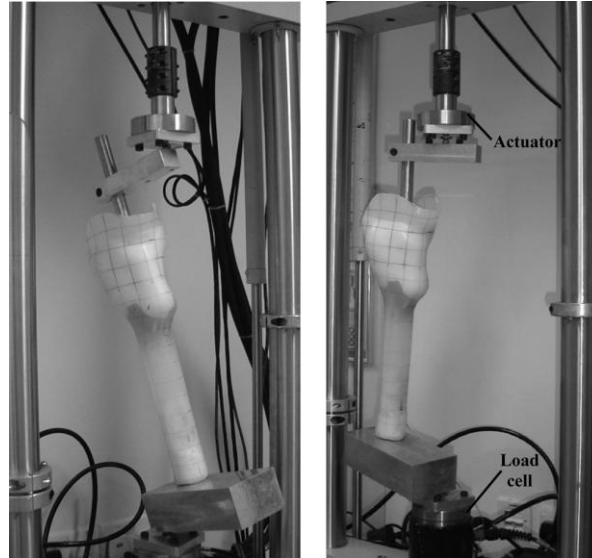


Figure 6: Fatigue Test Set Up (Lee 2006)

After the data was compiled, the elliptical system was found to perform the best in several different areas. The Elliptical monolimb weighed less and had higher flexibility than the circular design. During the gait analysis, the walking speed, stance time, and swing time were consistent between the two models; however, the step symmetry was better in the elliptical system. The subjects found the elliptical system to be more comfortable, stable and flexible while being lighter and easier to walk with (Lee 2006).

Through the testing, it was demonstrated that the elliptical system was a better system than the circular system. The advantage to using a monolimb is its low weight, low cost, and similar properties to the “energy storing” advanced prosthetics. In the end, the elliptical monolimb system led to an increase in comfort, a decrease in the energy required, and an increased level of control. It was also revealed that the flexibility increases as the cross sectional area of the monolimb shank is reduced (Lee 2006).

Jaiper Below Knee Prosthetic

The Jaiper Below the Knee Prosthetic system is comprised of the Jaiper foot, the total contact socket, the shank, and the suspension belt as shown in Figure 7. The materials used throughout the system are primarily rubber, High Density Polyethylene (HDPE), and leather. The foot is made of a rubber material and is molded to resemble a human foot. The total contact socket is made of an HDPE sheet which is thermoformed around a plaster mold of the

patient's existing stump. When molding the socket, special attention is paid to the tendons around the knee. The shank is also made using HDPE pipes in three different diameters: 75 mm, 90 mm, and 110 mm. These varying diameters have been incorporated into the design to account for the weight range of patients. The larger the diameter, the more weight the shank can successfully handle. Finally, the suspension belt is made of leather. The suspension belt has joints at two places to allow an increased range of motion while squatting and to ensure that the prosthetic limb stays in place on the patient (BMVSS).



Figure 7: Jaiper Below Knee Prosthetic (BMVSS 2007)

Fabrication Process

The Center for International Rehabilitation (CIR) uses the anatomically-based-alignment (ABA) system to properly cast a transtibial amputee. There are two varieties of this system: standing and supine. The supine system is more appropriate for weak patients and bilateral amputees. The standing system is better for stronger patients who are capable of holding up their own weight for a certain period of time. The standing system is explained in further detail in this report.

There are a number of measuring techniques that must be followed before the actual casting process can begin. The most important rule to remember is that anatomical landmarks must remain stationary. If they do not stay in their exact locations, the markings will be incorrect and the alignment will not be precise. There are four measurements that are made for dimensioning: medio-lateral (ML), anterior-posterior (AL), length of the tibia, and length of the residual limb. The elbow height, from the floor to the bottom of the elbow at a 90° angle, and width of hips must also be measured for use in the standing alignment process.

The preliminary casting techniques require a list of materials to be used in the process: nylon socks, approximately 120cm of 24mm elastic webbing, clamps, indelible pencil, 1 roll 15cm standard plaster, 1-2 rolls of elastic plaster, scissors, Vaseline, 52cm Dacron strap, pre-shaped clay reliefs, and a casting garment or 15cm elastic bandage. These materials and equipment are all used to cast the negative of the residual limb. This cast will be used to ensure proper alignment of the prosthesis.

The process for casting is rather short, but it plays the most significant role in molding the components that are extremely specific to each patient. The process starts by applying a damp nylon sheet over the residual limb. This sheet facilitates the placement and adherence of clay buildup for pressure relief. The knee center is then marked on this nylon sheet, at a point 20mm above the medial tibial plateau (MTP). This measurement is transferred around the knee using a square to mark the lateral and anterior surfaces. There are nine other areas that can be marked for improved application of the clay reliefs; these areas are not necessary but are helpful in the fitting process. The head of the fibula is an important feature to mark, as it could be a main weight-bearing area if improperly marked. Pressure reliefs are necessary to evenly distribute the weight-bearing throughout the socket of the prosthesis. These are 5mm thick clay reliefs that are measured and fit for each individual to provide the support they need.

To complete the casting process, a latex casting balloon is used to cover the residual limb. Six layers of plaster are added to make a splint that is slightly longer than half the circumference of the patella. Thumb indents are made on the plaster to establish the level of the patellar tendon. Since the following alignment techniques are done in the standing position, a 5-ply plaster splint needs to be added to allow for slight weight bearing on the distal end of the residual limb. The casting process is now complete and the patient is ready for alignment.

The standing alignment system, shown below in Figure 8, utilizes two structural components: the standing support fixture and the residual limb stand. The materials needed for these assemblies are: 2 weight bags, frame, 2 hitch pins with cotter pins, alignment bar components, mats, 3 extension bars, platform, and a base. The standing support fixture is the first to be constructed, and is placed on a grid-lined mat at the appropriate end points. The

fixture is placed at a width that accommodates average hip widths (38-49.5cm), with the sand-filled weight bags stabilizing the cross-bars of the structure. Adjustments must be made according to hip width and elbow height to ensure that the structure provides the proper support. The patient must stand on the mat with the center of the patient's body directly over the center line on the mat.

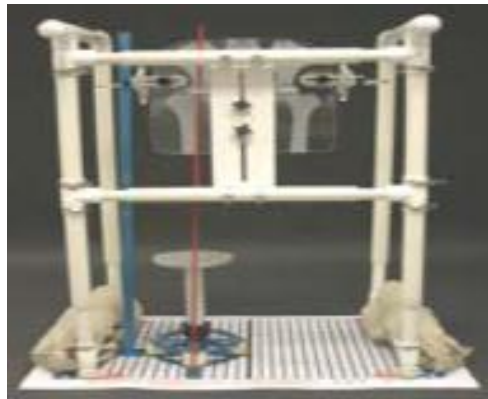


Figure 8: Standing Alignment System (CIR Manual)

Next, the residual limb platform is adjusted to accommodate for correct height. It should be altered to a height that allows the patient's residual limb to comfortably rest on the top of the platform. The height and rotation of the platform can be adjusted using the extension bars and collar at the base. It is very important to keep the hips at the same height during this process, so that they will be level when the prosthesis is complete. The centerline of the patient's body should be directly over the centerline on the mat. The distance from the centerline to both knees should be 6-10cm. Using the alignment bar, the correct AP positioning and the ML positioning are verified. Both axes should be re-checked at the end to ensure that there were no minor movements during the positioning process. Once the alignment marks have been made on both corresponding axes, the cast can carefully be removed.

Transferring the alignment is the next section in the fitting and alignment process. A commercially available Vertical Fitting Jig (VFJ) is used to transfer the alignment from the cast to the positive model. Alignment is an important aspect in designing a prosthetic device; it is what allows the user to have the correct posture and support from their device. The following materials are required to complete this alignment portion of the process: mandrel, pipe adapter, mandrel collar, t-handle hex wrench, plastic spacer, cast with Dacron strap, foot, ankle

busing, base plate, laser level, indelible pencil, flexible ruler, hole-saw or spade bit, utility knife, dish soap or talcum powder, tape, and a plaster mixing bowl.

Establishing the pylon (prosthetic shank) location is the first step in the alignment process. The coronal and sagittal alignment lines are extended using the ruler and pencil. They should perpendicularly intersect on a point, providing a mark through which the mandrel hole is drilled. The alignment lines must coincide with the centerline of the mandrel in both the coronal and sagittal views, which should be an automatic result due to the drill hole at the intersection point. Any necessary adjustments can be made in the AP/ML directions as well as the flexion and abduction/adduction angles. Once the appropriate alignment is reached, it must be secured in place using the four screws on the cast holder arm. A laser is then used to double check the alignment lines in the coronal and sagittal views.

The final stage before the creation of the actual monolimb is to craft the positive model. The first step is to lower the mandrel collar and wrap the bottom of the cast with tape. Plaster is then poured into the cast, taking about thirty minutes to set. After the plaster has hardened, the mandrel vice secures the positive model while the plaster cast is removed. Once this positive model has been created, the AP and ML dimensions must be checked to ensure no variation from the original alignment. Once this has been verified, all irregularities are filled and the model is smoothed.

At this point, the alignment and casting processes have been completed. The fabrication of the monolimb is the final step in fitting the prosthesis to the patient. The definition of a monolimb, according to CIR, is “a prosthesis in which the socket and pylon are formed from one piece of plastic” (CIR Manual). The following tools and equipment are needed for the fabrication process: oven and gloves, vacuum, pump, grinder, cast cutter, hand saw, mandrel vise, utility knife, and scissors. The monolimb is made from a thermoplastic material, however there are a number of other materials necessary for its fabrication including: mandrel with positive model, aluminum ankle bushing, nylon stockinet, talcum powder, scissors, string, tape, grease pencil, utility knife, plaster chisel and hammer, steel heat plate, anti-rotation pin template, 10mm x 25mm dummy bolt, 10mm x 500mm extractor bolt, 10mm x 70mm ankle bolt, Allen wrench, and a ratchet wrench with 17mm socket.

The first step in this section is to prepare the mandrel which must be polished with steel wool on the lower portion. The positive end is then covered in talcum powder with a stockinet added over the top. The 10mm dummy bolt is screwed into the ankle bushing, which is then slid over the distal end of the mandrel. The bushing must be rotated so that the flat sides are parallel to the line of progression. Finally, the vacuum line is connected to the top end of the mandrel.

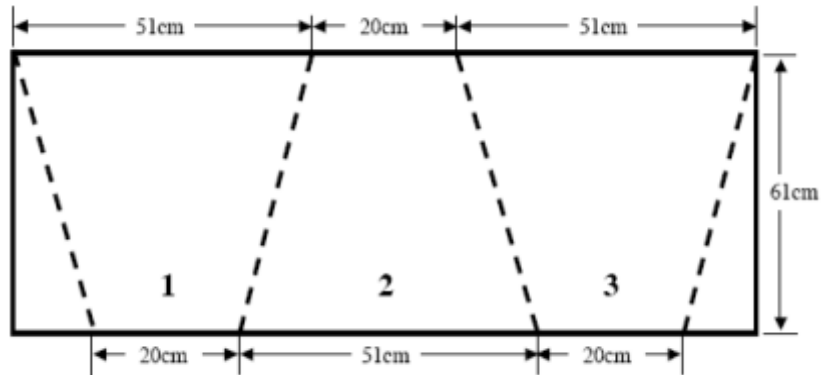


Figure 9: Trapezoidal Plastic Cut (CIR Manual)

As shown in Figure 9 above, the next step is to cut the thermoplastic sheet into three trapezoidal sections. The bases of these trapezoids are measured at 20cm and 51 cm. These trapezoidal pieces will later be used to create the actual monolimb. The plastic pieces must be heated in the oven for approximately 27 minutes to begin the process known as “drape-forming”. The plastic should be clear when it is completely heated and ready for drape-forming. The plastic seam is centered along the posterior aspect of the mandrel and the positive model, and then sealed at both ends. Starting at the distal end, the plastic is pinched together up to the proximal end. To draw the plastic into the model, the vacuum is turned on for twenty minutes. Once tight, the extra plastic is cut, leaving a 20mm seam from the bottom of the mandrel interface.

The next step, extracting the monolimb, starts with marking the trimlines. These lines must be traced around the top of the socket to mark the location of the cut. The cast cutter is used to remove the plastic from around the mandrel. The sander is used to grind down the distal end until the top of the bolt and the end of the ankle bushing are visible. The 10mm x 25mm bolt must be removed and replaced with the 10mm x 500mm extraction bolt.

In the final preparation stages, the sander is used to smooth and buff the trimlines, leaving a posterior seam of approximately 20mm. The distal end is flattened using a heated steel plate, after 15 minutes in the oven, and a heat gun. The distal end is heated until the plastic is semi-clear, then the dummy bolt must be inserted through the whole of the steel plate and tightened to the ankle bushing. The monolimb must now be prepared for delivery and the attachment of the foot. The anti-rotation pin is attached to the bottom of the monolimb to ensure proper alignment for the foot, and the lock-tite ankle bolt is applied. Once the necessary suspension sleeve or suspension cuff is added, the monolimb is ready for delivery to the patient.

Each monolimb is designed for a specific patient, and this process ensures that each will receive the best fitting prosthesis. The devices are designed to provide support and stability so that each user feels as though it is a true extension of their body. The process that was previously outlined in the section uses simple and effective techniques to provide such a comfort to the patients.

Materials

The material selection for prosthetic devices is important because the material directly affects the comfort of the socket and the level of mobility for the patient. The strength and weight of the material contribute to the comfort of the patient while walking. There is a necessary balance between enough strength without applying too much weight for the patient to walk with. In an ideal situation, the material choice should be selected based on the patient's needs and abilities.

There are many patients throughout the world who require the use of prosthetic limbs but do not have the funds to purchase a more advanced and comfortable prosthetic limb. The material associated with the prosthetic limb has a direct effect on the cost of the limb and choosing a material with a lower cost can make the prosthetic much more affordable for many people throughout the world. Many different types of materials are used for prosthetics, ranging from advanced carbon fiber materials to more simple co-polymers which are easily manipulated and require less technology to mold. Therefore, the material selection is one of the most important aspects to a prosthetic design.

Glass Fiber

Glass fiber comes in a variety of different types and has many different applications; however, E-glass fiber is the most commonly used fiberglass in commercial industries. E-glass is the Electrical type of fiber glass due to its low electrical conductivity and use as a dielectric. Fiberglass is made up of several different types of fibers: continuous fibers, discrete fibers, and woven fabric fibers. These are all layered to form a laminate. Optimal strength is achieved when continuous fibers are aligned, but only in the direction parallel to the fiber axes' alignment. This process of creating a laminate with fiberglass is used when making prosthetics (Shackerlford, 502).

A low cost prosthetic, developed by Sebastien Dubois, was created using glass fiber. Dubois' prosthetic project is called "Mobility for Each One" and is being implemented all over the world through the support of the non-profit organization, Handicap International. The prosthetic is shown below in Figure 10. Glass fiber was used for the prosthetic because it is rigid

and strong enough to transfer the forces associated with walking through the prosthetic to the ground, while also retaining its flexibility. The combination of these properties produce a reliable prosthetic limb, which can be produced using a fairly simple process (Dubois, Sebastien).



Figure 10: "Mobility for Each One" Fiberglass Prosthetic

The process to create this particular prosthetic limb follows several uncomplicated and easy to implement steps. First, the glass fiber is put into a wooden mold and shaped by hand. It is then put into a plastic bag and the air is removed, similar to a vacuum. Once the air has been taken out, the material is left to cure. Due to this simple process, the prosthetic can be built easily and fairly inexpensively. Using the material of glass fiber is less expensive than other materials used for prosthetics while also being easy to transform into a prosthetic limb (Dubois, Sebastien).

Thermoplastics

Thermoplastics, which are commonly used in household products such as packaging, toys and cars, have now been applied to prosthetics (Pritham, Charles). Due to their wide use in everyday products, these materials are widely available and produced fairly cheaply. Thermoplastics are often created in sheets, which are particularly useful for the purpose of prosthetics because they are easy to mold and they have sound structural components to work with. The sheets have versatility in the fact that they can be created in different thicknesses and lengths to account for a persons' physical requirements.

The molding of thermoplastics requires little technology and supplies, which makes it easier to implement in developing countries. Also, their structural components are sound for use with prosthetics, including strength, flexibility, and adjustable comfort. The most applicable quality for use in low cost prosthetics is their ability to be reshaped after their initial production. Thermoplastics can be deformed at temperatures of around 100 °C. In comparison, metals deform around 1,000 °C, which would be much too high of a temperature to realistically achieve. The ability to remold is important because if a patient is uncomfortable in their prosthetic, expensive liners cannot be used to increase the comfort level and the socket will need to be altered.

A heat gun is used to heat the material to its thermoformable temperature and then reformed as necessary (Uellendahl 1998). At the thermoformable temperature, the material becomes soft and easy to deform because the cells become thermally activated and the molecules slide past one another. As the material cools, the ductility is reduced and the material becomes rigid again and the new shape holds (Shackerlford, 476).

These materials are being used in many areas where metal alloys had been used due to their comparable strength, ease of fabrication, and reduced cost. These properties make them an ideal material for use with prosthetics for developing countries (Shackerlford, 477). The two most prominent thermoplastics are polypropylene (PP) and polyethylene (PE).

Polypropylene

Polypropylene (PP) is a thermoplastic material which is made for many different products, ranging from appliance housings to prosthetic limbs. It is used in combination with polyethylene (PE) quite often because of its low impact resistance, causing the material to be brittle. When combined with PE, its impact resistance increases, and the material becomes less brittle. Polypropylene can be made in various different grades, making its material properties fall within a broad range of values, as seen in the table below, Table 1 (MatWeb).

PP is a rigid thermoplastic which is used as the supporting structure within prosthetic designs. Stiffer materials are used as support to ensure that the forces applied with walking are transmitted to the floor from the amputee. These forces are crucial to the gait of the patient

and need to be addressed carefully by providing a material which transfers the forces through the prosthetic to the ground (Uellendahl 1998).

Table 1: Polypropylene Material Properties

Property	Value Range	Average Value
Poisson's Ratio	0.1 - 0.3	0.2
Elastic Modulus	1.16 - 1200 ksi	600.6 ksi
Density	0.032 – 0.052 lb/in ³	0.931lb/in ³
Tensile Yield Strength	1740 – 53,500 psi	27,620 psi
Compressive Yield Strength	5000 – 8000 psi	6500 psi
Ultimate Tensile Strength	1310 – 11600 psi	6455 psi
Coefficient of Friction	0.25	0.25

Polyethylene

Polyethylene (PE) is another thermoplastic material used for low cost prosthetics. Polyethylene is a material which consists of chains of ethylene and is used most often for automotive parts, plumbing parts, and containers. Polyethylene is considered the ‘general use polymer’ as it is the most commonly used thermoplastic. There are several different types of polyethylene, including Low Density Polyethylene (LDPE), High Density Polyethylene (HDPE), and Ultra-High Molecular-Weight Polyethylene (UHMWPE). High Density Polyethylene (HDPE) is the variety of polyethylene that is most commonly used for prosthetics because it has a higher tensile strength than lower density (History of Plastics, 2007). A table of the material properties of HDPE has been included below in Table 2.

Polyethylene has been used specifically in the Jaipur Project for the contact socket and shank of their lower limb prostheses. Sheets of HDPE are thermoformed around the mold of the individual requiring the prosthetic limb’s socket, creating a pocket for the patient’s limb to attach the prosthetic. Similarly, this material is thermoformed into the necessary shape of the leg, which acts as the shank for this limb (Kulshreshtha, Tarun Kumar).

PE is used to create the socket, mainly because PE is a flexible material, which makes it more comfortable and more appropriate to be used as the prosthetic interface. The flexible material is well suited for the interface because the flexibility brings a greater level of comfort to the patient. Often, these two polymers are blended together to combine the rigid properties

of PP and the flexibility of PE, which merges together two properties necessary for a quality prosthetic limb (Uellendahl 1998).

Table 2: Polyethylene Material Properties (MatWeb)

Property	Value Range	Average Value
Poisson's Ratio	.29	.29
Elastic Modulus	95 - 195 ksi	145 ksi
Density	.0333 –.0383 lb/in ³	.036 lb/in ³
Tensile Yield Strength	2600 – 4700 psi	3650 psi
Tensile Impact Strength	123 – 250 ft-lb/in ²	187 ft-lb/in ²
Tensile Ultimate Strength	3100 – 4390 psi	3745 psi

Polypropylene - Polyethylene (90/10)

The polypropylene - polyethylene co-polymer has a composition of 90 – 95 % polypropylene and 5 - 10% polyethylene. The combination of these two materials causes the material to be both rigid and flexible, which corresponds to a comfortable and functional lower limb prosthetic. The material properties for the specific material used are included below in Table 3. CIR is utilizing the combination of these thermoplastics because they are an easy to remold, and simple to fabricate low cost co-polymer. In turn, they are applying this material in their prosthetic campaign all over the world (CIR, 2007).

Table 3: Material Properties for Polypropylene-Polyethylene (90/10)

Property	Value
Poisson's Ratio	0.3
Young's Modulus	217,560 psi
Density	0.03 lbm/in ³
Tensile Yield Strength	4,456 psi
Compressive Yield Strength	7,034 psi
Tensile Ultimate Strength	5,337 psi

Other Low Cost Materials

In higher technological prosthetics, materials which have “energy storing” properties have been used because their material properties allow for the storing and releasing of energy while a person walks. This allows for a more natural gait, especially when compared to a stiffer and more rigid shank monolimb. However, there are several low cost alternatives to the

“energy storing” advanced materials, which are being utilized for the purpose of making artificial limbs in a more cost effective manner.

One of the materials used is Vinyl Ester Sheet Molding Compound (SMC). Vinyl Ester is a resin which is usually used in place of polyester or epoxy materials and the material properties for Vinyl Ester SMC have been included in Table 4. One of its most prominent features is its corrosion resistance and ability to withstand water absorption. These are important properties for a prosthetic which will be used during all types of weather and physical conditions. The material properties below are included to demonstrate its material properties. Some prosthetic designs are fabricated using several layers of vinyl ester resin containing fibers for structure. This orientation of the material allows for a rigid limb, which also allows for flexibility. (Houser, Patent #: 5571207).

Table 4: Vinyl Ester Material Properties (MatWeb)

Property	Value Range	Average Value
Elastic Modulus	540 – 3890 ksi	2215 ksi
Density	0.0372 - 0.0704 lb/in ³	0.0538 lb/in ³
Compressive Modulus	1,000 – 2,700 ksi	1,850 ksi
Compressive Yield Strength	15,000 – 45,000 psi	30,000 psi
Tensile Ultimate Strength	4400 – 120,000 psi	62,200 psi

Occasionally, certain metals are utilized for this purpose such as steel and titanium, which are used in advanced prosthetics due to their increased strength and light weight respectively. However, due to the low cost focus of these prosthetics, expensive metals are usually not utilized. Therefore, instead of the more expensive, heavier materials, aluminum is often used due to its fairly high strength, light weight, low cost, and availability (Bartkus 1993).

Comparison

The chart below, Table 5, has been compiled to compare the material properties at a glance. The property values are spread across a wide range because the properties can change due to different treating processes and other changes to the material. Looking at each of the properties, a comparison can be drawn about the material properties to justify the use of the Polypropylene/Polyethylene Copolymer.

The Ultimate Tensile Strength, the maximum stress that the material can withstand, is 5,337 psi for the PP/PE Copolymer. This value is slightly higher than the ranges of the polypropylene and polyethylene on their own, demonstrating the advantage to using the combination of the two materials. Vinyl Ester and E-Glass Fiber are both substantially higher, but the materials are not able to be remolded as the thermoplastics are, making them less desirable for use with monolimb prostheses. The elongation at break is within the same range for all of the materials, except the polyethylene. The high elongation percentage contributes to the high flexibility of polyethylene. The addition of the polyethylene into the Polypropylene adds a level of flexibility to the material properties, which contributes to an increased level of comfort in the socket.

The deflection temperatures of each material vary as well. E-Glass Fiber and Vinyl Ester have much higher deflection temperatures, making them unable to be remolded once they have been fabricated. The polypropylene copolymer and polyethylene have lower temperatures which demonstrate their ability to be manipulated after they have been created.

Table 5: Properties of Low Cost Prosthetic Materials

Material	90/10 PP/PE	Polypropylene Co-Polymer	Polypropylene Thermoformable Grade (PP)	Polyethylene (PE)	Vinyl Ester	E-Glass Fiber
Ultimate Tensile Strength	5,337 psi	1,890 – 5,000 psi	4,350 – 5,210 psi	3,100 – 4,390 psi	4,400 – 120,000 psi	500,100 psi
Tensile Yield Strength	4,456 psi	2030 - 8700 psi	4120 - 5600 psi	2600 – 4700 psi	4400 – 120,000 psi	
Elongation at Break	-	4.00 - 700 %	9.00 - 10.0 %	500 - 2800 %	1.20 - 7.90 %	4.80 %
Deflection Temperature	-	90.0 - 347 °F	205 - 266 °F	135 - 198 °F	320 - 520 °F	3137 °F *Melting Point
Modulus of Elasticity	217.56 ksi	65.3 - 261 ksi	1.16 – 1,200 ksi	95 - 195 ksi	540 – 3,890 ksi	10,500 ksi
Poisson's Ratio	0.3	0.1 – 0.3	0.1 – 0.3	0.29	-	0.2
Density	0.03 lb/in ³	0.0317 - 0.0589 lb/in ³	0.0325 - 0.0327 lb/in ³	.0333 – .0383 lb/in ³	0.0372 - 0.0704 lb/in ³	0.0918 - 0.0939 lb/in ³

This property is one of the key factors which set the PP/PE copolymer apart from the other materials. In the field, the prosthetics need to be easily manipulated with lower technology tools and processes in order to be effective. Therefore, lower temperatures can successfully be reached to adjust the original socket design in order to provide maximum comfort for each of the patients.

The modulus of elasticity, essentially the thickness of the material, is the slope of the stress-strain curve in the elastic region. It demonstrates the resistance of the material to permanent deformation (Shackelford, 191). The values for the materials below reveal that the thermoplastic materials all have fairly similar values; however, the fiber glass materials have much higher elastic modulus values. This fact demonstrates the increased rigidity of the fiber glass materials over the thermoplastic materials. Rigidity is an important factor, but the monolimb approach adds rigidity to the system by design already.

Finally, the density value for the PP/PE copolymer has the lowest density of any of the materials. This is a very important aspect to the material because lightweight prosthetics are much easier to walk with, especially using a rigid monolimb system. In the end, the thermoplastic material used by CIR is a quality material whose material properties are very similar to other materials used for prosthetics. The PP/PE copolymer's material properties demonstrate the ability to act as a high strength, flexibility, and low cost prosthetic for third world countries.

Objectives

The circular shank is the design currently utilized for the CIR's outreach programs, and several varying parameters of the circular cross sectional shank were tested in order to provide CIR with some information regarding the effect of each of the components of their design.

The overall objective of this project was to analyze the current shank monolimb, designed and utilized by the Center for International Rehabilitation, through a finite element analysis. In order to perform this task, the following objectives were completed:

1. Data were provided which verified that the current design utilized by CIR can withstand the loading conditions specified within the ISO Test Standard 10328 without failure. Several combinations of varying diameter and rib thickness parameters were analyzed and compared to determine which design would minimize displacement and overall stress distributions.
2. Four different sized elliptical shaped monolimbs were modeled and used to determine the stress distributions throughout the shank. These models underwent an analysis within the Finite Element Analysis program, COSMOSWorks, to compare their performance and reaction to the loading conditions.

A comparison was conducted to evaluate the results of the Finite Element Analyses of both the circular and elliptical shanks. These analyses were used to determine which shapes and parameters provide the most structural integrity for the patient. The shape that was found to minimize displacements and stress distributions throughout the monolimb was recommended to CIR as the most appropriate design for their programs. These objectives were accomplished through the following steps:

1. Twelve circular shank models of varying shank diameter and rib length and four elliptical models with varying minor and major diameters were modeled using the computer program, SolidWorks.

2. All sixteen models were input into the Finite Element Analysis program, COSMOSWorks and static loading tests were performed on each. These tests complied with the ISO Test Standard 10328.
3. An analysis of the von Mises stress distributions within the monolimb was performed on each of the models.
4. The displacement was analyzed on various areas of the model and graphed for further investigation. These results were utilized to further determine which monolimb shape is most appropriate for use in the field.

Methodology

To accomplish the objectives of this study, Finite Element Analysis was performed on models of several different shapes. The first task in this project was a parameter study which was performed by changing the outer diameter and rib length of a hollow, cylindrical shank model. Next, elliptical shapes were investigated in a similar fashion, using several different widths and an aspect ratio which was applied to each. The stress distributions and displacement were calculated through the finite element analysis program, COSMOSWorks. This chapter will detail the procedure that was followed in order to obtain results that were further analyzed and compared to complete the study.

Parameter Study of the Circular Cross Section

To better understand the effect of some of the parameters present in the circular model, several models were tested with varying combinations of different parameters. The parameters that were tested are the length of the rib on the posterior side of the shank and the outer diameter of the shank. The approach to this portion of the study was to test a model with each of the varying parameters to determine what combination of the varying parameters decreased the overall von Mises stresses and had some displacement throughout the shank which could mimic natural ankle motion; this was done to provide CIR with information regarding which monolimb was least apt to fail.

Shank Height

In order to fully comply with the International Test Standards, the length that was chosen to test needed to correspond with the numbers provided by the ISO Test Standard 10328. The measurement from the ankle to the knee plane in the standards is 420 mm. For a lower limb amputation, a minimum of 60 millimeters of the tibia must remain in order to retain full function of the knee joint (Orthoteers, 2005). In order to account for lower limb amputation, 60 mm has been subtracted from the ISO leg length, making the final length of the shank equal to 360 mm. This shank length was applied to all of the models for all of the

subsequent tests in order to test each of the parameters present on the monolimb shank under maximized conditions.

Test Plates

Additionally, a 20 mm test plate has been added to the distal end of the shank in order to provide a point of application for the offset load. During testing, this test plate has been bonded to the shank in COSMOSWorks and was included in the overall length. By bonding the two parts, the “bonded entities behave as if they were welded...the program merges coincident nodes along the interface” (COSMOSWorks Help File). This plate is 20 mm thick, making the final height of the shank to be tested as 380 mm.

Shank Diameter

Currently, the inner diameter of the shank is determined by the mandrel which is used to shape the polypropylene copolymer during the fabrication process. This size has been applied to every monolimb currently produced by CIR. However, to compare the performance of this cross sectional diameter, two other diameter dimensions were also tested. The diameters that have been chosen for testing are 48.5mm, 53.5mm, 58.5 mm, and 63.5mm. These diameters have been chosen to sample varying possible dimensions and demonstrate their respective stress distributions.

The first diameter chosen was 53.5mm because it corresponds to the diameter that is currently utilized by CIR for their monolimb design. When CIR fabricates the monolimb, they use a mandrel to size the inner diameter making the inner diameter consistent throughout their monolimbs; therefore, the outer diameter that corresponds with the 43.5 mm mandrel and the 5 mm thick material on each side was used. Next, the 63.5mm diameter was chosen because it is the measured width of the raised ankle portion of a SACH foot. CIR pairs their monolimb design with the SACH foot due to the cost effectiveness of the SACH foot. In order to allow for the combination of these two prosthetic systems, the monolimb should not exceed the width of the ankle area of the SACH foot. Once these two values were selected, a diameter that is 5 mm less than the current diameter was chosen in order to determine the effect of a slightly smaller diameter on the overall stress distribution of the monolimb. Finally, the 58.5 mm diameter was

chosen to provide a consistent increase in diameters by 5 mm increments. Below, Figure 11, shows the cross section of the monolimb.

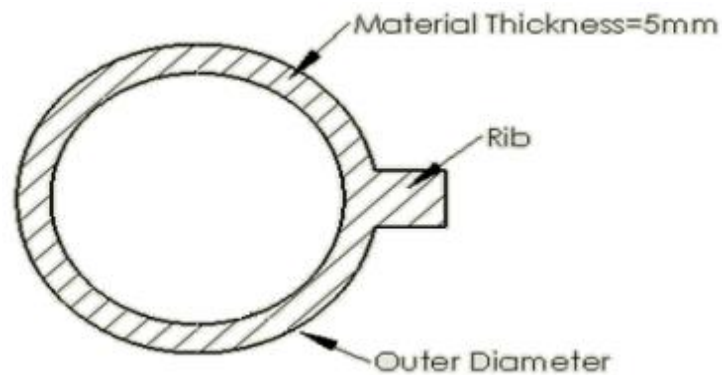


Figure 11: Monolimb Cross Section

Length of the Rib

The rib is a feature of the CIR monolimb design which has been added to increase the rigidity as well as to seal the posterior edge of the monolimb. In order to further understand its role within the design, several lengths of the rib were tested to demonstrate how the rib length affected the overall stress distribution and displacements. To provide a model for comparison, the first length to be tested was 0 mm. This provided insight as to how the monolimb shank reacted to the applied loads without the addition of the rib.

The next lengths were chosen after measuring the rib length of several of the produced monolimbs. These measurements ranged from 10 mm to 20 mm. In order to account for these varying lengths, both 10 mm and 20 mm rib lengths have been incorporated into the parameter study of the monolimb.

Thickness of Material

The material used to fabricate the monolimbs is a polypropylene copolymer, which is purchased in sheets. The fabrication manual dictates that the sheet purchased is 61 centimeters wide by 122 centimeters long and has a thickness of 5 mm. The material purchased by CIR for these programs depends on what is available within their cost bracket; however, they have been consistently using the 5 mm sheets and have included this dimension

in their fabrication manual. Therefore, a 5mm thickness is a constant parameter throughout the modeling and testing.

Parameter Combinations

The parameters chosen above were combined into a table to make sure that each of the diameters and rib lengths were tested with one another. The shank length remained consistent throughout the tests, while the diameter and rib length vary in accordance with the chart below, Table 6. Each parameter was tested with each of the other parameters; therefore twelve circular models and cross sections were tested overall. A table of each of the parameter combinations has been included in the Appendix. A table detailing the parameters that were tested in combination with one another in different models has been included below:

Table 6: Circular Test Parameters

Shank Length	Diameter (mm)	Rib Length (mm)
360 mm (380 mm, including plate)	48.5	0
	53.5	10
	58.5	20
	63.5	

Elliptical Cross Section

The elliptical shape of the monolimb design has been previously researched, physically tested, and published in the Journal of Rehabilitation Research and Development (Lee JRRD 2004). The CIR does not currently use this shape in the field, but they would like to gain a greater understanding of how the stresses are distributed and whether it fails under the loading conditions dictated by the ISO Test Standard 10328. Also, CIR would like to investigate how the circular and elliptical shapes compare to one another regarding the stress distributions and displacements throughout the monolimb.

There are four different models that were designed for the elliptical cross sectional analysis. The dimensions are maximized in accordance with the SACH foot that is usually

attached to a CIR monolimb. The interface plane between the SACH foot and the monolimb has a width of 63.5mm and a length of 98.42mm. The ratio of the major and minor diameters of the SACH foot was used to find an aspect ratio. The minor diameters used for these models corresponded to the circular diameters and the aspect ratio was applied to these values in order to determine the proper major diameter. The aspect ratio used was 0.645. These values all measure the outer dimensions and are included in Table 7 below. Further, Figure 12, displays a drawing of the maximized elliptical shape.

Table 7: Elliptical Parameters

Shank Length	Ellipse Width (mm)	Ellipse Length (mm)
360 mm (380 mm, including plate)	48.5	74.17
	53.5	82.92
	58.5	90.67
	63.5	98.42

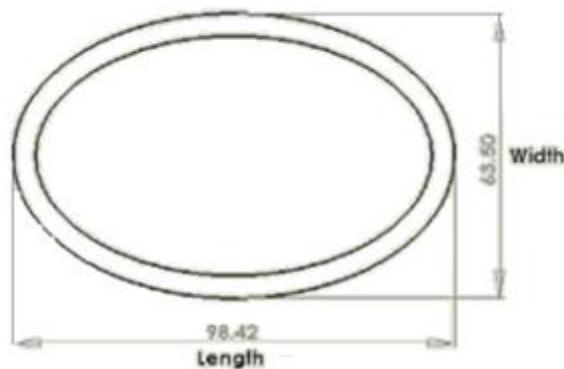


Figure 12: Drawing of Elliptical Shape

ISO Standard

The International Test Standard, ISO 10328, has been used as the basis for the testing. This standard details the testing procedure for lower limb prosthetic devices. The standard dictates the proper coordinate system to use while testing, as well as the required forces and loading locations. The purpose of these standards is to ensure that all prosthetic devices are properly tested and will perform to a certain level of excellence before being distributed to patients; therefore, our coordinate system, forces, and force locations have all been derived from the specified values in the standards.

Testing Level

In the ISO Test Standard 10328, there are four testing levels which can be applied to the test setup and procedure of adult lower limb prostheses. These levels are P3, P4, P5, and P6. “Field experience has shown that there is no need for lower limb prostheses which sustains loads above the level covered by the test loading level P5” (ISO 10328 7.2.3, note 1). The prostheses produced by CIR are utilized by people of all statures, making it appropriate to test for the highest level to account for larger adults who may use the prosthetic device. Therefore, the highest realistic loading condition, P5, was determined to be the appropriate level for the testing in this study. The loading values associated with this level have been applied to the models to be tested.

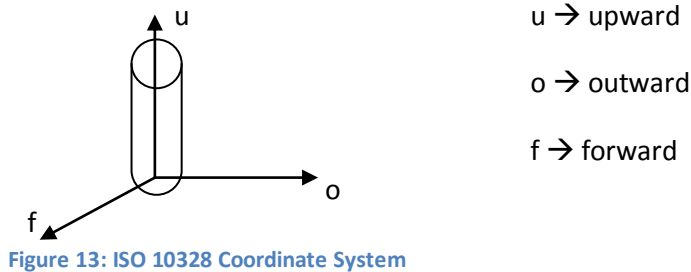
Type of Testing

The type of testing deemed as most appropriate for this analysis is called the ultimate strength test in the ISO Test Standard 10328. The ultimate strength test is a “static load representing a gross single event, which can be sustained by the prosthetic device/structure but which could render it thereafter unstable” (ISO 10328 3.2). This test procedure has been extracted from the ISO Test Standard 10328 and detailed throughout this report. The ultimate strength test was used to demonstrate the capabilities of the device under extreme loading conditions. The two loading conditions, heel-strike and toe-off, were both applied in the testing.

These two sets of loads have been incorporated into our tests by running each model twice. In the first test, the load present will be the “heel strike” load which is placed on the Shank Loading Plane. The Shank Loading Plane is located at the base of the shank. This has been called Loading Condition I throughout the body of this report. The next test will be run on the model with the “toe off” loading condition, referred to as Loading Condition II. The location point for this load is also on the Shank Loading Plane. Together, these two loading conditions will provide a complete picture of how the monolimb performs under the conditions in each of these phases of the gait cycle.

Coordinate System

The ISO Test Standard 10328 specifies the coordinate system that should be used for testing; it shows the directions of the axes for testing prostheses and has been included below as Figure 13. It is important to note that this system only applies when the device is configured to the upright position.



The coordinate system used by the ISO Standards correlates with a standard three-dimensional axes system. For the purpose of transferring this given coordinate system into one that applies to the three dimensional models that will be used, the o-u-f coordinate system has been translated into the x-y-z coordinate system. From the origin, o corresponds to the positive x-axis, while u is the positive y-axis, and f is the positive z-axis. The o-u-f coordinate system will be used throughout the report regarding the orientation of force loads, force locations, and points for investigation on the monolimb.

The o-u-f coordinate system was found in section 6.7 in the ISO Test Standard 10328, which dictates the process for locating the effective joint centers for the knee and ankle joints. In order to calculate the location of the ankle joint center, the SACH foot that is available in the Biomechanics lab was examined. The joint center is located at a point that is equidistant in the medio-lateral direction and at one-quarter the length of the foot, measured 60.75mm from the heel of the foot.

The shanks that are being tested in this study were designed to connect to the SACH foot at the screw-hole location, which is measured at 56mm from the heel and is equidistant in the medio-lateral direction. The ankle joint center coordinate system was input into the Solidworks data, as it is located 4.75mm in the anterior direction from the axis through which

the foot is connected. The location of the applied force as specified through COSMOSWorks is measured from this point labeled “Joint Center System.”

Alignment

During fabrication, the alignment of the monolimb is adjusted from the socket to shank positioning. There are reference alignment lines which are used to position the socket on the proper position on the shank; this point is called the “socket-to-pylon” contact point. This cast is properly positioned and placed on the mandrel. The mandrel is then placed on top of the aluminum bushing, which has been set on a flat surface. The material is shaped around the mandrel to make the shank portion of the monolimb. Therefore, the axis of the shank is aligned with the center of the aluminum bushing.

Reference Planes

There are three reference planes that are used in the modeling of the monolimb. These planes lie parallel to each other and perpendicular to the u -axis. In the ISO Test Standard 10328, the three planes used to determine the force loading location are the Knee Plane (u_K), Ankle Plane (u_A), and the plane which can be applied at any height (u_X). The u_X plane has been placed at the distal end of the shank. In this study, this plane (u_X) is referred to as the “Shank Loading Plane” as it is where the load is applied.

Figure 14, from ISO Test Standard 10328, visually depicts the reference planes for the left leg which will be used during testing. The reference planes are described in the standards as follows:

- 1: Top Reference Plane, T
- 2: Knee Reference Plane, K
- 3: Plane at Any Height, $U=U_X$
- 4: Ankle Reference Plane, A
- 5: Bottom Reference Plane, B

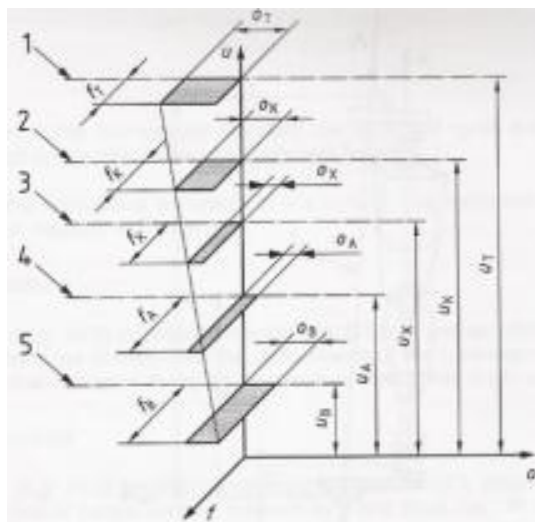


Figure 14: ISO 10328 Reference Planes (ISO 10328)

The ISO Test Standard 10328 provides the line of action along which the load is applied at the levels of the Knee Plane, Ankle Plane, and the Bottom Plane on the monolimb. These values, which are included in Table 8 below, provide the necessary values to solve for the loading point in the f and o directions. To remain consistent throughout the models, the base plane is described at the Shank Loading Plane with $u_X=0$, with the Ankle Plane at $u_A=20$, and the Bottom Plane at $u_B=-60$ on the model. The values provided in the ISO Test Standard 10328 detail the intersection points of the line of action with the Ankle Plane and the Bottom Plane. These values were manipulated to determine the intersection of the line of action with the Shank Loading Plane.

The Shank Loading Plane has been chosen to lie at 0mm in the u direction for all of the models. This height was chosen because this study is only examining the effect of the loading conditions on the shank portion of the monolimb; the socket portion of the monolimb is not being examined. The Shank Loading Plane is the location of the applied loads and it lies on the bottom of the plate. The Shank Plane, u_X , is the value of the height of the shank plus the thickness of the 20mm test plate. With addition of the test plate, the total height of each model is 380 mm. Using the standards, the values for the coordinates of the inner section of the line of action with the bottom and ankle planes in the f and o directions were utilized to determine the intersection of the line of action with the loading plane. The points of

intersection of the line of action on the Ankle and Bottom Planes are different for each of the two loading conditions, and the respective coordinates have been included in Table 8.

Table 8: Loading Offset Locations

Loading Condition I		Loading Condition II	
Variables	Values (mm)	Variables	Values (mm)
f_B	-48	f_B	129
f_A	-32	f_A	120
o_B	45	o_B	-19
o_A	30	o_A	-22
u_B	-60	u_B	-60
u_A	20	u_A	20

These values were then input into the equations shown below to find the location for the load in these directions on the Bottom Loading Plane. The location of the loading point in the f-direction at height $u=u_x$ is:

$$f_X = f_B + \left\{ \frac{(f_A - f_B) * (u_X - u_B)}{(u_A - u_B)} \right\}$$

The location of the loading point in the o-direction at height $u=u_x$ is:

$$o_X = o_B + \left\{ \frac{(o_A - o_B) * (u_X - u_B)}{(u_A - u_B)} \right\}$$

After the coordinates were input into these equations, the values for f_x and o_x were obtained. A table detailing the values of these loading locations for each condition, I and II, has been included below as Table 9.

Table 9: Loading Condition Load Locations

Loading Condition I		Loading Condition II	
Variables	Values (mm)	Variables	Values (mm)
o_x	33.75	o_x	-21.25
u_x	0.00	u_x	0.00
f_x	-36.00	f_x	122.25

Forces

The next step in determining the loads required for the P5 testing level in the ISO Test Standard 10328 was to calculate the force components in each of the principal directions: o, u, and f. The plane locations specified above were utilized to find the line of action of the force vector and then solve for the components of the force vector, the angles of this vector, and finally the magnitude of each component.

The first step in this process was to find the line of action of the force vector. This was done by subtracting the coordinates in the three principal directions of the Bottom Plane, from the point on the Shank Loading Plane. For Loading Condition I, the following vector components were obtained and displayed below.

$$s_1 = o_X - o_B = -11.25mm$$

$$s_2 = u_X - u_B = 60.00mm$$

$$s_3 = f_X - f_B = 12.00mm$$

The process was also followed for Loading Condition II with the specified coordinates used for each vector equation. The vector components for Loading Condition II have been displayed below.

$$l_1 = o_A - o_X = -2.25mm$$

$$l_2 = u_A - u_X = 60.00mm$$

$$l_3 = f_A - f_X = -6.75mm$$

The equations for each of these vectors for Loading Condition I, \vec{S} , and Loading Condition II, \vec{L} , are shown below in vector form.

$$\vec{S} = -11.25\vec{i} + 60.00\vec{j} + 12.00\vec{k}$$

$$\vec{L} = -2.25\vec{i} + 60.00\vec{j} - 6.75\vec{k}$$

Once these vector equations had been calculated, the distance formula was used to find the magnitude of this three dimensional vector. The equation used was:

$$|\vec{S}| = \sqrt{(-11.25)^2 + (60.00)^2 + (12.00)^2} = 62.21 \text{ mm}$$

$$|\vec{L}| = \sqrt{(-2.25)^2 + (60.00)^2 + (-6.75)^2} = 60.42 \text{ mm}$$

Once the vector equations were found, the Direction Cosines of Vectors principle was applied in order to find the components of the load vector. The equations are displayed in a table below, Table 5. These were used to determine the cosine of the angles between the o, u, and f planes. The inverse cosine of each of the values has been included in Table 10.

Table 10: Cosine Values

Loading Condition	Equation	Cosine Value	Equation	Cosine Value	Equation	Cosine Value
I	$\cos \alpha = \frac{s_i}{ s }$	-0.18	$\cos \beta = \frac{s_j}{ s }$	0.96	$\cos \gamma = \frac{s_k}{ s }$	0.19
II	$\cos \alpha = \frac{l_i}{ l }$	-0.04	$\cos \beta = \frac{l_j}{ l }$	0.99	$\cos \gamma = \frac{l_k}{ l }$	-0.11

The ISO Test Standard 10328 specifies that the value of the applied force for Loading Condition I is 3360 N and for Loading Condition II is 3019 N. These force load values were multiplied by their respective cosine values in the alpha, beta, and gamma directions. The product of each provided the force components in the three directions. These component values are detailed in the table below, Table 11.

Table 11: Force Components

Force Component Table	Loading Condition I	Loading Condition II
o-component	-607.58 N	-112.42 N
u-component	3240.44 N	2997.99 N
f-component	648.09 N	337.27 N

The values have been used as the components of the force vector to be applied on the Shank Loading Plane for each of the tests for the varying elliptical dimensions and circular parameters.

Shank Models

The first step in determining how the monolimb responds to the testing loads was to create the models. These models were created with the three-dimensional modeling program, Solidworks. The models were built using the coordinate system dictated by the standards and described previously. The models will each have one of the circular or elliptical parameter

combinations detailed in Appendix D. These size differences have been applied to better understand the affect of the cross sectional shape on the monolimbs' stress distributions and displacements.

Once the models had been made, a plate was added to the distal end of the shank. This plate has been added to the model to ensure proper distribution of the applied force. In physical testing, the socket portion of the monolimb and attached prosthetic foot would serve the purpose of distributing the load. In this study, the socket and foot have not been included and the line of action of the force lies outside of the area of the shank, which makes a plate necessary to distribute the force across the bottom of the shank. The force loads dictated by the ISO Test Standard 10328 are point loads, which need to be distributed to the model to better represent the natural forces which would be experienced during the gait cycle. Beyond distributing the load, the plates need to be able to withstand the load with minimal deformation in their geometry. To determine the material to be used for these purposes, material properties were consulted to find a material with a high yield strength, because the this property demonstrates the stiffness of the material. A material with a high yield strength has a lower chance of permanent deformation. This material property was necessary for the test plate to ensure that the load was distributed through the shank, rather than deforming the plate. AISI 1020 steel proved to be the best choice for the plate. AISI 1020 steel has the highest yield strength of all the materials within the COSMOSWorks Material Library, making it the most stiff and best for loading in this test.

Force Application

Upon completion of the construction, the models were opened in COSMOSWorks to begin the Finite Element Analysis testing. The Ultimate Static Test Forces were applied according to the ISO Test Standard 10328. To account for the two main stages of the gait cycle, the 'heel strike' and 'toe off' phases were both applied on the Shank Loading Plane, which lies on the test plate located at the base of the shank. At the height of the shank, a fixed constraint has been applied to ensure that there is no movement from this end of the shank while testing is being completed.

Finite Element Analysis Testing

For the purposes of the FEA software, the model will be assumed as linearly elastic, isotropic, and homogeneous. The values in the table below will be applied as the material properties for the model created and run in COSMOSWorks. The values being applied to the model are listed in Table 12.

Table 12: Polypropylene/Polyethylene Copolymer Material Properties

Material Property	Value (English Units)	Value (SI Units)
Poisson's Ratio	0.3	0.3
Young's Modulus	217,560 psi	$1.5 \times 10^9 \text{ N/m}^2$
Density	0.03 lb/in ³	830.4 kg/m ³
Tensile Yield Strength	4,456 psi	$3.07 \times 10^7 \text{ N/m}^2$
Compressive Yield Strength	7,034 psi	$4.85 \times 10^7 \text{ N/m}^2$
Tensile Ultimate Strength	5,337 psi	$3.68 \times 10^7 \text{ N/m}^2$

A new study was performed for every combination of the parameters; a table detailing the parameters of each circular has been included as Appendix A. Each study created a solid mesh in order to perform a static analysis on the models that have been designed to the specifications described above. Once the study was defined, the proper constraints and point loads were applied. For the first study, the forces as described for Loading Condition I were applied to the Shank Loading Plane while a fixed constraint was applied at the proximal end of the shank. The components of the "heel strike" loading conditions were applied in the specified location. This point load is applied to the plate to distribute the force throughout the plate to the shank. Once all of these conditions were specified within COSMOSWorks, the mesh was created on the model, and the load was applied for the analysis to be performed.

After the mesh was successfully applied to the model and the program had finished running the model, the results were extracted to observe the von Mises stresses and displacements that occurred due to the applied loads. The results have been reported in the form of several contour plots, which are displayed through colors that correspond to different stress and displacement value levels. The color scale of the contour plots was adjusted to ensure that the same values corresponded with the same stress and displacement values

throughout all of the models. This was done to provide consistency throughout the testing and analyses of this study. These plots were then used for the comparative analysis that is described later in this report.

Finite Element Analysis

Failure Criteria

Von Mises Stress

The material used for manufacturing the CIR prostheses is a thermoplastic material. This material has a percent elongation of 5%, which places it into the ductile materials category. The failure of ductile materials is considered to occur when the yield strength is reached under static loading (Norton, 241), which is when the von Mises stresses become equal to the stress limit. The yield strength for this material is $3.07 \times 10^7 \text{ N/m}^2$, which was also referred to as the stress limit. Therefore, the von Mises stresses were used as the first criterion for comparison between the shank models.

The von Mises stresses were used for this comparison because these stress values “allow the most complicated stress situation to be represented by a single quantity” (Shigley, J.E., 2004). In essence, the von Mises stress values are a combination of all of the stress components present in the model into one value. This is a good measure of the overall reaction of the shank monolimb to the loading condition, because it takes all of the stress components and outputs one stress value. This value was compared to the Yield Strength to ensure that the material did not exceed the stress limit presented by the polypropylene copolymer material. The contour plot for the von Mises stresses will be examined for each of the models. These contour plots were used to display the overall distribution of the von Mises stresses throughout the material, as well as determine the approximate location and value of the maximum von Mises stresses. These contour plots were examined and presented in the results section of this report.

Within the COSMOSWorks program, the failure analysis that was run was the von Mises stress distribution test. This test is based on the von Mises-Hencky theory, which is “the most

accurate” (Norton, 241) of the numerous failure theories for ductile materials. The Yield Strength specified is what the program uses to determine whether or not the model has reached its stress limit.

$$\sigma_{\text{Von Mises}} \geq \sigma_{\text{Limit}}$$

Another one of the features of the COSMOSWorks program which was used to further illustrate the overall von-Mises stresses was the Design Check. The Design Check isolated the shank and illustrates the stress distributions throughout this part of the model, which disregarded the metal plate for this portion of the analysis. As the purpose of the metal plate is to distribute the force, the stress distributions present in the metal plate did not need to be investigated further in this study. The Design Check has various comparison criteria, but the first criterion to be used will involve the von Mises stresses, which are applied in the program per the equation below to determine whether or not the model fails at any point within the model.

$$\frac{\sigma_{\text{von Mises}}}{\sigma_{\text{Limit}}} < 1$$

The Design Check applies the Yield Strength as σ_{Limit} to highlight the areas where this ratio is greater than 1 and displays these regions in red.

Using the next feature within COSMOSWorks, ISO Clipping, these areas can be isolated so that only the areas where the ratio is above 1 are shown in the contour plot of the shank. These isolated areas allow a better understanding of where the shank is experiencing von Mises stresses that exceed the stress limit. The tests were performed on all of the models and the areas where the ratio is greater than 1 were compared through an observational analysis of the location of these areas and the value by which this failure criterion is exceeded.

Displacement

The next area for comparison is in the displacement of each model due to the applied loading conditions. The displacements were investigated to determine the overall effect of the parameters and their reaction to the loading conditions in the varying directions. The displacements were examined in component form to determine how the model has moved from its original position in each of the three principal directions, o, u, and f. These component values were used to find the resultant displacement in each model. These were graphed and analyzed to gain a better understanding of how the combined loading affected the models.

The measurements of the displacements were taken at 12 points distributed equidistant throughout the shank of each model. The first point was located 10mm above the interface of the shank and the plate, and the u (y) coordinate of the following points was increased by 30mm. These points were located on the outer edge of the monolimb, at a point that is 180° from the load application point. For Loading Condition I, measurements were taken along the plane that lies 46.86° from the positive f axis, in the negative o direction. For Loading Condition II, this plane lies 9.84° from the positive f axis, in the negative o direction. These planes were chosen as they pass through the point of application of the load vector and the axis of the shank for their respective loading conditions. The plane has been displayed in Figure 15 below; the green line represents the plane used for measurement of the stress and displacement values. In the figure below, the coordinate system corresponds to the traditional x-y-z system, with the x and o direction the same, and the z and f direction the same.

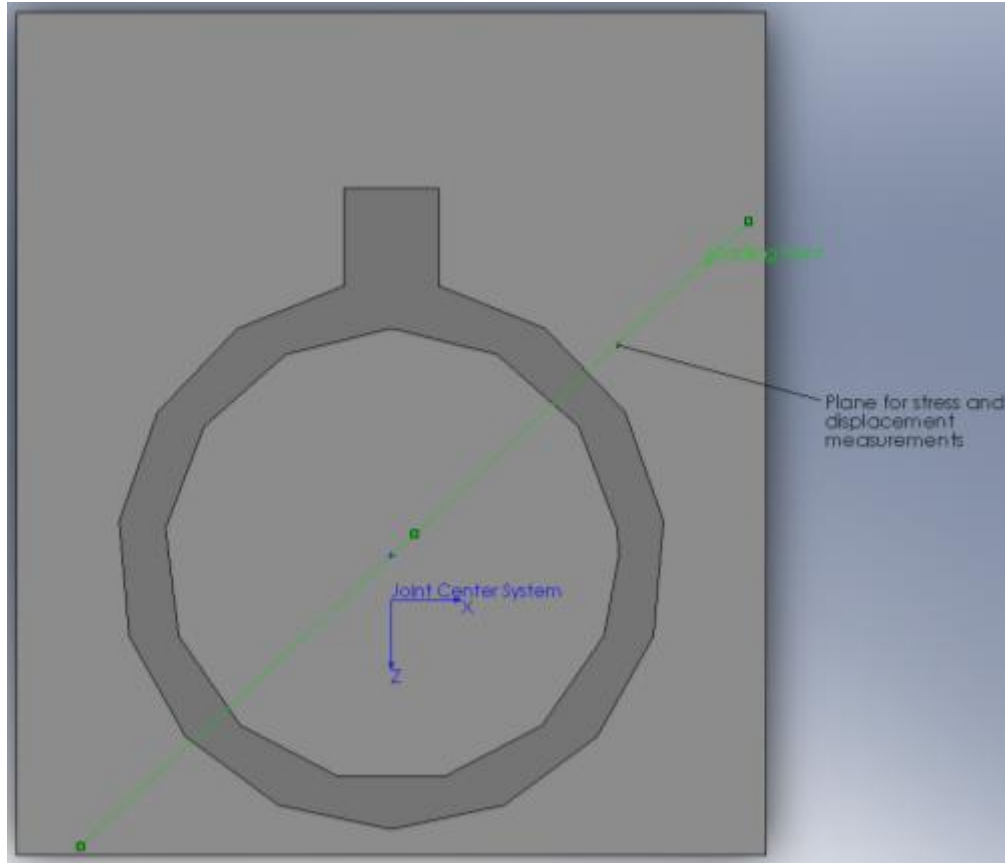


Figure 15: Plane for stress and displacement measurements

These points were probed in the COSMOSWorks program to determine the displacements at each of these points. The data for the X and Z displacements at each point were transformed to correspond to the plane on which we had previously measured the von Mises stresses. The given data from COSMOSWorks was exported into Excel and the resultant displacement was transformed into components to correspond to the new plane. The scalar resultant value was found using the formula $R = \sqrt{x^2 + z^2}$. The direction of the resultant was found as $\theta = \tan^{-1}(x/z)$. The angles described in the earlier section, 46.86° and 9.84° (symbolized by φ), were used to find the values of the “In-Plane” and “Out-of-Plane” displacement. The “In-Plane” value describes the value that lies within the plane described above, and was found using: $I = R * \cos(\theta + \varphi)$. The “Out-of-Plane” displacement, which describes the values that are 90° to the plane, were found using a similar equation: $= R * \sin(\theta + \varphi)$. The “In-Plane” displacements are related to the bending loads, while the

“Out-of-Plane” displacements are related to the torsional loads and the transverse bending loads.

The displacements at each of these probed points were output into multiple graphs to better understand the displacement throughout the model. The values of the resultant displacement in each model were graphed according to outer diameter. Graphs were also created to depict the “In-Plane” and “Out-of-Plane” displacements.

The output from COSMOSWorks was manipulated in Excel to achieve the appropriate graphs to scale. The COSMOSWorks values do not correspond to the values originally described for the probed points (10mm, 40mm, 70mm, etc.) because they are based on a coordinate system that is located near the centroid of the model. In order to account for this change, the difference was found between the y value in the probed point, and the original y value of the point. This difference was added to each of the points to keep the u-values in the same relative position as they were in the exported data. For example, in the figure below, the point at the distal end of the shank has a y-value of -163mm. In order to have the appropriately scaled data, 173mm will be added to every u-value of each node.

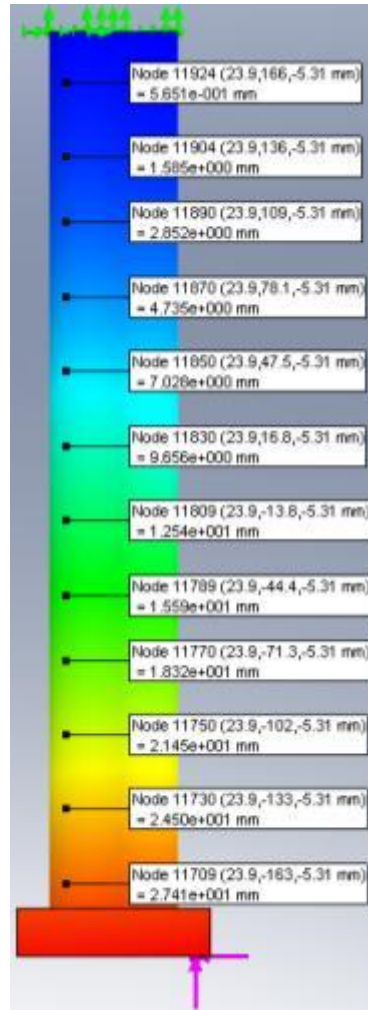


Figure 16: Front View of Probed Points

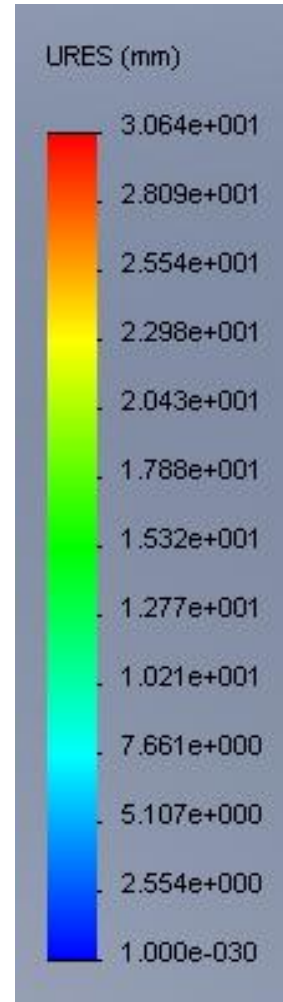


Figure 17: Scale of Displacement Values

Figure 16 and Figure 17, shown above display the values of the resultant displacement at each of the probed points. The above example is from the 53.5 Outer Diameter model with a 10 mm rib length under Loading Condition I and the points are clearly located on the plane that lies 46.86° from the f-axis. The displacement was investigated because flexibility in the shank can mimic that of natural ankle motion, which is a desirable quality in a prosthetic. It demonstrated how the shank responds to the loading, and which set of parameters provided sufficient rigidity for the patient. For this reason, the analysis of the displacements was of particular interest for this report.

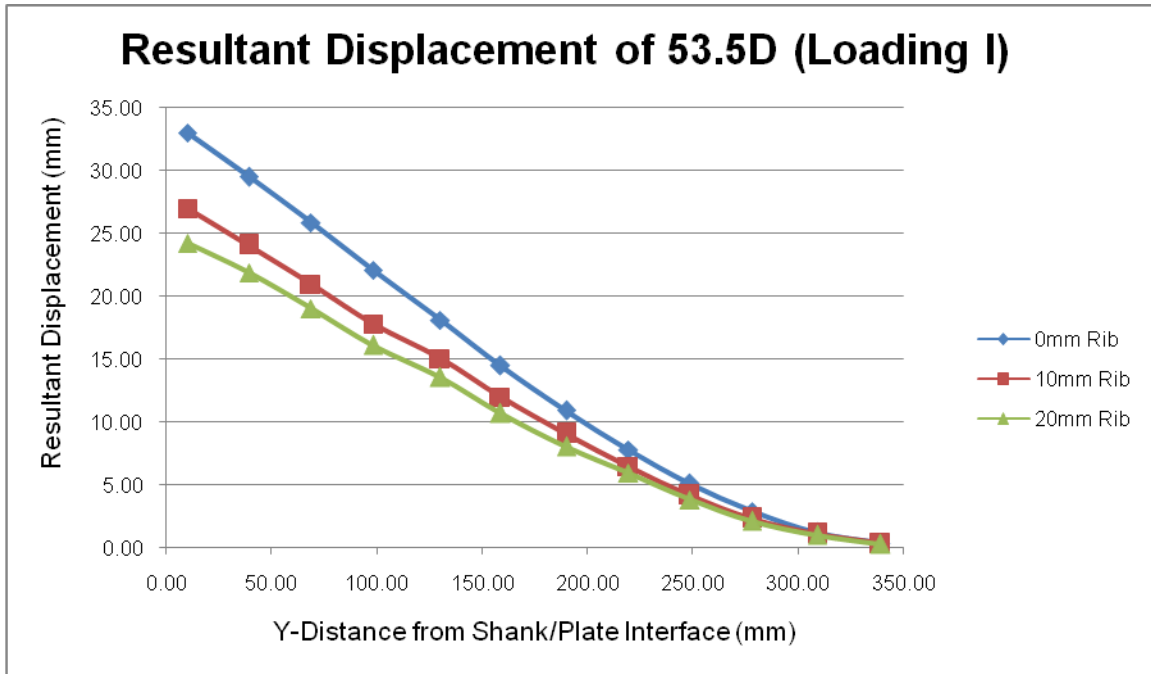


Figure 18: Graph of Resultant Displacement

Figure 18 displays the graph of the displacement in the shank model. The 10 mm distance on the graph corresponds to the area present 10 mm above the interface between the shank and the metal plate; this area of the monolimb corresponds to the ankle region of the model. The 340 mm points correspond to the height of the shank where there is a fixed constraint on each of the models.

Within the monolimb, the displacement throughout the shank is often considered a positive quality of the design, because this displacement will mimic ankle movement for the patient (Lee 2006). Therefore, we will pay special attention to the displacement throughout the monolimb to determine if the shank is undergoing slight displacements around the ankle and up through the height of the shank. The displacement is expected to be larger toward the distal end of the shank as it is closer to the loading; however, the displacements throughout the entire shank will be examined.

Results

Von Mises Stresses

The von Mises stresses were analyzed through the contour plots which were displayed from the results of the finite element analysis performed in COSMOSWorks. These models have been included showing the *Front View* from COSMOSWorks for each of the models. The *Front View* was chosen as the most appropriate view to display because the maximum stresses and probed points were clearly visible with this view in the computer program. The point which was probed on each of the models lies 180 degrees from the load application point. This plane lies 46.86° and 9.84° from the f-axis in the negative o-direction, which according to manual calculations, should be the plane upon which the highest von Mises stresses are located for loading condition I and II, respectively. To provide better comparisons between the data for each diameter, one color scale for the von Mises stress contour plots has been used per diameter per loading condition.

Loading Condition I

The contour plots in this section will display the von Mises stresses caused by Loading Condition I, which is the “Heel Strike” load from the ISO Test Standard 10328.

Circular Shanks

Circular Shank: 48.5 mm Outer Diameter

The von Mises stresses are displayed through the contour plots below in Figure 19, these plots are for the 48.5 mm OD shank. From left to right, the models are for the 0 mm rib, 10 mm rib, 20 mm rib, and finally the color scale for the model. As shown in these stress plots, there are definite areas where maximum von Mises stresses are occurring on the anterior region of the shank. These areas can be visually seen below as red regions on the shank; the maximum von Mises stresses are displayed through the color red in the contour plots. The von Mises stresses are 100% higher in the model with a 0 mm rib length than the Yield Strength for the thermoplastic material being used for the monolimb. The stresses in each of these models are

above the Yield Strength, with the 20 mm rib length being 38% higher than specified 3.07×10^7 N/m² value.

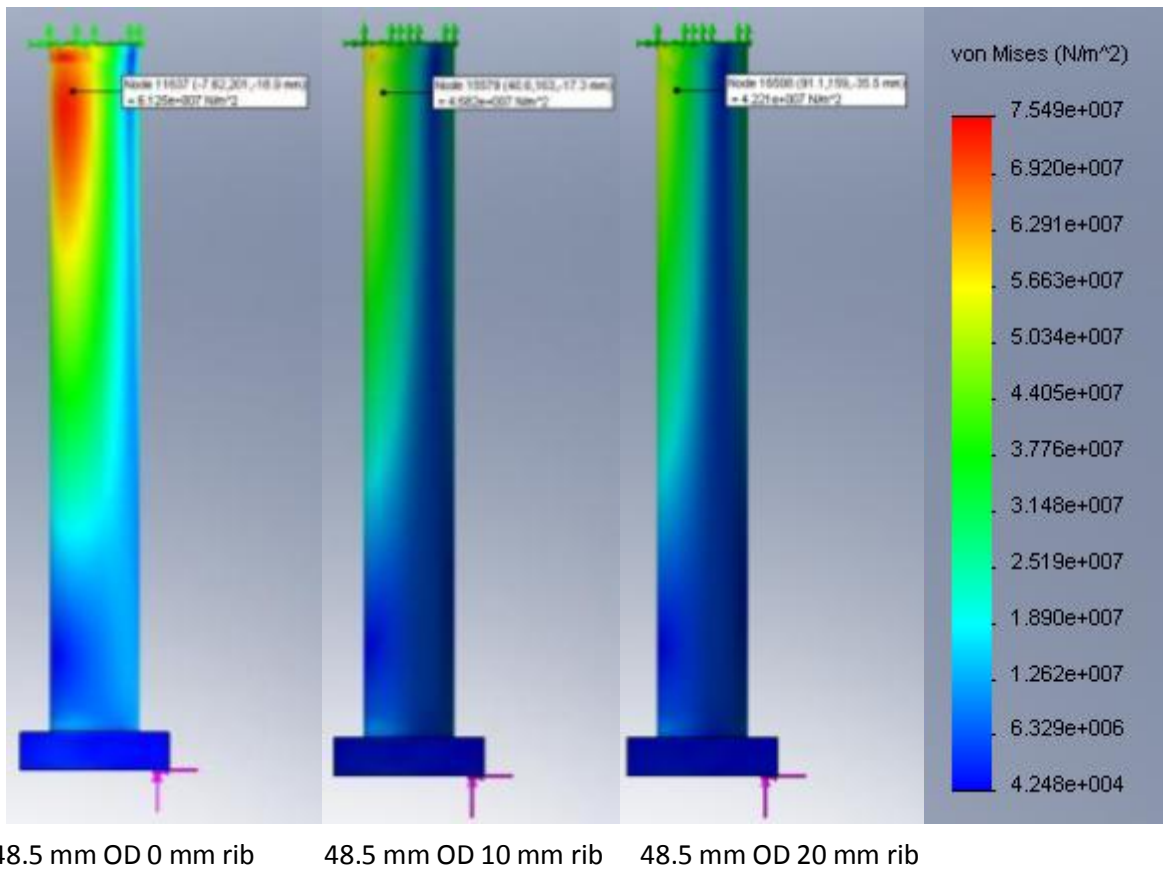


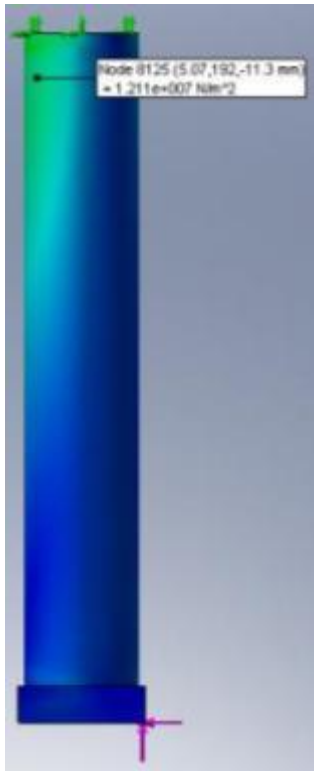
Figure 19: 48.5 mm OD von Mises Stress Contour Plots (Loading Condition I)

The below table, Table 13, displays the probed von Mises stress values for all of the circular models under loading condition I. The overall stress distributions for each of the circular shanks follow a similar pattern as shown in the models above; therefore, the remainder of the contour plots has not been included in the body of the report, but they are included in Appendix G for further reference.

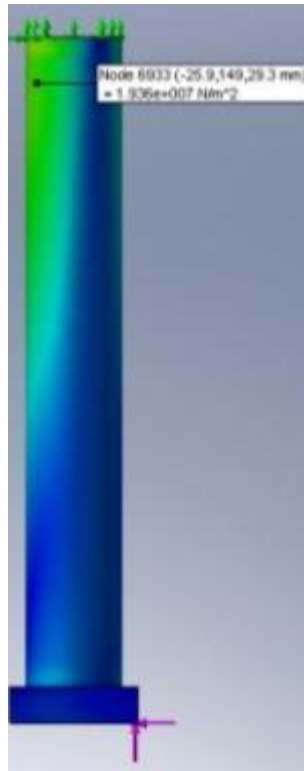
Table 13: von Mises Stress Values for circular models (Loading Condition I)

Outer Diameter	0mm Rib Length	10mm Rib Length	20mm Rib Length
48.5 mm	6.125×10^7 N/m ²	4.682×10^7 N/m ²	4.221×10^7 N/m ²
53.5 mm	3.666×10^7 N/m ²	3.200×10^7 N/m ²	2.889×10^7 N/m ²
58.5 mm	3.215×10^7 N/m ²	2.212×10^7 N/m ²	2.062×10^7 N/m ²
63.5 mm	1.962×10^7 N/m ²	1.843×10^7 N/m ²	1.759×10^7 N/m ²
Yield Strength	3.07×10^7 N/m ²		

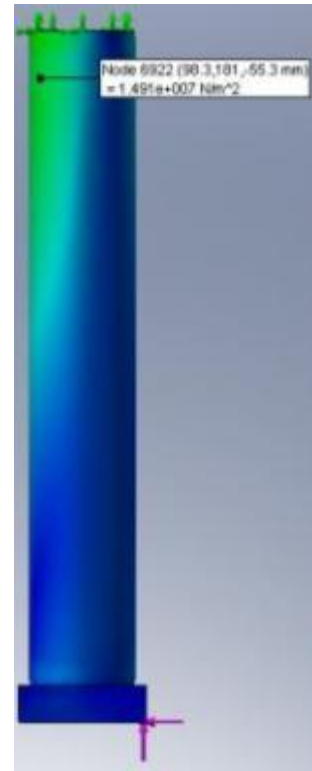
Elliptical Shanks



48.5mm minor diameter



53.5mm minor diameter



58.5mm minor diameter



63.5mm minor diameter

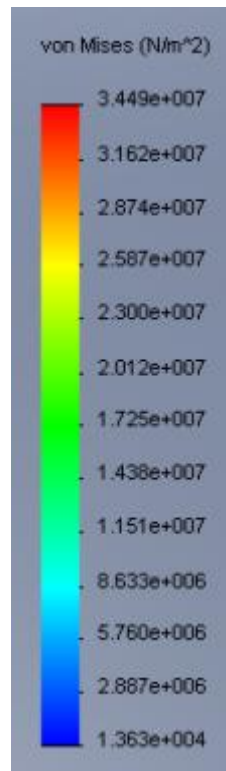


Figure 20: von Mises Stress Contour Plots for Elliptical Shanks (Loading Condition I)

As shown above in

Figure 20, the von Mises contour plots have been included to illustrate the stress distributions present throughout the elliptical shanks. The pattern of stresses mimics that of the circular shanks for Loading Condition I, with a stress concentration located on the front area of the shank and the stresses decreasing as the distance from this area increases. A chart of the values for the elliptical shanks at the probed point that lies 25 mm below the proximal end has been included below as, Table 14.

Table 14: von Mises Stress Values for Elliptical Shanks (Loading Condition I)

Elliptical Minor Diameter	48.5 mm	53.5 mm	58.5 mm	63.5 mm
Von Mises Stress Value	$2.838 \times 10^7 \text{ N/m}^2$	$1.938 \times 10^7 \text{ N/m}^2$	$1.491 \times 10^7 \text{ N/m}^2$	$1.211 \times 10^7 \text{ N/m}^2$

These values detailed above all below the Yield Strength of $3.07 \times 10^7 \text{ N/m}^2$, which demonstrates that the elliptical models all successfully pass the von Mises failure criteria.

Loading Condition II

The next sets of contour plots will display the von Mises stresses caused by Loading Condition II, which is the “Toe Off” load from the ISO Test Standard 10328.

Circular Shanks

Circular Shank: 48.5 mm Outer Diameter

The below contour plots display the von Mises stresses that were caused by Loading Condition II on the 48.5 mm OD shank. These contour plots have been included as Figure 21. The model with a 0 mm rib has an area where maximum stresses occur, which can be seen as the red portion of the shank in the leftmost model below. This area is not visually present in the other two models with rib lengths of 10 mm and 20 mm. The 10 mm rib shank has an area of yellow, which is still fairly high on the color spectrum, but there is not a maximum stress displayed in this area. In the model with a 20 mm rib length, the front area of the shank is primarily green and blue, demonstrating much lower stress values.

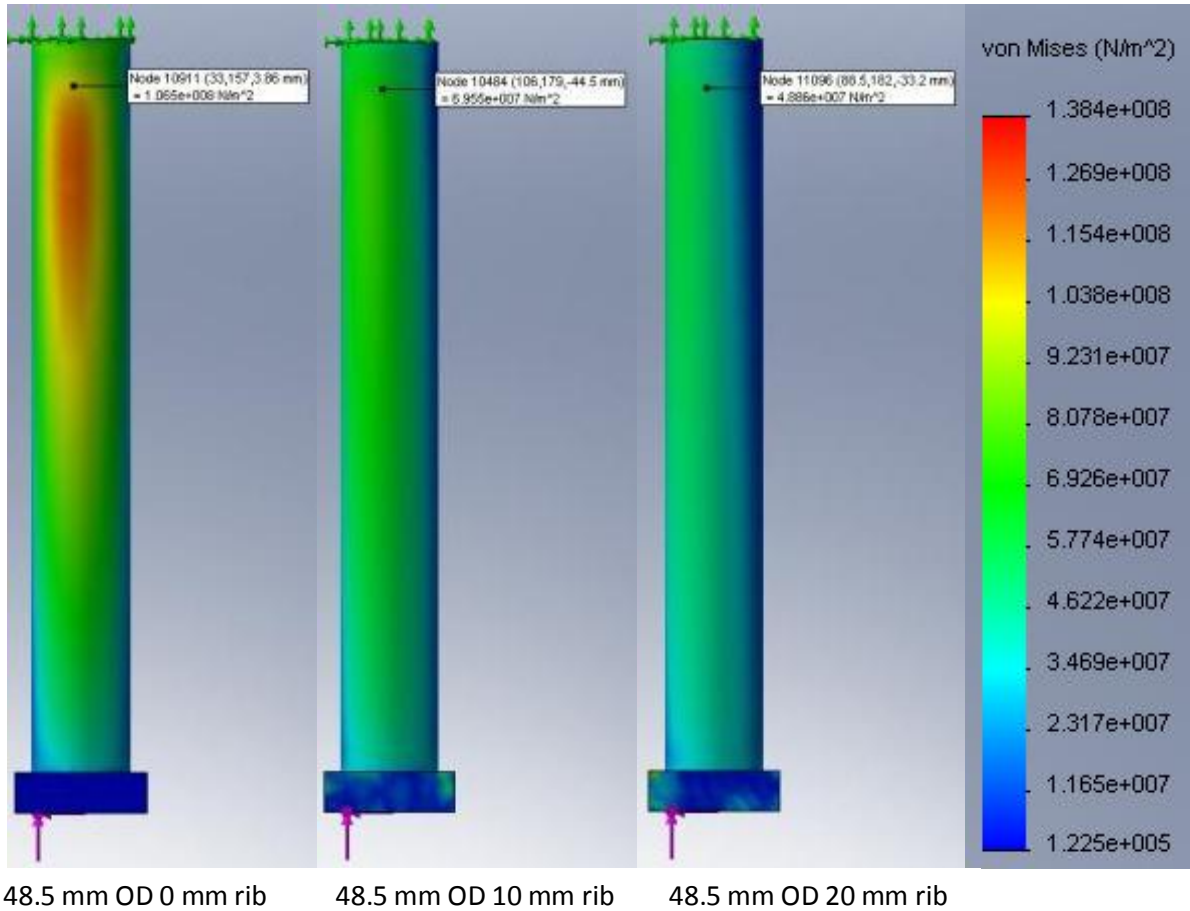


Figure 21: 48.5 mm OD von Mises Stress Contour Plots (Loading Condition II)

Table 15: 48.5 mm OD von Mises Stress Values (Loading Condition II)

Loading Condition	0 mm rib length	10 mm rib length	20 mm rib length
II (Toe Off)	$1.065 \cdot 10^8 \text{ N/m}^2$	$6.955 \cdot 10^7 \text{ N/m}^2$	$4.886 \cdot 10^7 \text{ N/m}^2$
Yield Strength	$3.07 \cdot 10^7 \text{ N/m}^2$		

As shown in the table above,

Table 15, the stresses decrease by 35% with the addition of the 10 mm rib; however, all of the von Mises stresses in the 48.5 mm models are at least 59% higher than the Yield Strength of the thermoplastic material.

The table containing all of the von Mises stress values for the circular models under loading condition II is below,

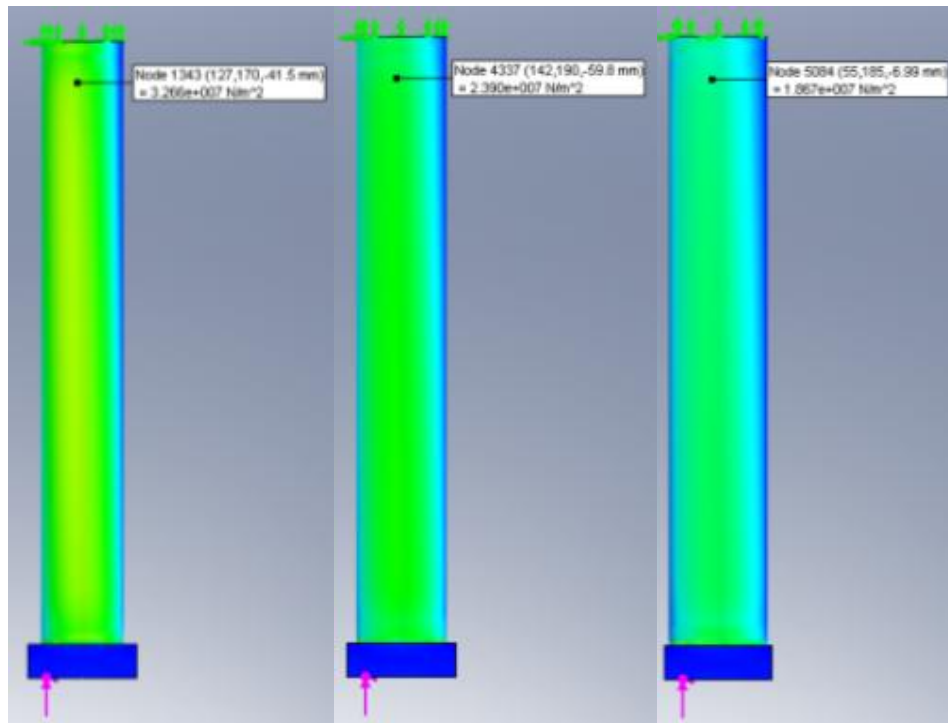
Table 16.

Table 16: Probed von Mises values for elliptical shanks (Loading Condition II)

Outer Diameter	0mm Rib Length	10mm Rib Length	20mm Rib Length
48.5 mm	$1.065 \cdot 10^8 \text{ N/m}^2$	$6.955 \cdot 10^7 \text{ N/m}^2$	$4.886 \cdot 10^7 \text{ N/m}^2$
53.5 mm	$6.842 \cdot 10^7 \text{ N/m}^2$	$4.867 \cdot 10^7 \text{ N/m}^2$	$3.592 \cdot 10^7 \text{ N/m}^2$
58.5 mm	$6.847 \cdot 10^7 \text{ N/m}^2$	$3.609 \cdot 10^7 \text{ N/m}^2$	$2.830 \cdot 10^7 \text{ N/m}^2$
63.5 mm	$3.460 \cdot 10^7 \text{ N/m}^2$	$2.802 \cdot 10^7 \text{ N/m}^2$	$2.326 \cdot 10^7 \text{ N/m}^2$
Yield Strength	$3.07 \cdot 10^7 \text{ N/m}^2$		

The remaining contour plots and observations for each of the models have been included in Appendix G.

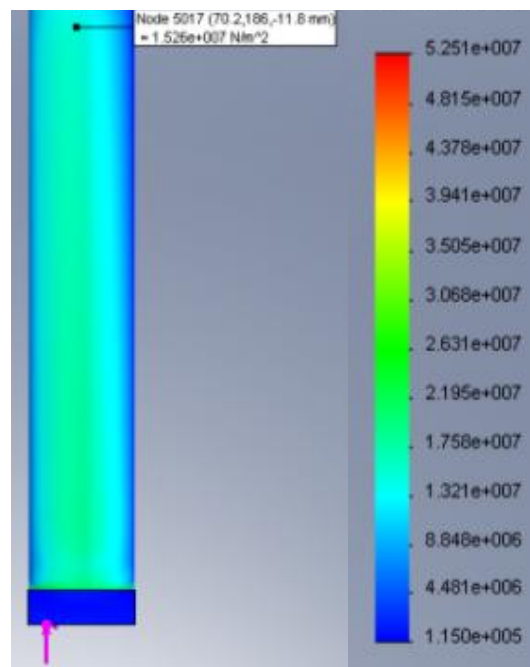
Elliptical Shanks



48.5mm minor diameter

53.5mm minor diameter

58.5mm minor diameter



63.5mm minor diameter

Figure 22: von Mises Contour Plots for Elliptical Shanks (Loading Condition II)

The value of the von Mises stresses for the 48.5 mm width elliptical shank is more than double the Yield Strength, and also nearly three times the stress value for the 53.5 mm width shank. This can be seen through the chart, included as Table 17. The stresses decrease as the minor diameter of the ellipse increases. Each of the values lies below the Yield Strength for the thermoplastic material, as long as the minor diameter is greater than or equal to 53.5 mm.

Table 17: von Mises Stress Values for Elliptical Shanks (Loading Condition II)

Elliptical Minor Diameter	48.5 mm	53.5 mm	58.5 mm	63.5 mm
Von Mises Stress Value	$6.955 \cdot 10^7 \text{ N/m}^2$	$2.390 \cdot 10^7 \text{ N/m}^2$	$1.667 \cdot 10^7 \text{ N/m}^2$	$1.526 \cdot 10^7 \text{ N/m}^2$

Displacement

Loading Condition I

Circular Shanks

Circular Shank: 48.5 mm Outer Diameter

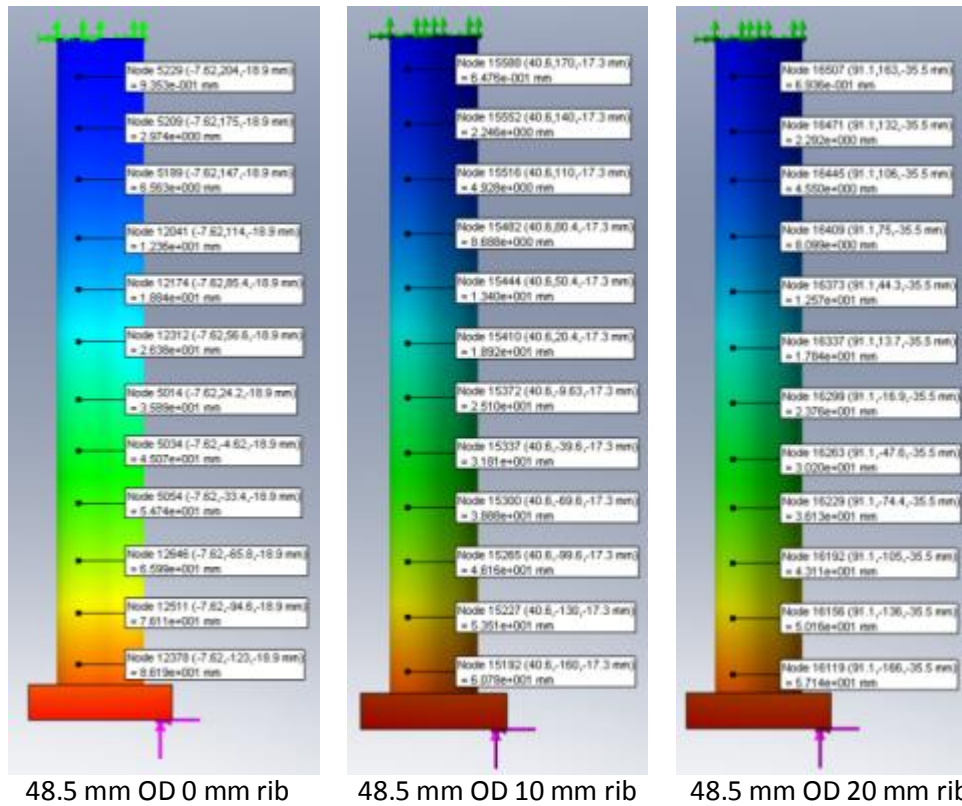


Figure 23: 48.5 mm OD Displacement Contour Plots (Loading Condition I)

Figure 23 shows that the displacements are highest the closer they lie to the load location in the u direction. As the distance from the load location increases, the displacement values decrease. This trend was similar in each of the models tested and the displacement plots have been included in Appendix H. Below, Figure 24 displays this trend graphically. These displacement values output from COSMOSWorks are substantially larger than originally expected. The resultant displacement for a shank of this diameter is nearly twice the dimension of the full diameter, 48.5 mm.

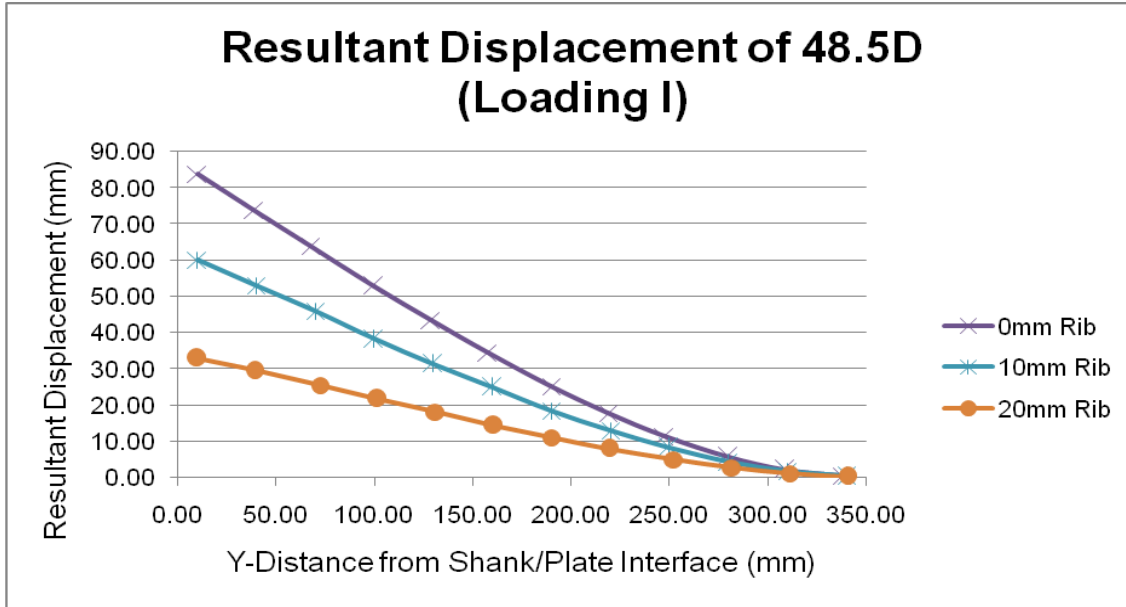


Figure 24: Resultant Displacement (48.5 mm OD)

Circular Shank: 53.5 mm Outer Diameter

The resultant displacement values on the 53.5 mm OD shank are quite large; the resultant displacement is close to 10% of the height of the shank. The overall trend in the above graph shows that as the rib length increases, the magnitude of displacement decreases which can be seen in Figure 25 above.

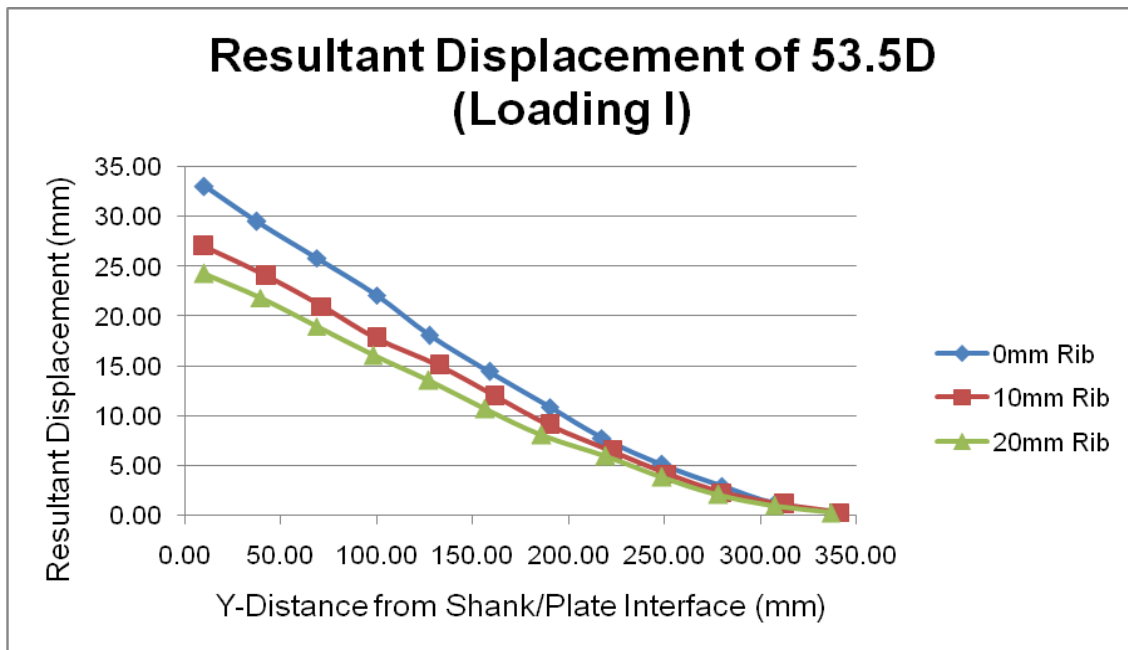


Figure 25: Resultant Displacement of 53.5 mm OD

Circular Shank: 58.5 mm Outer Diameter

Through the use of the graph below in Figure 26, the existing trend can be seen, which is that as the distance from the load increases, the displacement decreases.

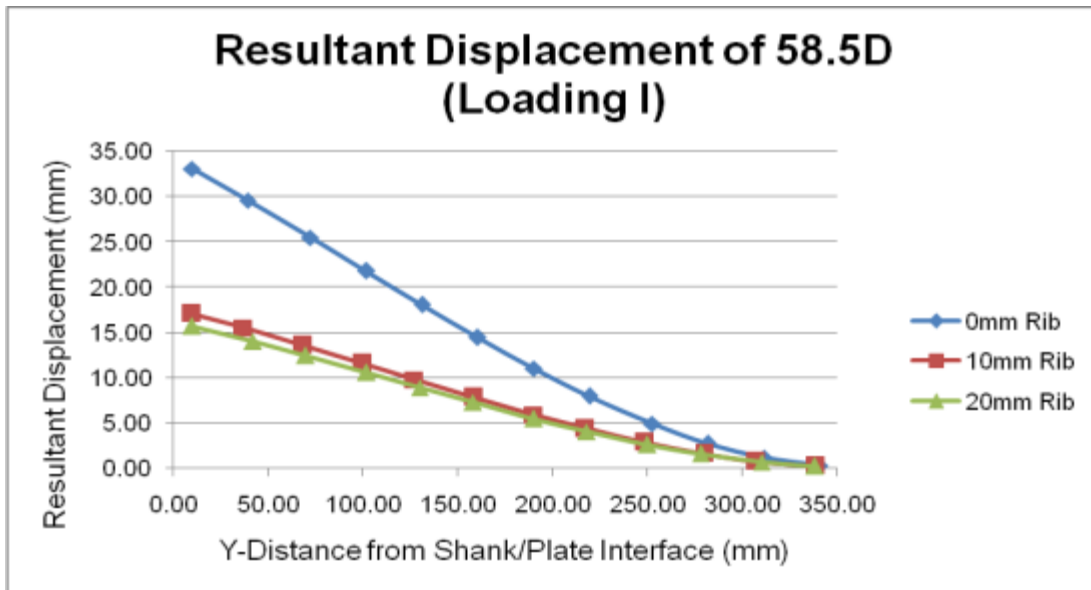


Figure 26: 58.5 mm OD Resultant Displacement (Loading Condition I)

Circular Shank: 63.5 mm Outer Diameter

The displacement values decrease as the rib length increases; however, the difference between the 10 mm and the 20 mm shank is not substantial enough to make a significant difference. This can be seen through the displacement graph below, Figure 27.

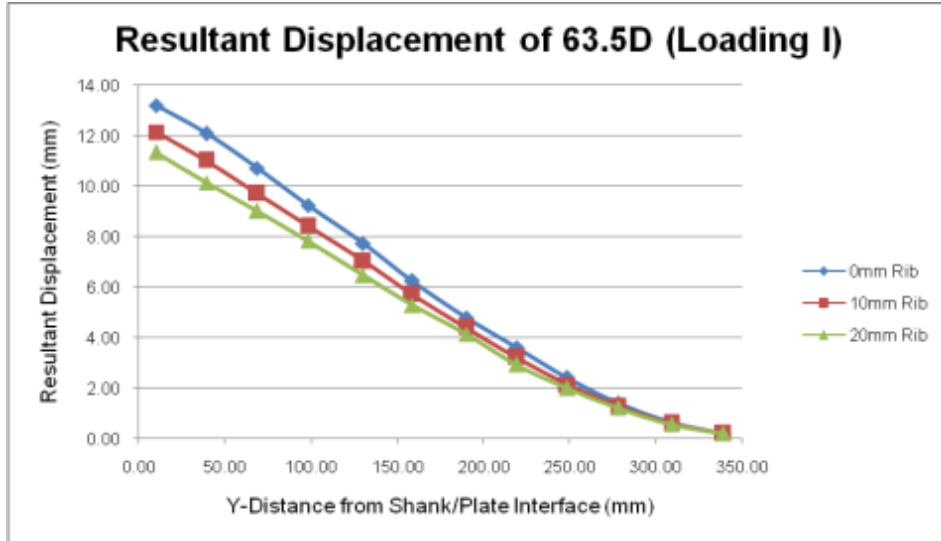
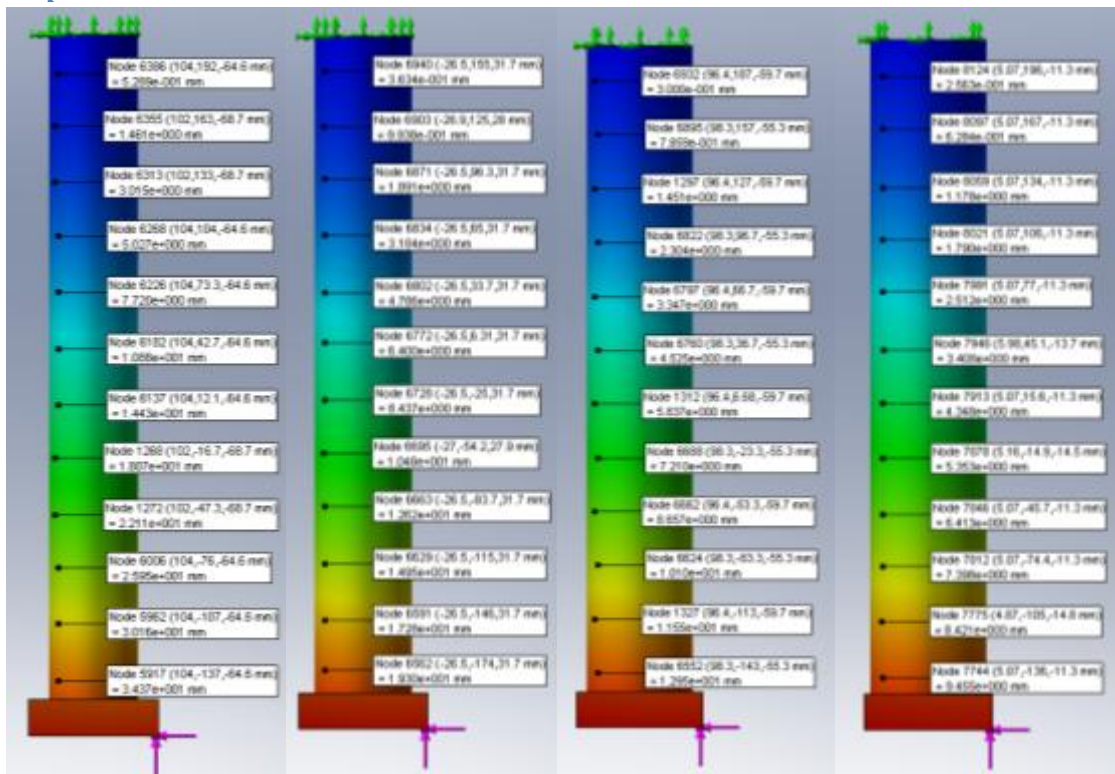


Figure 27: Resultant Displacement of 63.5 mm OD

Elliptical Shanks



48.5 mm width

53.5 mm width

58.5 mm width

63.5 mm width

Figure 28: Displacement Plots for Elliptical Shanks (Loading Condition I)

As shown in the displacement plots above,

Figure 28, the displacement is greatest at the point where the shank and the metal plate meet. Below, Figure 29, displays this data in a graphical format. The displacement values

decrease as the minor diameter of the elliptical shape increases. The elliptical shank with a minor diameter of 63.5 mm has displacement values which are less than 10 mm, which is more than three times lower than the displacement values for the 48.5 mm width shank.

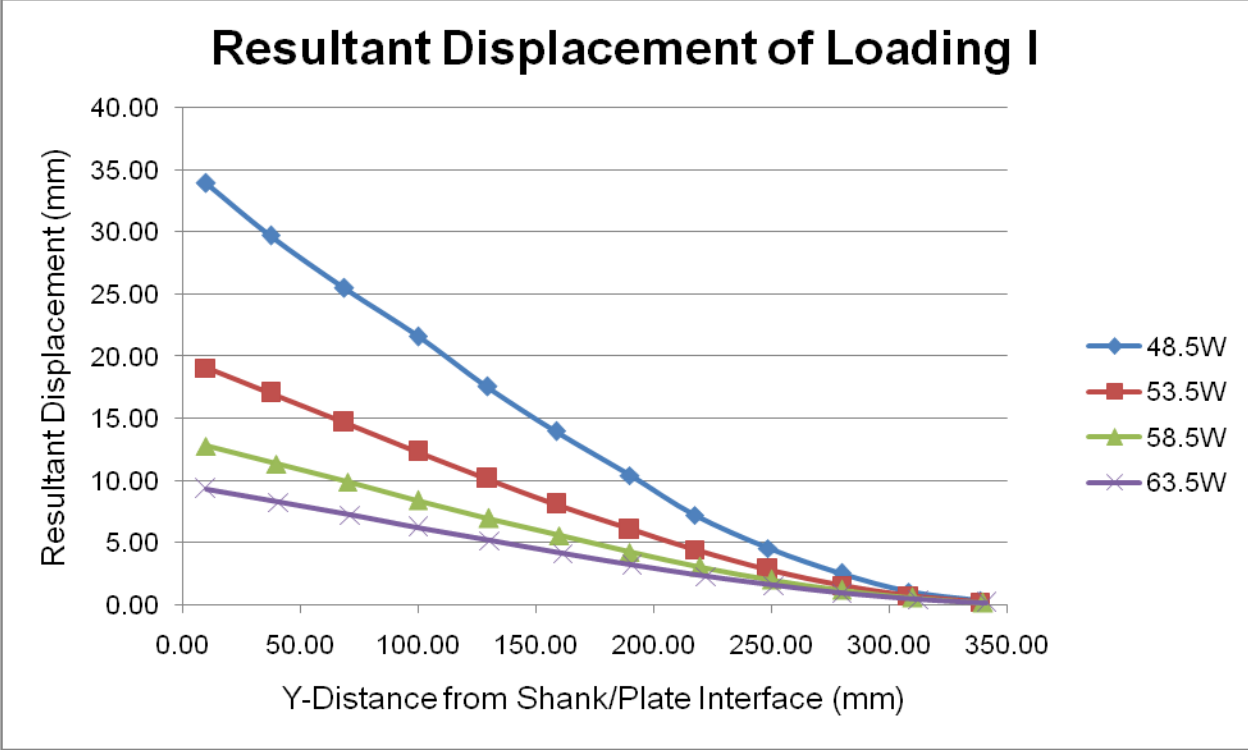


Figure 29: Resultant Displacement Graph for Elliptical Shanks (Loading Condition I)

Loading Condition II

Circular Shanks

Circular Shank: 48.5 mm Outer Diameter

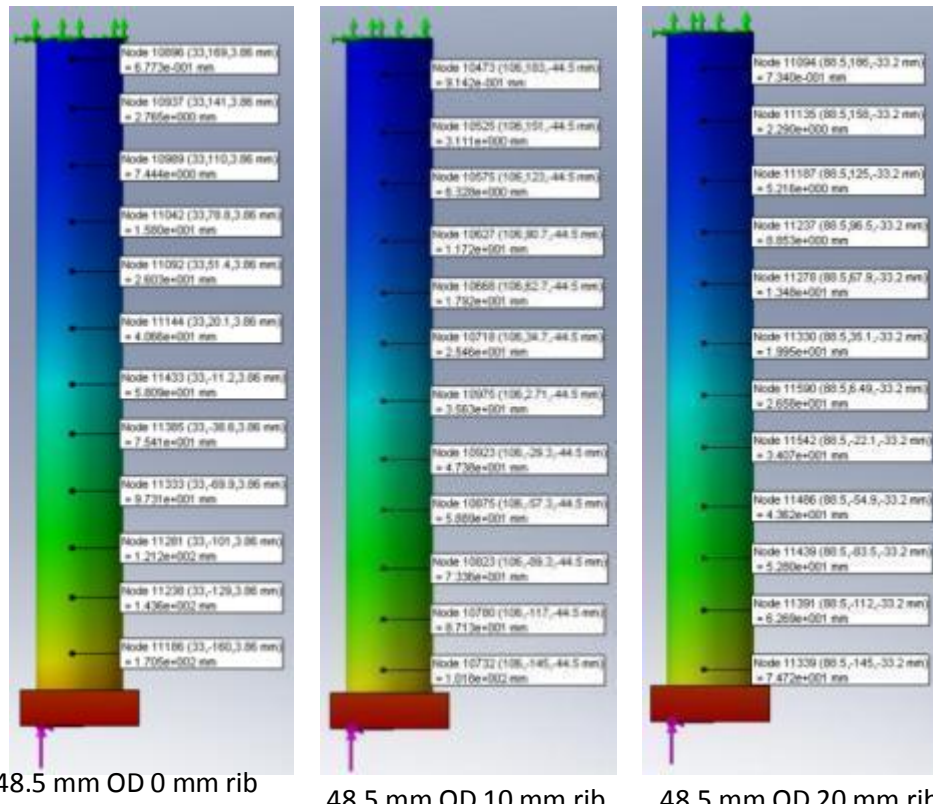


Figure 30: 48.5 mm OD Displacement Contour Plots (Loading Condition II)

In the above contour plots, Figure 30, the displacements of the 48.5 mm OD shank have been presented. In these plots, the blue portion represents the minimum displacement values and this area takes up nearly half of the shank. Again, these contour plots are fairly similar for each model and have been moved to Appendix H.

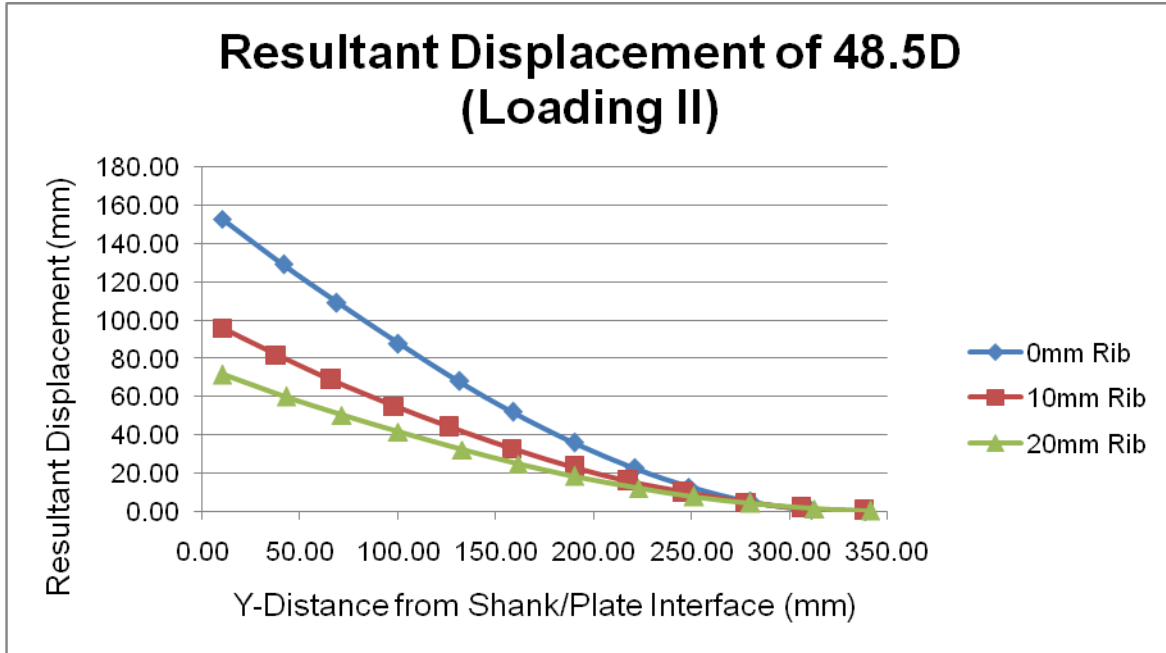


Figure 31: 48.5 mm OD Resultant Displacement (Loading Condition II)

Circular Shank: 53.5 mm Outer Diameter

The displacement for models with 53.5 mm OD has been included through contour plots,

Figure 57, and graphically as Figure 32. As depicted in the graph below, the displacement is considerably large; the resultant value representing up to nearly double the diameter. The addition of the rib in this case decreases the displacement values by 80% when comparing it to the model with no rib. This demonstrates that the rib length can make a substantial difference in decreasing the resultant displacement of the shank.

It is also important to notice the slope differences between the lines on this graph. For the 0 mm rib shank, the displacement is largest at the ankle, but lowers as the points continue up the height of the shank. The slope of this line is a more drastically negative line than the line of the 20 mm rib length model, which fairly remains much more horizontal as it approaches 0

mm of displacement at the fixed end.

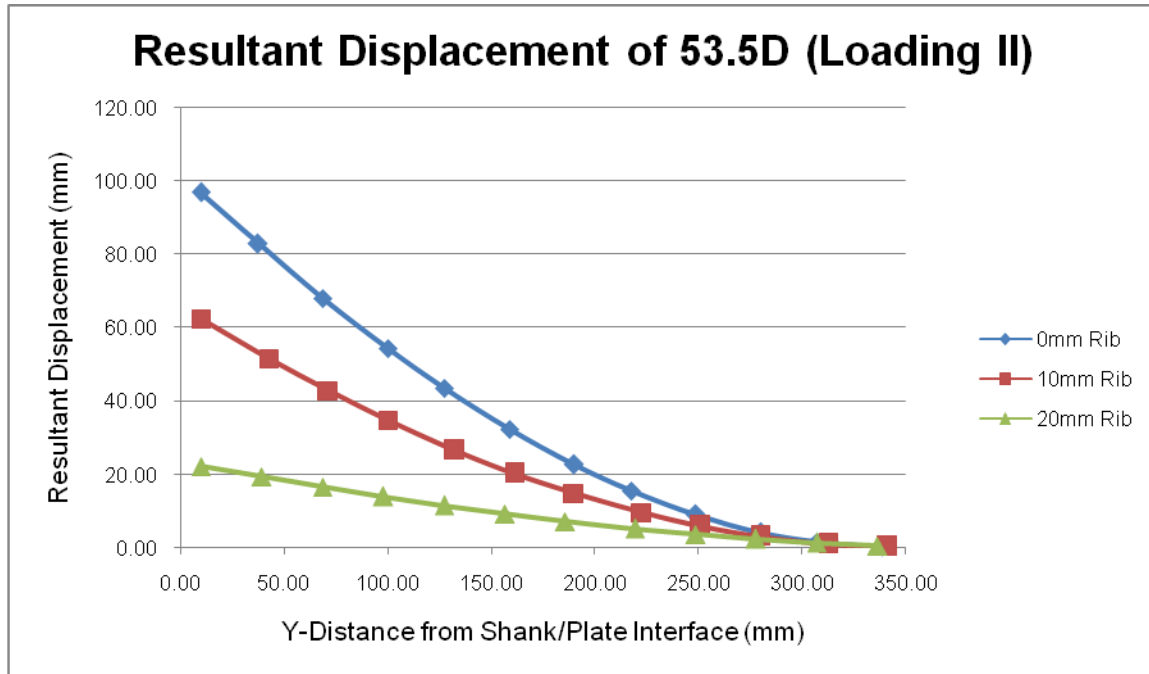


Figure 32: Resultant Displacement (Loading Condition II, 53.5 mm OD)

Circular Shank: 58.5 mm Outer Diameter

In the contour plots above, the displacement for the 58.5 mm OD shank, under loading condition II has been included as Figure 58. The data has been furthered represented through the use of the graph below, Figure 33. Similar to the 53.5 mm OD shank, the 20 mm rib decreases the displacement by 75% when compared to the 0 mm rib shank. This is a considerable amount of displacement which is being decreased by the presence of the rib.

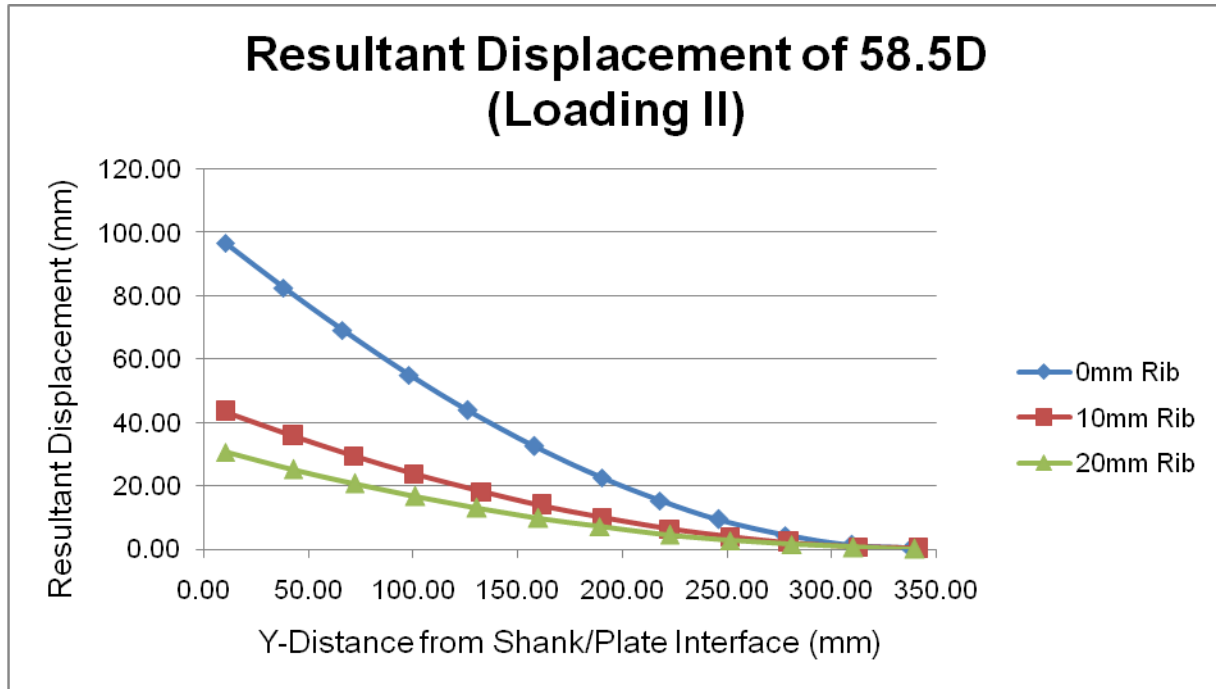


Figure 33: 58.5 mm OD Resultant Displacement Graph

Circular Shank: 63.5 mm Outer Diameter

The above displacement contour plots, Figure 59, were generated through COSMOSWorks to detail the displacement caused by Loading Condition II. This data was further investigated through the graph included below, Figure 34. As shown below, the displacement decreases as the rib length increases. The displacement also decreases as the point gets further away from the load application point at $u=-20$ mm. The majority of the displacement is taking place around the ankle portion of the shank.

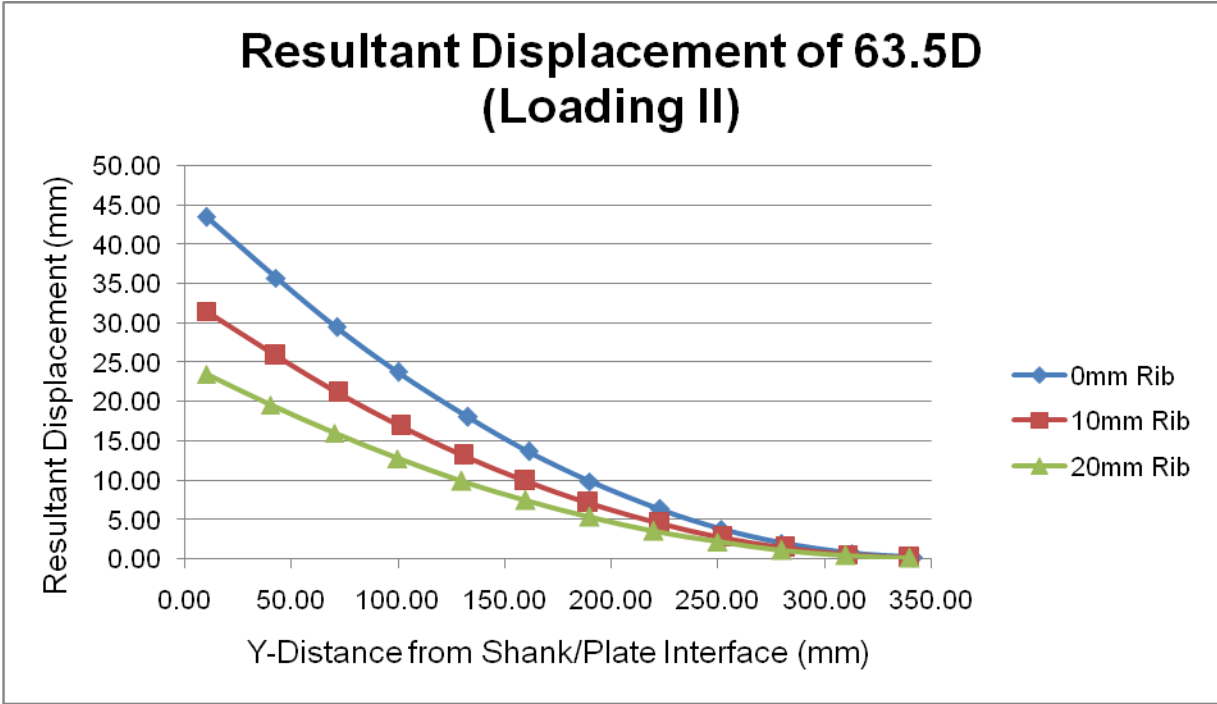


Figure 34: 63.5 mm OD Resultant Displacement (Loading Condition II)

Elliptical Shanks

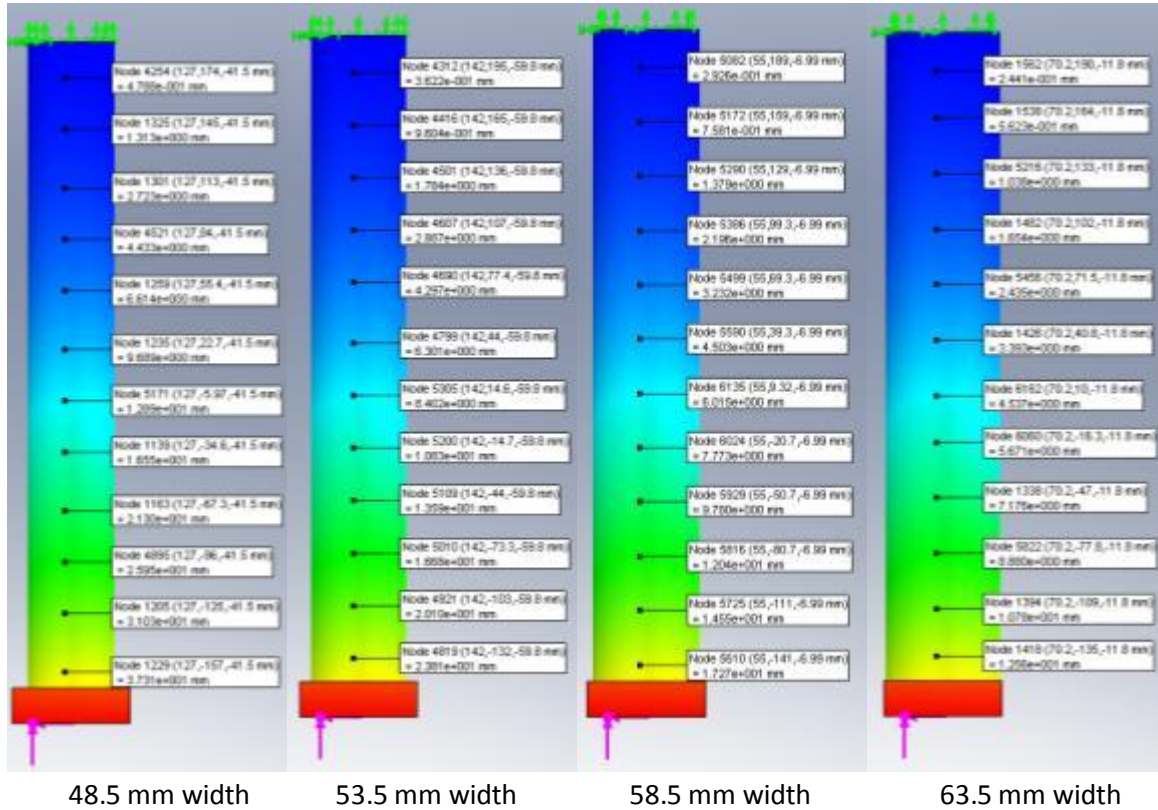


Figure 35: Displacement Plots for Elliptical Shanks (Loading Condition II)

For Loading Condition II, the elliptical shank has less red areas of displacement values, which signify the maximum stresses as shown in Figure 35. The displacement values in the graph below are fairly consistent with the values found for Loading Condition I demonstrating that the elliptical shank reacts to the loading conditions consistently. Again, the displacements decrease as the width of the shank increases.

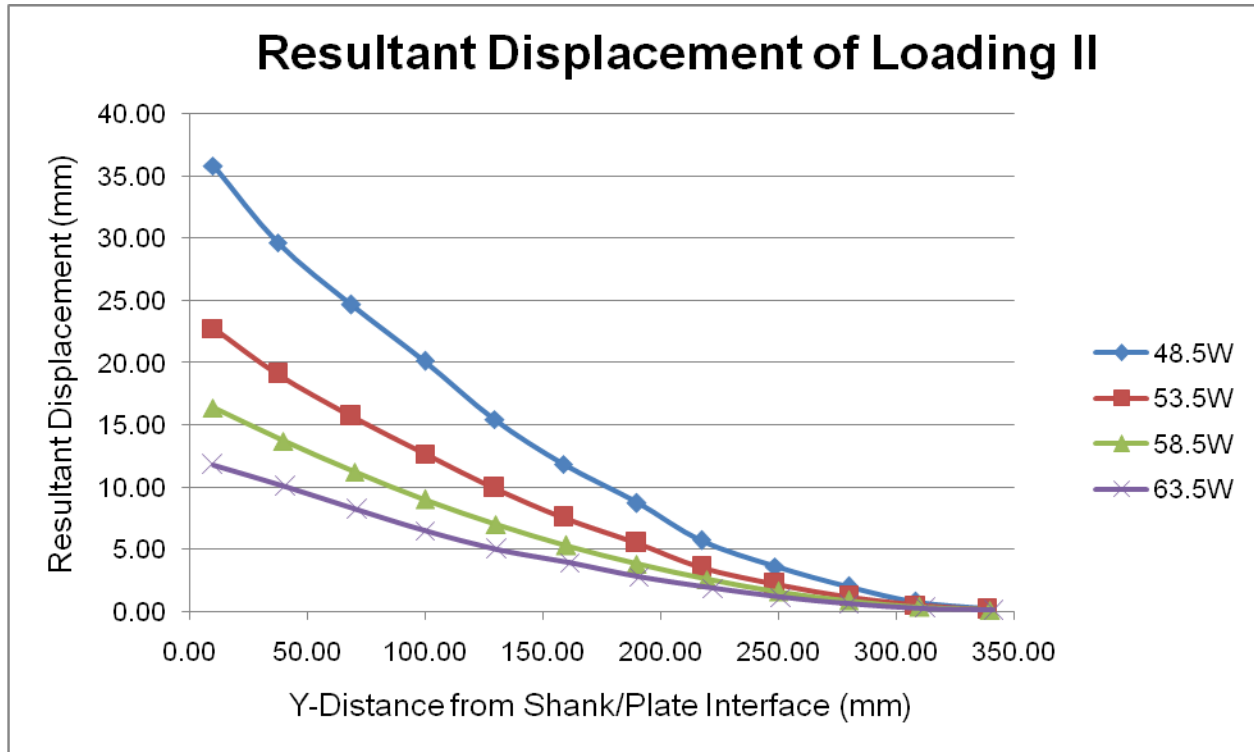


Figure 36: Resultant Displacement for Elliptical Shanks (Loading Condition II)

Comparisons

To gain an understanding of the effect of the parameters on the performance of the monolimb, several comparison graphs have been generated to provide a visual base from which to draw conclusions. Each graph has a dashed line marking the yield strength of the thermoplastic material to be used for comparison of the von Mises stresses.

Von Mises Stresses

The first mode for comparison of the von Mises stress is the difference between the models' reaction to the loading conditions. The first loading condition, heel strike, had much lower von Mises stress values than the second loading condition; toe off, for all models. This was primarily due to the off-set load location differences. In the first loading condition, the offset load was 36 mm from the center of the shank in the -f direction; however, the second loading condition had an offset load of 122.75 mm in the f direction. These high stresses are most likely occurring because the load location is 122.25 mm offset in the f direction from the

origin of the model. With such a large offset, the bending stresses increase substantially, causing higher overall stresses throughout the shank under Loading Condition II.

As shown in the table below, Table 18, the results from Loading Condition I in the 0 mm rib length column are generally about half of the value found for Loading Condition II. As the rib length increases, the stress values between the two different loading conditions are closer in value. Through this comparison, it can be concluded that Loading Condition II has much higher stress levels overall due to the increased bending loads.

Table 18: von Mises Stresses at probed point - Comparison by Loading Condition

Shank Diameter (mm)	Loading Condition	0 mm rib (N/m ²)	10 mm rib (N/m ²)	20 mm rib (N/m ²)
48.5	I	6.13E+07	4.68E+07	4.22E+07
	II	1.07E+08	6.96E+07	4.89E+07
53.5	I	3.67E+07	3.20E+07	2.89E+07
	II	6.84E+07	4.87E+07	3.59E+07
58.5	I	3.22E+07	2.21E+07	2.06E+07
	II	6.85E+07	3.61E+07	2.83E+07
63.5	I	1.96E+07	1.84E+07	1.76E+07
	II	3.46E+07	2.80E+07	2.33E+07

In the below figure, the stresses are being compared between the various rib lengths and cross sectional diameters.

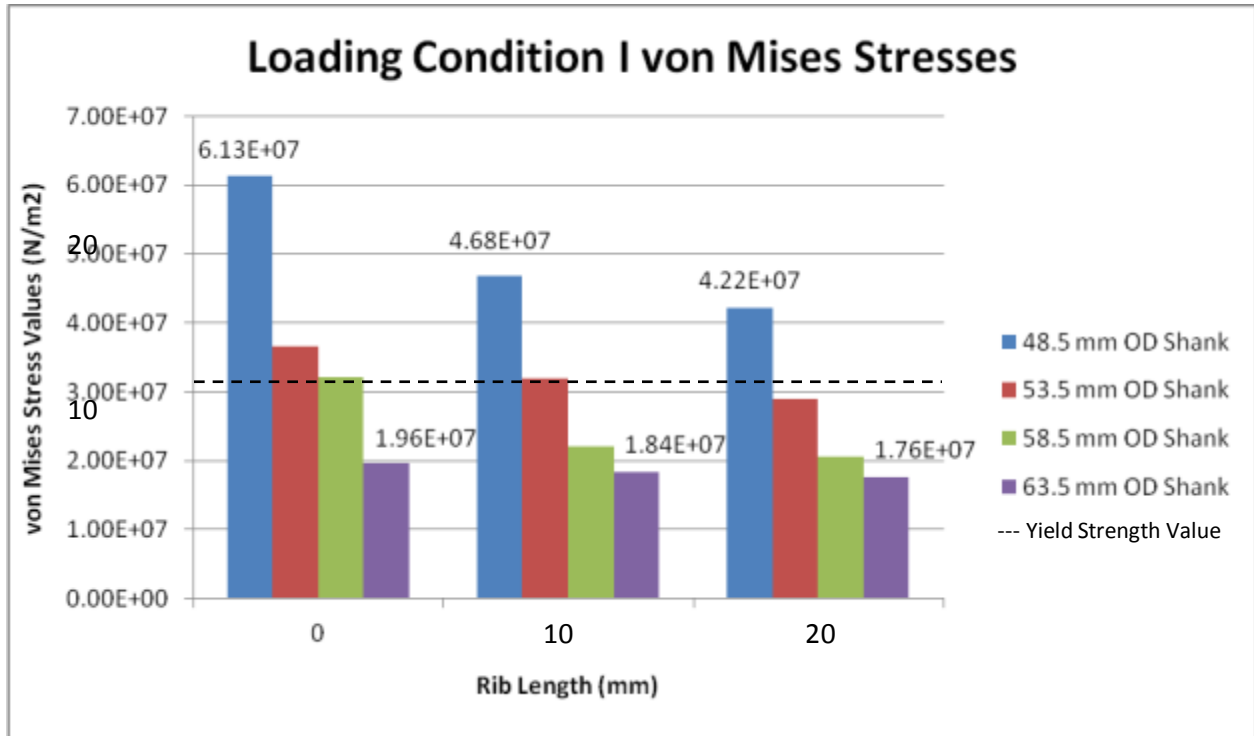


Figure 37: von Mises stresses at probed point- Rib Length Comparison (Loading Condition I)

A similar pattern is seen when investigating the stress value distribution for Loading Condition II and has been displayed as Figure 38.

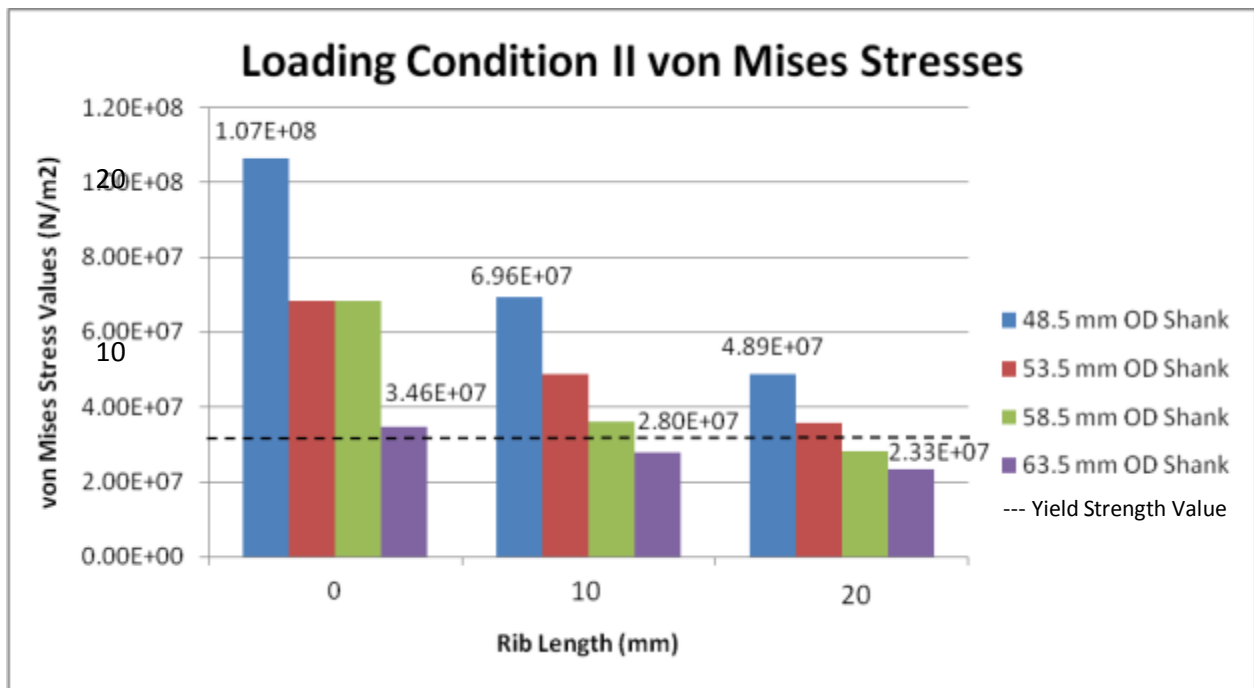


Figure 38: von Mises stresses at probed point- Rib Length Comparison (Loading Condition II)

In this graph, the 53.5 mm and 58.5 mm shanks with a 0 mm rib length are almost identical; there appears to be an anomaly in the data, as it does not follow the expected trend of a decrease in stresses as the diameter increases. This value should be re-evaluated; however, time does not permit further investigation of this suspicion. The stress value for the 48.5 mm shank is 250% higher than the Yield Strength for the Polypropylene Copolymer, which is an unacceptable stress value. The trend remains similar to Loading Condition I in the manner that the stress values decrease as the diameter increases and also as the rib length increases.

This comparison did provide insight regarding the positive effect of the rib on the maximum stress values of the shank models. The addition of the rib to the monolimb design contributes to the monolimb design by decreasing the stress levels throughout the model.

A decrease in von Mises Stress values is an important aspect of the design to consider; however, there are other effects of a decrease in these values. As the stresses decrease, the displacement values also decrease which causes the shank to become more rigid. A more rigid design is not optimal because flexibility within the shank mimics natural ankle movement, which is a desirable quality in the overall shank design. Also, an increase in diameter or rib length requires more material which contributes to an increase in weight for the monolimb. An increase in weight would be a negative attribute to the patient as the monolimb would become heavier and harder to walk with. Although it is important that the von Mises stresses fall below the Yield Strength line included on the graphs above, the amount that the stresses lie below this value is not as important. Finding a light, flexible monolimb with von Mises stresses that are below the Yield Strength is the underlying goal of this project.

Elliptical Shanks

As shown in the figure below, Figure 39, the von Mises stresses decrease as the minor diameter of the hollow elliptical shank increases. For loading condition I, the von Mises stresses found at the same location on each model are below the Yield Strength, which demonstrates the models were all successfully loaded and withstood the applied loads for Loading Condition I. For Loading Condition II, the stress values are almost three times larger than the value found for Loading Condition I in the model with a 48.5 mm minor diameter

elliptical shank; however, on the other three models, the stress values are roughly equivalent to each other. This observation differs from that of the circular shanks where the stress values for Loading Condition II are often almost double the values found for Loading Condition I.

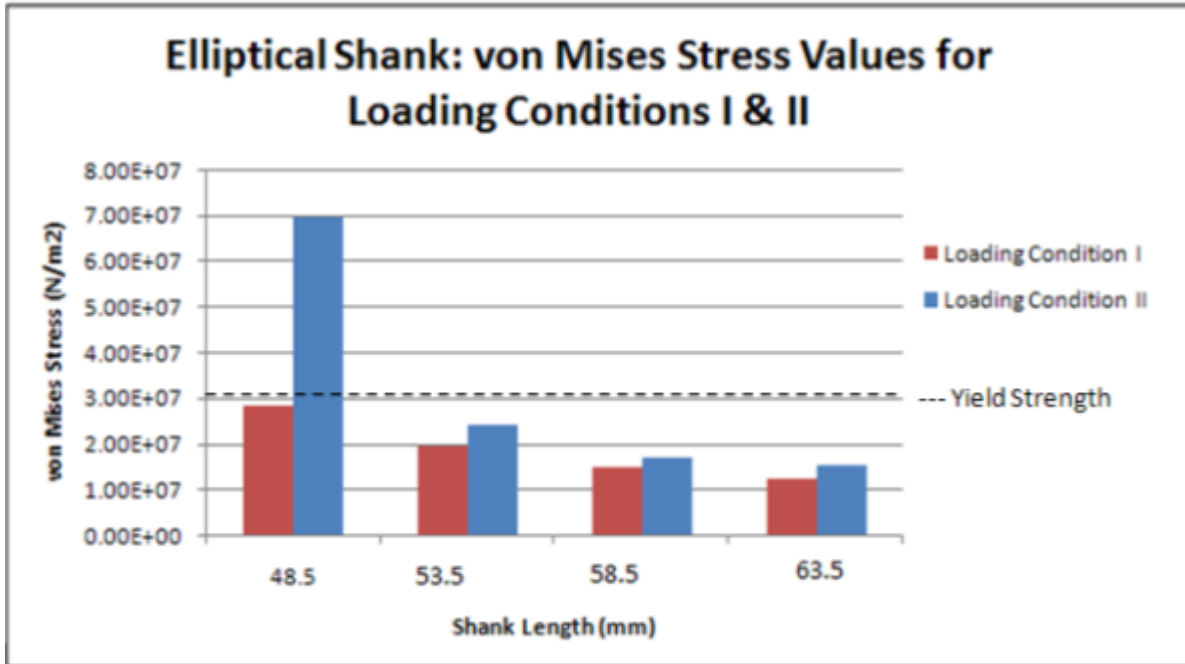


Figure 39: von Mises Stress Values for Elliptical Shanks

Elliptical Shank and Circular Shank Comparison

In the graph below, the circular shanks and elliptical shanks of the same diameter or elliptical minor diameter have been included for comparison between the two shapes. The trend below demonstrates that for each diameter, the shank with a 0 mm rib length has the highest von Mises stresses and the elliptical shank has the lowest stress values. The circular shank with a 10 mm rib has lower stress values than the 0 mm rib, but still higher than the 20 mm rib length and the elliptical shank. Through analysis of this graph, it can be seen that the elliptical shank decreases the stress values present in each shank width/diameter.

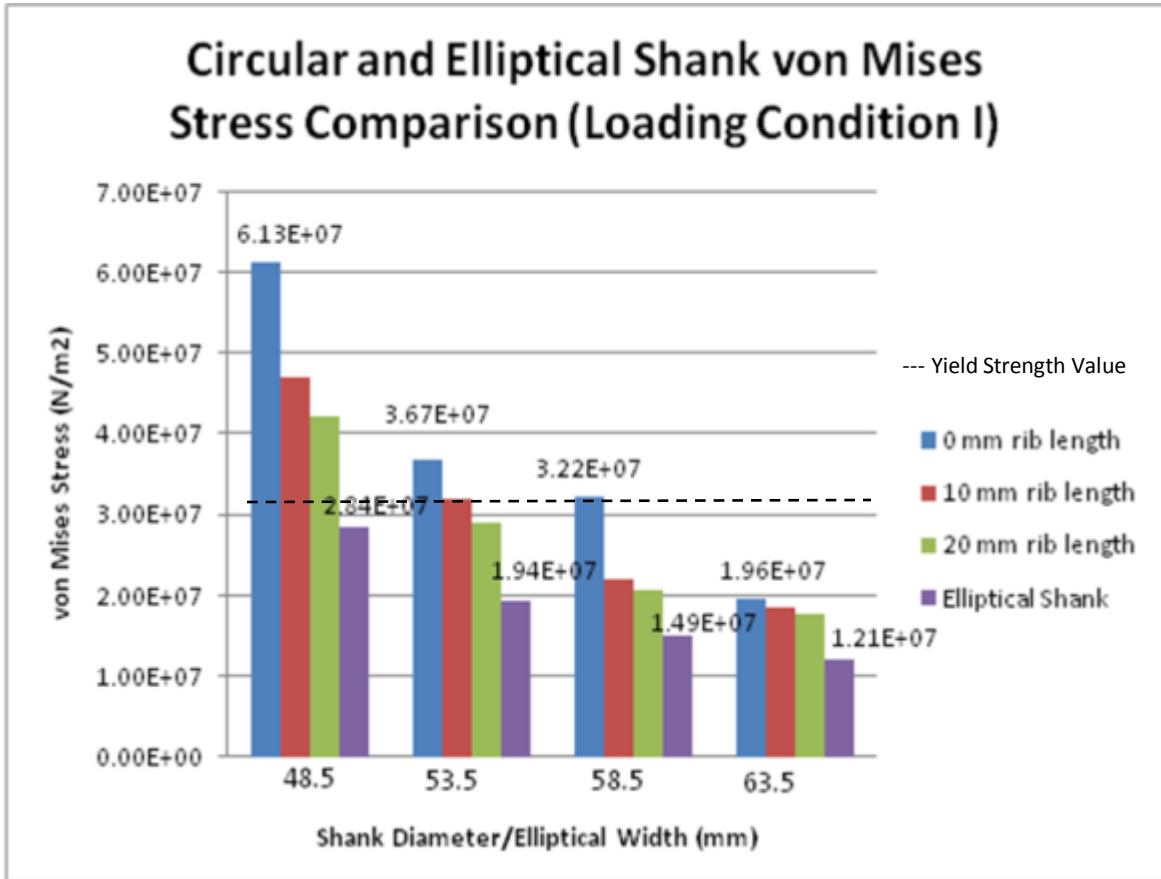


Figure 40: Circular and Elliptical Shank von Mises Stress Comparison (Loading Condition I)

Performing a similar comparison on Loading Condition II, a very similar trend is seen in Figure 41 below. The stresses in the circular shank with a 0 mm rib length are substantially higher than the other models. In all, but the 48.5 mm diameter/elliptical minor diameter, the elliptical shank significantly decreases the von Mises stress values. This appears to be irregularity with this data. The elliptical shank should follow the same trend as seen in the rest of the models by measuring the lowest von Mises stresses of shank models of the same diameter. The elliptical shank decreases the stresses more than the 20 mm rib length does in the circular shank, which is an important quality in comparing these models.

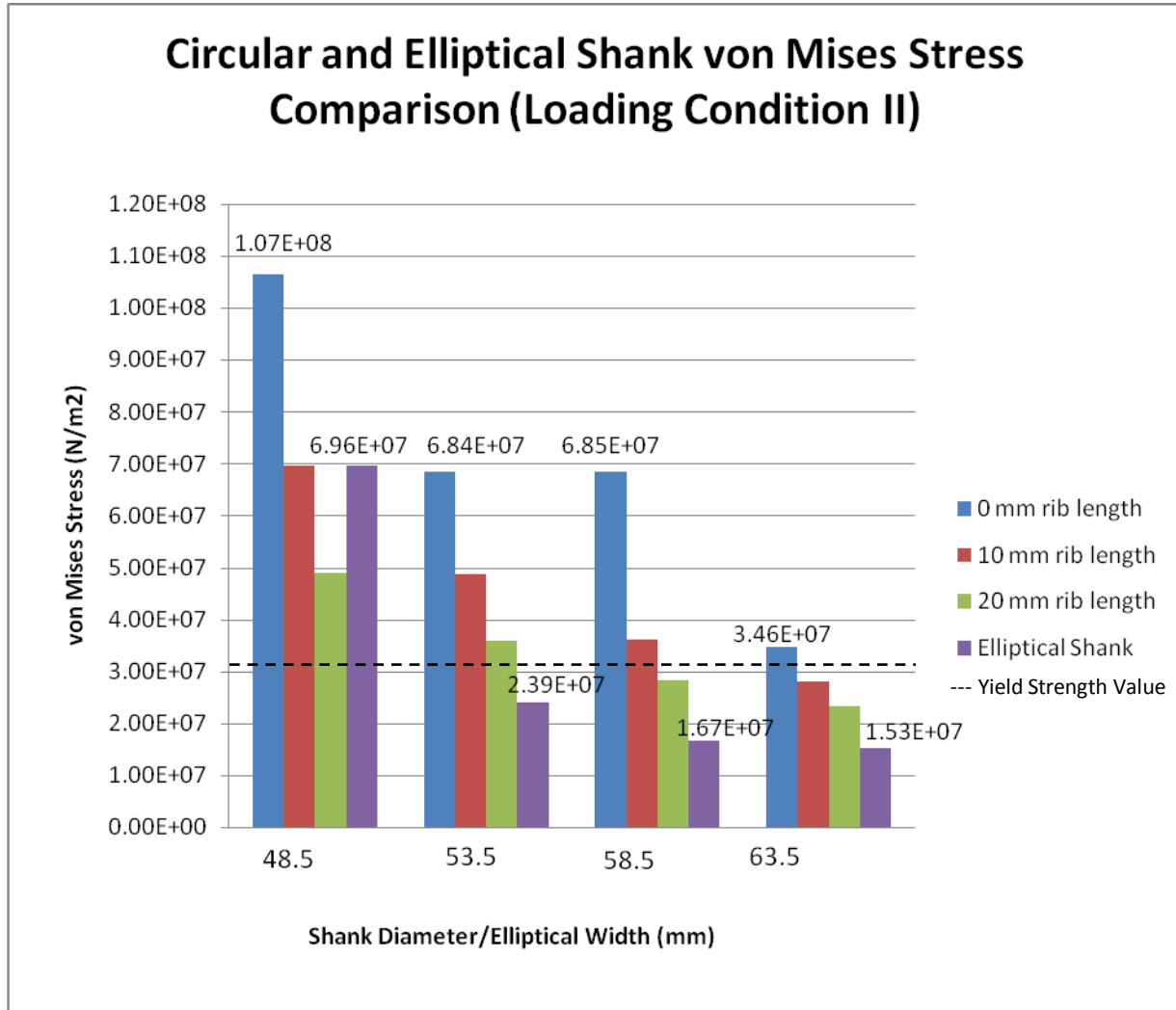


Figure 41: Circular and Elliptical Shank von Mises Stress Comparison (Loading Condition II)

Displacement

Next, the displacement was analyzed through its components out of plane and in-plane. These data were obtained through COSMOSWorks and transformed per the methodology described above. The In-Plane displacement is caused by the bending loads occurring through the model and has been shown in several graphs below.

First, the in-plane displacement trends for Loading Condition I have been included as Figure 42. The data provided in this graph only represent the maximum displacement of the points probed along the shank, which lies 10 mm above the interface between the metal plate and the shank. Charts which detail the displacement throughout the entire shank have been included in Appendix G. The in-plane displacement has been found in order to further

understand the affect of the bending loads on the shank. Displacements due to the bending loads were the primary component of the overall displacement throughout the models, which is why the in-plane displacement values are higher than the out-of-plane displacement values, which will be discussed in the next few pages.

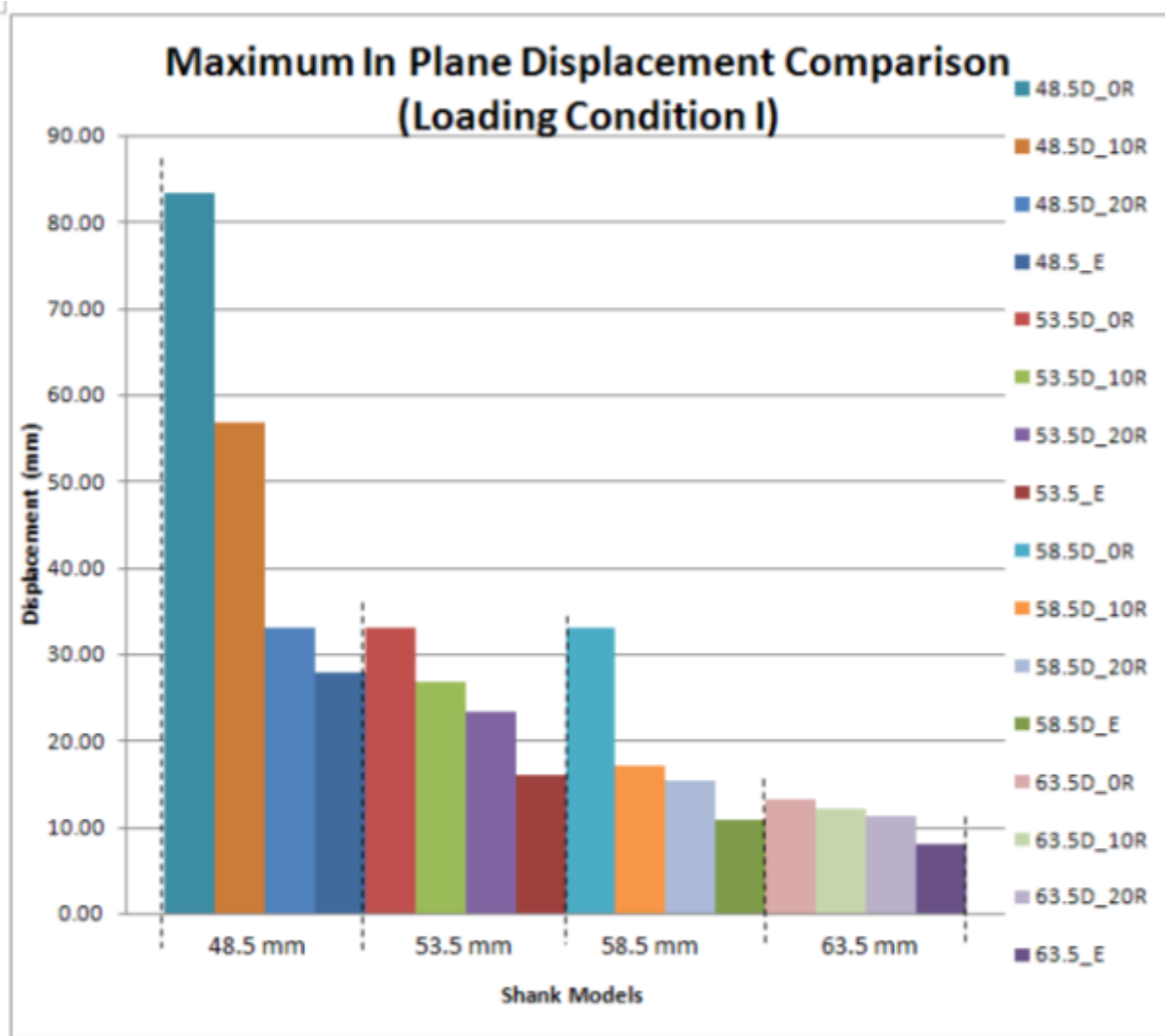


Figure 42: In-Plane Displacement Trends for Loading Condition I

The model with the most displacement was the 48.5 mm shank with a 0 mm rib. This demonstrates that the smallest diameter, paired with the smallest sized rib do not contribute to realistic displacement values. For each diameter, the models with a 0 mm rib length have the highest displacement values when compared to the models with 10 mm and 20 mm shanks.

The lowest displacement values were from the 63.5 mm OD shank with a 20 mm rib length and the 10 mm rib length. This demonstrates that an increase in diameter increases the overall rigidity of the monolimb. It can also be seen that as the rib length increases, the displacement values decrease because the rib is further adding to the rigidity of the design. In addition, as the diameter increases, the displacement values decrease, which further substantiate the conclusion that a larger diameter would contribute to lower stresses as well as displacement caused by bending loads.

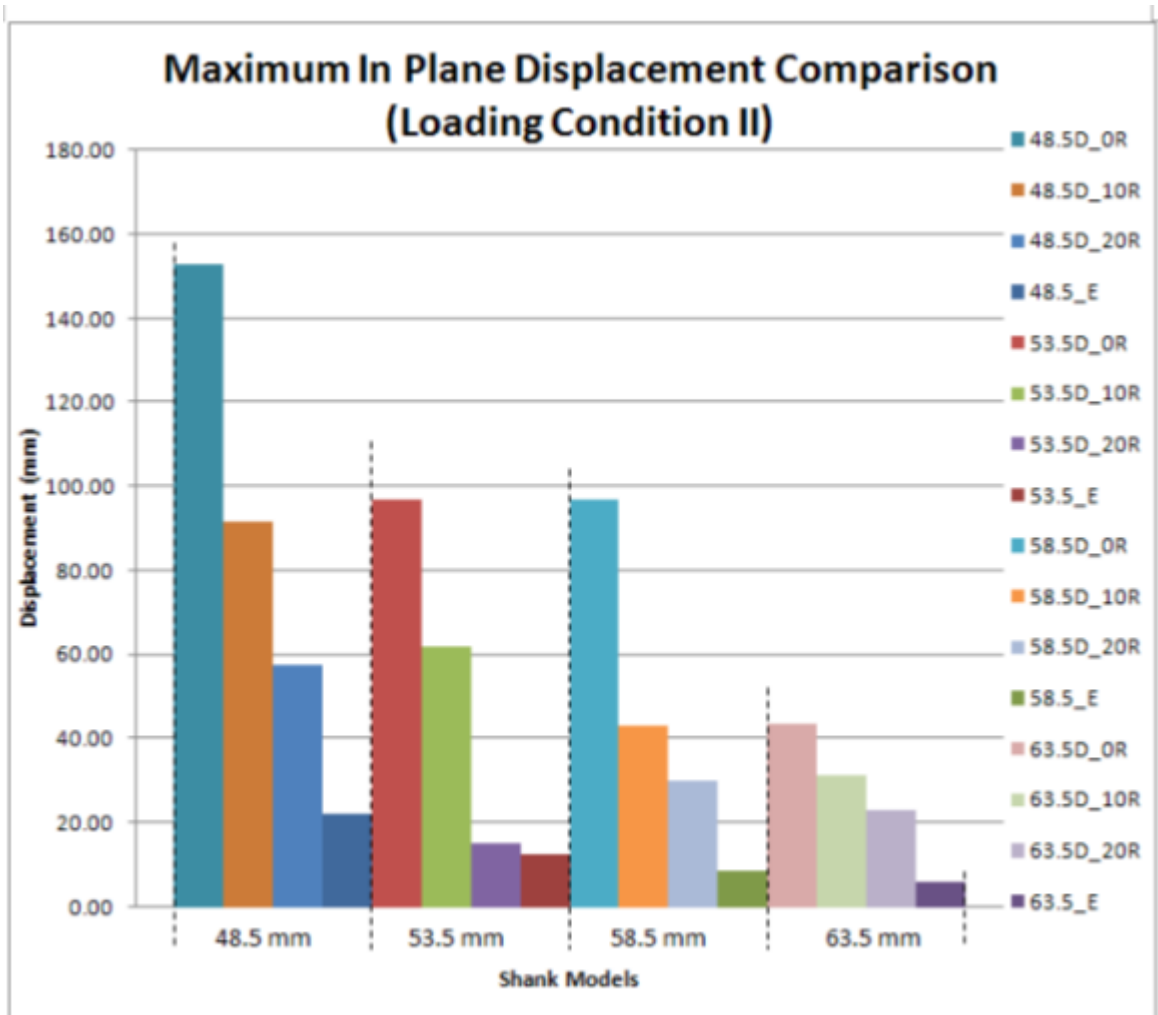


Figure 43: In-Plane Displacement Trends for Loading Condition II

The In Plane Displacement proves to be very similar between Loading I and Loading II. The trend for displacement follows that the model with a 0 mm rib has the highest displacement values while the elliptical model with the same minor diameter has the lowest

values; this proves true for loading conditions I and II. It would be assumed that the monolimbs would not see such large displacement values in the field, as they would never be exposed to such extreme conditions; however, it should be noted that the loading conditions dictated by the ISO Test Standard 10328 and the maximized height parameters allow for substantial displacement in the shank region of the monolimb.

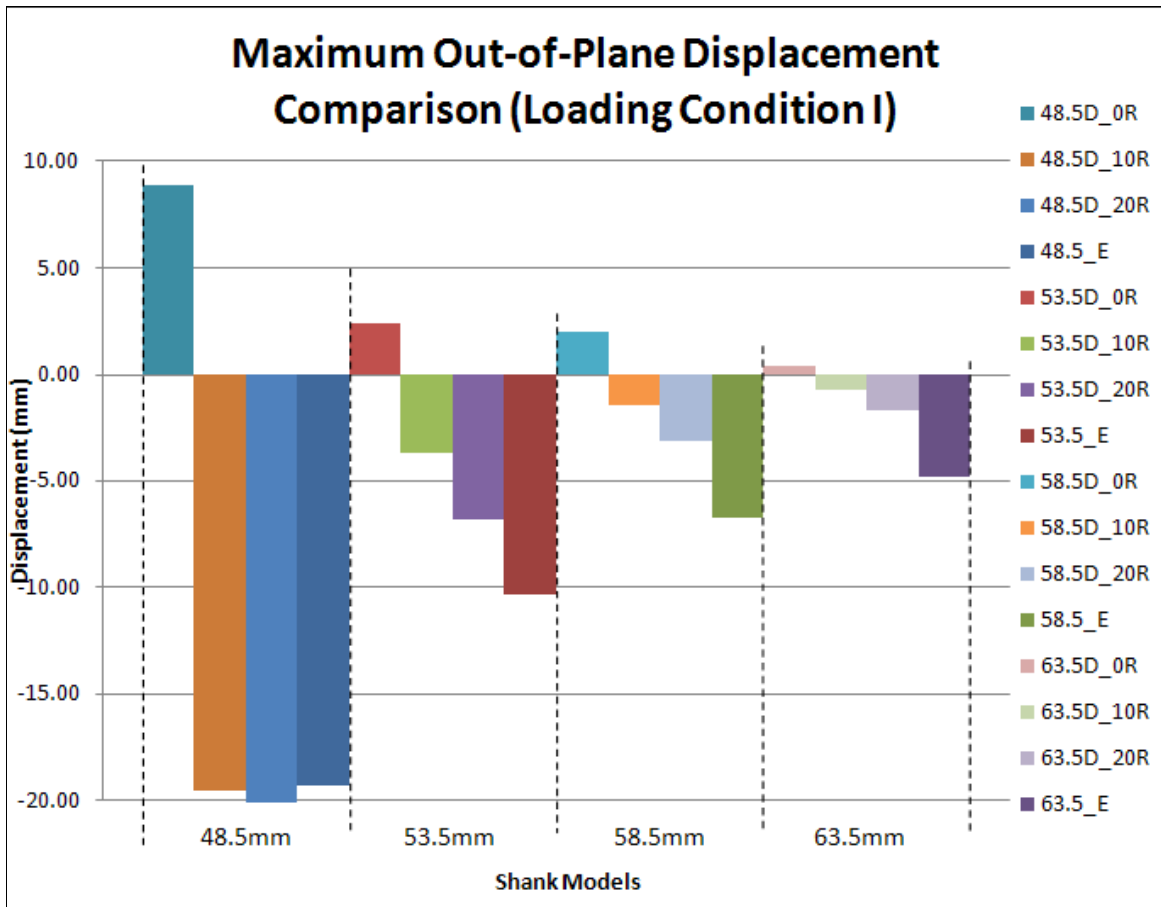


Figure 44: Maximum Out-of-Plane Displacement Comparison (Loading Condition I)

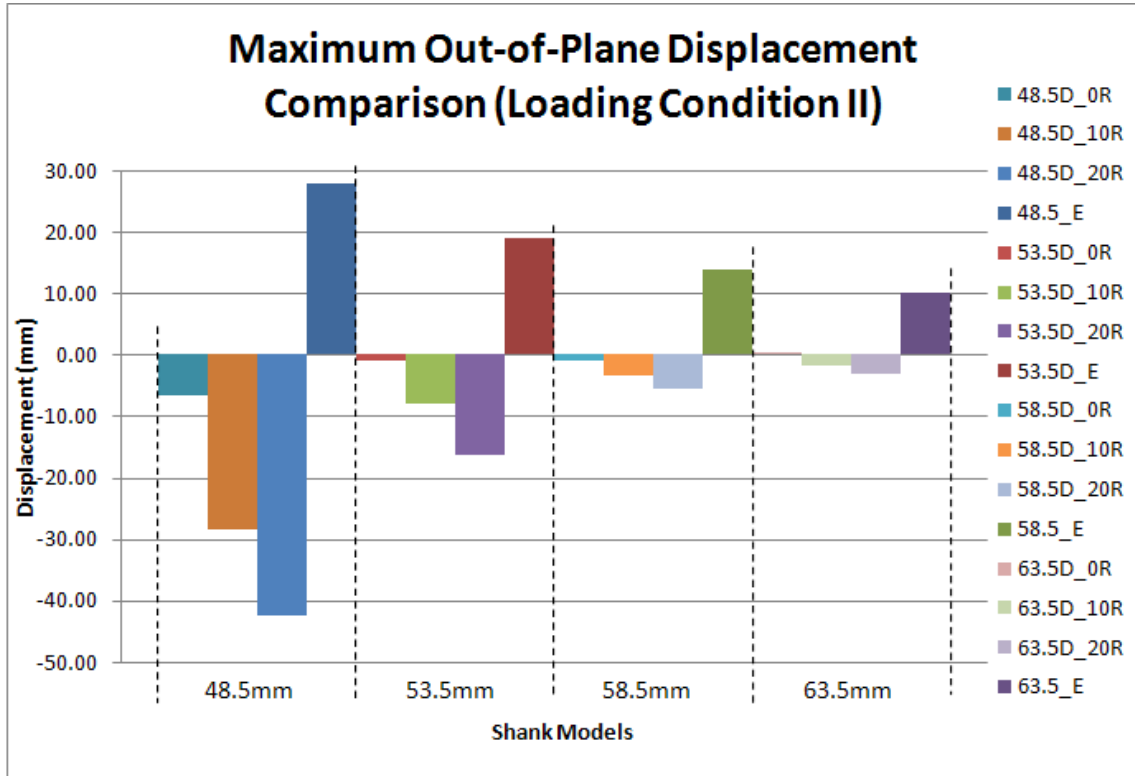


Figure 45: Maximum Out-of-Plane Displacement (Loading Condition II)

The Out-of-Plane displacement demonstrates the affect of the transverse loads on the shank models. These values are much lower than those caused by the bending loads in the previous few graphs. It is important to notice that the displacement is positive for the models that have a 0 mm rib and negative for those models that have a 10 mm or 20 mm rib length. The positive displacement means that the displacement is towards the anterior part of the shank while the negative displacement is directed towards the posterior part of the shank.

In both loading conditions, the 48.5 mm shank has the highest displacement values and the 63.5 mm shank has the lowest displacement values. The values increase as the diameter decreases and also as the rib length decreases. These trends again substantiate the claim that the rib length contributes positively to the overall design of the monolimb. An increase in diameter would cause a decrease in displacement, but still allow displacement throughout the shank, which would still allow for flexibility for the patient.

The most important aspect to displacement is that it should be present in the models because it contributes to the overall flexibility of the shank which can mimic natural ankle movement. Decreasing the displacements is a positive influence, but it should be taken into

consideration that displacement should still be present in the models to provide this flexibility. As the diameter and rib length increase, the displacements decrease; however, this makes the design more rigid and less like the natural movement of walking.

Material Analysis

Through an analysis of the displacement and the von Mises stresses present with the sixteen models tested within COSMOSWorks, conclusions have been made regarding an increase in diameter and increase in rib length and their positive effect on the shank models. In an ideal world, this change to the fabrication could be easily made; however, other factors are important to consider, such as the amount of material used in the fabrication. The material used by CIR is 61 cm by 122 cm and it is cut into 3 even trapezoidal shapes for use with three monolimbs. This is done because CIR is focused on providing low cost prosthetics for third world countries and the material needs to be used in such a way as to minimize material waste to decrease costs. Each monolimb requires a 51 cm by 20 cm side trapezoidal piece for fabrication. In order to determine which models that were tested could be made with these size parameters, the following chart has been made. The outstretched length was calculated by finding the perimeter of the circle and adding twice the rib length. This accounted for the material on each side of the monolimb being pressed together to form the rib on the posterior end of the shank. The lengths which lie beyond the 200 mm limit have been highlighted with red text.

Table 19: Material Length Requirements

Diameter (mm)	Rib Length (mm)	Outstretched Length (mm)
43.5	0	136.6592804
43.5	10	156.6592804
43.5	20	176.6592804
48.5	0	152.3672437
48.5	10	172.3672437
48.5	20	192.3672437
53.5	0	168.075207
53.5	10	188.075207
53.5	20	208.075207
58.5	0	183.7831702
58.5	10	203.7831702
58.5	20	223.7831702
63.5	0	199.4911335
63.5	10	219.4911335
63.5	20	239.4911335

This table shows that the 63.5 mm shanks with 10 mm and 20 mm rib lengths lie outside of the boundaries of the available material; however, if CIR could add 1 cm of material for each monolimb and purchase sheets of material that are 124 cm wide and 51 cm long, CIR could apply the largest set of parameters, which is a 63.5 mm OD shank with a 20 mm rib.

Next, the elliptical shank perimeters were found in order to determine the amount of material necessary to fabricate prostheses with the same widths and lengths as the models. This has been included as Table 20. With a minor diameter greater than 48.5 mm, the elliptical shank perimeters are all above the maximum 200 mm, which demonstrates that the elliptical cross section would require more material than their circular counterparts.

Table 20: Elliptical Shank Perimeters

Minor Diameter (mm)	Perimeter (mm)
48.5	185.66
53.5	207.03
58.5	239.72
63.5	260.19

Another important factor that needs to be taken into account is the cost of producing a larger monolimb. Although thermoplastic sheets are sold in many different dimensions, purchasing thermoplastic sheets that are not of standard sizes can call for a sudden increase in

price. As CIR is a non-profit organization that produces low-cost prosthetics, these prices are very important. Therefore, it would not be worthwhile to increase the dimensions of the sheet if it would cause a decrease in the number of devices produced by CIR. This makes the maximum length for a shank 200 mm as it complies with the material sheet parameters currently being used in their outreach programs.

In order to determine the feasibility of the manufacturing and use of the circular and elliptical models, the mass values were found for each model. Note that these values represent only the shank portion of the monolimb, and do not include the metal insert and the socket. “Although previous research was not able to conclude an optimal weight of a prosthesis...some studies indicated that lightweight provided by a monolimb is welcomed by amputees” (Lee 2006). Through this background research, it was determined that there is not a specific limit for weight; however, the lighter the monolimb, the more comfortable the patient’s experience.

Table 21: Circular Shank Weight

Mass (kg)	0mm Rib	10mm Rib	20mm Rib
48.5D	0.204	0.234	0.264
53.5D	0.228	0.258	0.288
58.5D	0.251	0.281	0.311
63.5D	0.284	0.314	0.344

Table 21: Circular Shank Weight displays the mass of each circular monolimb. These values were calculated by multiplying the cross sectional area by the shank length to find the volume and then multiplying this value by the density of the polypropylene copolymer. The current monolimb used by CIR is 53.5 mm with a 10 – 20 mm rib length. The average value for this monolimb is about 0.27 kg, which is roughly .6 pounds. This was used as a measure for comparison between the shanks to ensure that the mass value is not much higher than the current weight of the monolimb. The highest mass found was the 63.5 OD with 20mm rib which was 0.344 kg. This value is roughly 25% higher than the current weight of the monolimbs distributed by CIR. This weight gain still provides CIR with a shank which is three quarters of a pound.

Table 22: Elliptical Shank Weight

Minor Diameter	Mass (kg)
48.5 mm	0.264 kg
53.5 mm	0.296 kg
58.5 mm	0.327 kg
63.5 mm	0.357 kg

The table above, Table 22, displays the mass values for the four elliptical models. These values were solved for in the same fashion as the circular models. The volume was found for the elliptical shape and the density properties of the polypropylene copolymer were used to find the mass of the shank. The masses are still below 0.4 kilogram, which is equivalent to about 0.9 lb. The weights of the elliptical shanks are comparable to the weights of circular shanks of the same diameter with 20 mm ribs.

The information displayed throughout this report has shown that a rib length between 10mm and 20mm is very beneficial to CIR. This range contributes to decreases in displacement and overall stress distributions throughout the shank. An increased diameter has also shown to be beneficial in the fabrication of the monolimb. In order to continue to utilize the thermoplastic sheets that are currently purchased by CIR, a model with a 53.5mm OD and a rib length of 15mm could maximize material use.

Based on the analysis described above, the elliptical shanks have demonstrated the ability to substantially lower von Mises stress values with a more consistent distribution of stresses between Loading Conditions I and II; however, the masses associated with the elliptical are on the higher end of the weights when compared to the circular models. Although a decrease in stresses and displacement is important, the other factors contributing to the properties of the monolimb cannot be disregarded. The weight of the monolimb contributes to the overall comfort of the patient and was considered before making final recommendations. If the stresses are lower than the Yield Strength under the ISO Test Standard Loading Conditions, the model is deemed appropriate for use in the field.

Another aspect to the monolimb which should be addressed is the insertion of the aluminum bushing. This metal piece is used to attach the foot to the monolimb, making it a vital portion of the monolimb. Currently, the mandrel rests on top of the aluminum bushing during fabrication, which centers this piece within the shank. If an elliptical shank were to be adopted, the aluminum bushing size and shape would also need to change as the interface between the shank and the aluminum bushing needs to be a tight fit to ensure that the connection between the foot and the monolimb is as rigid as possible.

For fabrication of a monolimb of a differing diameter or elliptical shape, CIR would first need to acquire mandrels of different sizes. The thermoplastic sheets would still be wrapped around the mandrel during the fabrication process. One of the negative impacts of an increase in shank diameter is the necessity of larger mandrels. These would need to be distributed to the outreach program locations to ensure that the new design was being implemented.

The information displayed throughout this report has shown that a rib length between 10mm and 20mm is very beneficial to CIR. This range contributes to decreases in displacement and overall stress distributions throughout the shank. An increased diameter has also shown to be beneficial in the fabrication of the monolimb from their current design is necessary to comply with the ISO Test Standard 10328. The current design did not pass the von Mises failure criteria under the specified loading conditions.

The elliptical models show drastically lower von Mises values with a more consistent distribution of stresses throughout the different model dimensions for Loading Conditions I and II; however, the weight is higher for the 58.5 mm and 63.5 mm minor diameters than that of their circular shank models of the same diameters. Although a decrease in stresses and displacement is important, it can also lead to a more rigid design, which does not allow for flexibility throughout the shank. A drastic decrease in overall stresses is not necessarily required to produce a valuable monolimb as the shank was considered to successfully withstand the applied loading conditions if the stress values were below the Yield Strength.

Furthermore, the increase in weight between the elliptical shank and the circular shank models makes them a less attractive option for CIR. The increase in weight will not allow the necessary amount of flexibility throughout the shank and would also require an increase in the

material sheet size properties. The circular model currently used by CIR was not found to successfully withstand the ISO Test Standard 10328 loading conditions for a P5 test. Due to these results, it is highly recommended that CIR uses 58.5 mm circular shank with a 20 mm rib length or a 63.5 mm circular shank with either a 10 mm or 20 mm rib length. These three models were the only models within the parameter study that reported von Mises stresses that were lower than the Yield Strength.

Conclusions

Through an analysis of circular and elliptical models, several trends regarding the parameters of each of these and the resultant displacement and von Mises stresses have been demonstrated. The COSMOSWorks contour plots provided information regarding the von Mises stresses as well as the displacement values through each of the sixteen models that were tested.

The von Mises stresses were shown to decrease as the diameter increased. Also, the von Mises stresses decreased as the rib length increased, which demonstrated that the rib length is a positive addition to the overall design of the circular shank. The elliptical models that were tested measured the lowest von Mises stresses when compared to the stress values of circular shanks of the same diameter as the minor diameter of the elliptical shanks. The models were all compared to the Yield Strength of the material used to fabricate the monolimb in order to determine whether or not the models exceeded the stress limit under the ISO loading conditions.

The von Mises stresses of the majority of the models did not pass the von Mises failure criteria, which means that under the ISO Test Standard 10328 loading conditions, models of this height and with the varying parameters would not be deemed appropriate for use in the field. The 58.5 mm shank with a 20 mm rib length; 63.5 mm shank with a 10 mm and 20 mm rib length all had stresses below the Yield Strength of the polypropylene copolymer for both loading conditions. This demonstrates that these three models can be successfully used in the field under the ISO Test Standard criteria. These models have been recommended to CIR as possible changes to their current prosthetic design.

The displacement values were analyzed through several different avenues. First, the resultant displacement was found for each of the diameters to determine how the addition of the rib affects the displacement values. In order to determine the effect of the bending loads, the in-plane displacement was calculated and the maximum values for each model were compared graphically. Through this graphical analysis, it was determined that the displacement

decreases as the diameter increases. Although a decrease in displacement is important, it is important to ensure that some displacement is still present throughout the model as this contributes to the flexibility of the shank and its ability to simulate natural ankle movement. Similarly, the out-of-plane displacement was analyzed to determine the presence of torsion within the models. The out-of-plane displacements were much lower than the in-plane displacements, which confirmed that the bending loads had a much more substantial effect on the resultant displacement in the shanks.

Finally, the amount of material needed to fabricate the shanks was determined because CIR uses 61 X 122 cm sheets of material to cut a trapezoidal piece that is used to fabricate three monolimbs. This is done to minimize wasted material as well as keep the costs as low as possible. Through this analysis, several of the larger circular models would require a slight increase in material in order to account for the increase in diameter and/or rib length. The elliptical shanks were on the heavier end for each diameter. An increase in weight can negatively impact the performance of the monolimb for the patient because a heavier monolimb and requires more energy to walk with. It is important to decrease the von Mises stresses and displacement without increasing the weight. As the elliptical shanks have been reported to be roughly the same mass as the heaviest circular models, the elliptical shanks were deemed less appropriate for CIR's low cost prosthetic outreach programs despite their positive effect on von Mises stresses and displacement.

Recommendations

It is being recommended to CIR to continue to use the hollow cylindrical model with a rib design within their programs. The presence of the rib allows for a decrease in both von Mises stresses as well as displacement. An increased diameter would substantiate the monolimb, as the 58.5 mm shank with a 20 mm rib and the 63.5 mm shank with a 10 and 20 mm rib all pass the von Mises failure criteria under the ISO Test Standard 10328 specified loading conditions. The other models have not been validated to withstand the loads without surpassing the Yield Strength of the polypropylene copolymer. Therefore, it is being

recommended that at 58.5 mm shank with a 20 mm rib should be adopted as it requires a slight increase in amount of material, but it does not increase the weight enough to change the performance of the monolimb and this model successfully withstood the ISO Test Standard Loading Conditions.

The feasibility of a change in mandrel size should be investigated further to determine whether or not this change would be cost appropriate for CIR. Also the interface between the aluminum bushing and an elliptical shank should be further investigated as the elliptical shank substantially decreased the von Mises stresses and had displacement values which remained fairly consistent for both Loading Condition I and II.

Works Cited

- “A Plastics Explosion: Polyethylene, Polypropylene, and Others.” *An Introduction to the History of Plastics*. <http://www.packagingtoday.com/introplasticexplosion.htm>. [November 14, 2007].
- “Angarami, Geraldo; Samaria, Carlos. “An Efficient Low Cost Prosthetic Structural System.” *Journal of Prosthetics and Orthotics*. Volume 1, Number 2. Pp. 86 – 91. http://www.oandp.org/jpo/library/1989_02_086.asp
- Bartkus, Eric; Colvin, James; Arbogast, Robert. “Composite Prosthesis Joins Performance, Economy, Comfort.” *Modern Plastics*. Volume 70, Number 7. July 1993.
- Bartkus, Eric K.; Colvin, James M.; Arbogast, Robert E. “Development of a Novel Limb Prosthesis Using Low Cost Composite Materials.” 1994.
- Bhagwan Mahaveer Viklang Sahayata Samiti (BMVSS). <http://www.jaipurfoot.org/>
- Funk, Len. Orthoteers – Orthopedic Resource. British Orthopedic Association. 2007. < <http://www.orthoteers.com/>>
- Gailey, Robert. "Functional Value of Prosthetic Foot/Ankle Systems to the Amputee." Journal of Prosthetics & Orthotics 17(2005) 39-41. 20 Nov 2007 <http://www.oandp.org/jpo/library/2005_04S_039.asp>.
- Handicap International. <http://www.handicap-international.us/hi/>
- International Standard. Prosthetics – Structural testing of lower-limb prostheses – Requirements and test methods. ISO 10328: 2006.
- Kim, Donghak. “Finite Element Analysis of Monolimb.” December 12, 2006.
- Kulshreshtha, Tarun Kumar. “The Jaipur Below Knee Prosthesis HDPE” Fabrication Manual. [November 1, 2007].
- Lee, Winson; Zhang, Ming; Boone, David; Contoyannis, Bill. "Finite-element analysis to determine effect of monolimb flexibility on structural strength and interaction between residual limb and prosthetic socket." Journal of Rehabilitation Research and Development. Volume 41. 2004. 775-786.

Lee, Winson C. C.; Zhang, Ming; Chan, Peggy P. Y.; Boone, David A. "Gait Analysis of Low-Cost Flexible-Shank Transtibial Prostheses." IEEE Transactions on Neural Systems and Rehabilitation Engineering, VOL. 14, No. 3 September 2006.

Loos, Bonnet, Petermann J. "Morphologies and mechanical properties of syndiotactic polypropylene (sPP)/ polyethylene (PE) blends" Polymer. Volume 41, Issue 1. PP 351 – 356. January 2000.

MatWeb (Material Property Data). "Overview of materials High Density Polyethylene (HDPE), Sheet/Thermoplastic Sheet"
<http://www.matweb.com/search/DataSheet.aspx?MatID=78285>

MatWeb (Material Property Data). "Overview of materials for Polypropylene, Molded"
<http://www.matweb.com/search/DataSheet.aspx?MatID=78370&ckck=1>

Mobility India. "SATHI: Trans-Tibial Prosthetic Modular Component (TTPMC)". www.mobility-india.org/download/sathimanual.pdf . [October 30, 2007].

Muilenburg, Alvin L. "The Definitive Prosthesis ." A Manual for Below-Knee Amputees. 1996. Orthotics and Prosthetics Online. 20 Nov 2007
 <<http://www.oandp.com/resources/patientinfo/manuals/7.htm>>.

Norton, Robert. Machine Design - An Integrated Approach. 3rd Edition. Prentice Hall, 2006.

Shigley, J.E., Mischke, C.R., Budynas, R.G., Mechanical Engineering Design, 7th Ed., McGraw-Hill, 2004, p. 163.

Orthoteers. "Lower Limb Amputations".
[http://www.orthoteers.org/\(S\(dptvir45mji03n55mdg50155\)\)/searchresults.aspx?section=35&article=260&searchterm=Lower+Limb+Amputations](http://www.orthoteers.org/(S(dptvir45mji03n55mdg50155))/searchresults.aspx?section=35&article=260&searchterm=Lower+Limb+Amputations). 2005

Pearce, G.; Kibble, K; Zorn, M. "A Simple, Cheap, and Effective Lower Limb Prosthesis for Use by Landmine Victims in the Third World."

"Prosthetic History." Ampulove. 03 Nov 2007
 <<http://www.ampulove.com/amputee/proshistory/proshistory.htm>>.

Reswick, James B. "How and when did the rehabilitation engineering center program come into being? " Journal of Rehabilitation Research and Development 39. Dec 2002 11-16. 03 Nov 2007 <<http://www.rehab.research.va.gov/jour/02/39/6/sup/reswick.html>>.

Shackerlford, James F. Introduction to Materials Science for Engineers. Sixth Edition. Pearson Prentice Hall, Upper Saddle River, New Jersey. 2005.

Southern California Orthopedic Institute. "Anatomy of the Knee".

<http://www.scoi.com/kneeanat.htm>. 2004

The Center for Orthopaedics and Sports Medicine. "Knee Joint – Anatomy and Function".

<http://www.arthroscopy.com/sp05001.htm>. April 3, 2003.

Uellendahl, Jack E. "Prosthetic Primer: Materials Used in Prosthetics. Part I." InMotion. Volume 8, Issue 5. September/October 1998. www.amputee-coalition.org/inmotion/sept_oct_98/matinprs.html

Uellendahl, Jack E. "Prosthetic Primer: Materials Used in Prosthetics. Part II." InMotion. Volume 8, Issue 6. November/December 1998. www.amputee-coalition.org/inmotion/nov_dec_98/matinprs.html

Appendix A: History of Prosthetics

The history of prostheses dates back to a time in the BC era. There has always been a need for humans to feel whole and complete; however when a body limb is missing, this feeling of completeness is missing as well. To satisfy this need, humans began to design devices to artificially replace the missing limb. For a lower limb, these devices were originally a peg design in order to provide the necessary support. A hook design was used for a missing hand, which gave the client some function and use of an extension of the arm. As the years progressed, the design capabilities advanced. Prosthetic devices were built into the armor that was worn for battles. This often was simply a continuation of the metal to make the upper limbs symmetrical and lower limbs symmetrical. This allowed the user to have a balanced feeling armor, even if there was nothing underneath.

The advancement of prostheses continued into the Renaissance period. This was an era of rebirth and rediscovery for prosthetic devices. There was a major discovery in regards to independent joint movement and control. Designers were experimenting with spring loaded joints to allow for a smooth return. This was a new feature that gave the user freedom to bend at the joint. This was especially helpful for upper arm and upper leg prostheses, in which the elbow and knee joints, respectfully, were impacted.

The 16th century was a time for great advancements due to a French army surgeon, Ambroise Paré. He was a very skilled surgeon and was capable of performing successful surgeries in a very timely manner. In working with the army at a time of frequent battles, he had to amputate a large number of limbs. He had approximately 30 seconds to amputate the limb, and 3 minutes to complete the surgery. There was no availability of anesthesia or tourniquets at this time and he had to complete all surgeries without an aide. Paré had the ability to invent both upper and lower limb prostheses, showing promise of basic function. His above the knee prosthesis included a kneeling peg leg, with an adjustable harness, and a foot

prosthetic addition. This lower limb prosthesis included a knee lock control, which was the first in the history of prostheses.

Medical advancements in the period from 1600-1800 helped to increase the surgery survivor rate. Great strides were taken for modern medical practices including: tourniquets, anesthesia, analeptics, blotting styptics, and disease fighting drugs. During this time, amputations were becoming a more accepted solution to a severe wound suffered during battle, as opposed to an effort to quickly save a life. More time and attention was given to the surgeries, which allowed for cleaner amputations and better fit prostheses. Antiseptic techniques were not adopted until the end of the 19th century. This delay in cleanliness resulted in a higher mortality rate, especially for amputee patients. There is a saying in reference to the sanitation during this time, “it was safer to have a limb amputated by gunfire than by a surgeon”.

Also during this time period, there were advancements in prostheses, which were largely due to two men. In the 17th century, the Dutch surgeon, Pieter Andrianszoon Verduyn brought the belief that function was more important than aesthetics when he invented the first non-locking, below the knee prosthesis. This device featured external hinges, leather cuffs, and was lined with leather. The prosthesis was made of a copper shell and a wooden foot. Verduyn’s device served as a starting point for Dr. Benjamin F. Palmer, who added an anterior spring and concealed tendons, which helped with the fluidity of the motion. Palmer also focused on giving the device a smoother appearance to combine both function and aesthetics. Palmer’s prosthesis was honored at the 1851 London World’s Fair because “it imparted a life-like elasticity and firmness to the step”.

The Civil War era (1861-1865) brought about the creation of more advanced prostheses. In 1863, Dubois D. Parmlee designed a device with a suction socket, polycentric knee, and a multi-articulated foot. In 1912, Marcel Desoutter invented a prosthesis that later became a foundation for the Hanger company. He was an English aviator who lost his leg in an airplane accident and developed the first aluminum prosthesis. This was further developed by Hanger, who was promoting the use of pelvic suspension versus shoulder suspension. The Hanger

Company found that the pelvic suspension was much more efficient and stable. This realization led to important control systems, such as the knee brake.

The World War I era (1914-1918) provided a great opportunity for the advancement and organization of prosthetists. The European prosthetists had an extreme increase in experimentation as they had ten to twenty times more amputees in their armies than the US Army did. This influenced the Surgeon General of the US Army to invite US prosthetists to Washington, DC to discuss the current technologies and developments. This meeting was a great occasion for the development of prostheses including: ethical standards, scientific programs, educational programs, and establishing relationships with other health professionals. This forum resulted in the creation of the American Orthotics and Prosthetics Association (AOPA).

The Belgian prosthetist, Dr. Martin, began to emphasize the connection between prosthetic devices and the anatomy and physiology of the human leg. He could produce both the static and aesthetic appearances. He created a modified cast of a residual limb and used the measurements from this cast to develop his prosthesis. This focus on appearance influenced future prosthetists in their designs, as this had never been a focus before Martin.

The developments and technologies brought about in the 1940s have had a great affect on the prosthetic world as it is today. In 1945, Normal Kirk, Surgeon General of the United States Army, requested that the National Academy of Sciences (NAS) investigate the prosthetic state of the art. General Kirk, in conjunction with the NAS, created the Committee on Prosthetic Devices (CPD) for US health professionals. The purpose of this committee was to provide leadership and coordination among the nation's leading specialists. The committee strived to join together health professionals, physicians and surgeons, with engineers and technical support to aid in the improvement of the quality of life of people with disabilities. In 1946, General Kirk brought a team of engineers and surgeons to Europe to learn about the European advancements regarding prostheses. This visit demonstrated how far behind the US was in terms of development, which helped the US to focus on the development and organization of disability services. In 1947, the University of California Berkeley held

educational seminars on the prescription, fabrication, and alignment of above the knee prostheses.

A Congressional Act was passed in 1948 that allowed the Veterans Administration (VA) to fund research and development programs in the US. The first facility that was opened was the Veterans Administration Prosthetic Center (VAPC) in New York. It was made available to both veterans and the general public in the greater New York City area. The staff included a large number of engineers, physicians, and prosthetists who had a desire to improve prosthetic design and construction. The VA also opened the Prosthetics and Sensory Aid Service (VA-PSAS) at its Central Office in Washington, DC. This center oversaw the orthotics and prosthetics services at VA hospitals throughout the United States. The VA, in cooperation with the Department of Health, Education and Welfare (H.E.W.) and the Armed Services also began the Artificial Limb Program, which established numerous research laboratories throughout the nation.

The creation of higher education prostheses programs began in the 1950s. The first institution to offer a course was the University of California Los Angeles (UCLA) when, in 1956, they began formal above the knee prosthetic courses. At about the same time, the VA established a prosthetic post graduate program at New York University (NYU). In 1959, Rehabilitation Services Administration and H.E.W. established a prosthetic program at Northwestern University in Chicago, Illinois. This decade was a great time for universities to display the many advancements they had made. In 1956, the University of California introduced the SACH foot, which has a wooden heel wrapped in rubber, with a rubber cushion heel (Gailey, 2005). In 1959, the PTB prosthesis was created at the University of California Berkeley. This device has a soft lined socket which completely covers the stump and attaches to the shank of the prosthesis (Mullenburg, 1996).

The latter half of the 1950s proved to be an important period for leadership and organizations. During this time, the Committee on Prosthetic Research and Development (CPRD) was developed with the goal of providing leadership in the world of prostheses. This committee was comprised of solely volunteer medical and engineering personnel. The focus of the committee centered on amputations, artificial limbs, rehabilitation engineering, and

assistive technology. The CPRD combined true leaders in the industry and provided them with the chance to exchange research ideas, evaluate devices, and discuss publications regarding such topics.

The Social and Rehabilitation Services (SRS) funded physical medicine and rehabilitation programs. The SRS also developed the Rehabilitation Research and Training Centers (RRTC), which received grants to support training programs for health professionals. According to the RRTC, the important objective regarding prosthetic devices was to research and advance the technologies.

The growth and development of prosthetic devices has continued to flourish into the present. There are many companies and organizations throughout the world that focus on the improvement of the lives of people with disabilities, with a special focus on their mobility. The patient plays an even greater role for the design and manufacturing of the device. Technology levels have a wide range: from high tech devices for paralympians, to low tech devices for developing countries. No matter the audience, all prosthetics are designed with the common goal to provide a comfortable and functional prosthesis that allows the user to live a “normal” lifestyle.

Appendix B: Center for International Rehabilitation (CIR)

The Center for International Rehabilitation (CIR) is a Chicago based non-profit organization, whose mission is “to assist people with disabilities worldwide in achieving their full potential” (CIR 2007). The creation of the CIR began in 1996 when Dr. William Kennedy Smith founded the organization Physicians Against Land Mines (PALM). In 1997, one year after its inception, this organization received the Nobel Peace Prize. The CIR was opened in 1998 by PALM to expand its facilities to include victim assistance in rehabilitation services and advocacy. The center is now present in six countries, educating over seventy students to date who treat approximately 8,600 amputees yearly.

The CIR has created a Rehabilitation Engineering Research Center (RERC) which has been titled a “national center of excellence in rehabilitation engineering” by the National Institute of Disability and Rehabilitation Research (CIR 2007). This program works to develop new technologies and techniques to improve access to mobility aid for survivors of landmines and other amputees. The program focuses on technologies that are appropriate for use in regions with limited technical and human resources.

The CIR has been developing the “Comprehensive and Integral International Convention to Promote and Protect the Rights and Dignity of Persons with Disabilities”. There are over forty disability organizations working toward the creation of this UN treaty. The organizations are all members of the International Disability Caucus, of which the CIR is a founding member. The CIR is also an active part of the International Disability Right Monitor Program. This program includes a network of researchers in over 30 countries who are working to collect data and report on the experiences of people with disabilities throughout the world.

The International Disability Educational Alliance Network (IDEAnet) website was officially launched by the CIR in 2005. The mission of IDEAnet is “to foster collaborative efforts to use distributed learning and telemedicine to address health disparities and foster effective, sustainable health services” (CIR 2007). This mission may be achieved through the two communities within the network: the Rehabilitation Services Community and the Tele-Medicine Resource Center. Tools such as forums, chats and document sharing are used to promote idea sharing and to generate strategies to improve health services worldwide.

There are currently four collaborative projects in process on the IDEAnet website. These projects are broken down into two categories: appropriate technology and education. The appropriate technology groups work on technologies that can meet economic, cultural, financial and functional needs of people with disabilities. The first project utilizes the RERC to “Improve Technology Access for Landmine Survivors”. The second is a “Project on International Guidelines for Wheelchair Provision”. This project is to develop guidelines that focus on the education, training, design, and service provisions to meet the needs of wheelchair users around the world.

The education category also includes two projects. The first is an “International Model Curriculum Consortium which focuses on creating a model distance learning curriculum. This will lead to improved care and quality of life for amputees. Second is the “Train the Trainer Project” whose goal is to help prosthetic educators train each other and advance ideas. It allows the members to offer advice, support, and constructive feedback on each other’s ideas.

Appendix C: Programs for Third World Countries

Mobility India

Recognizing that millions of people undergo amputations every year due to trauma and the majority of these people being unable to afford the aid they require, Chapal Khasnabis formed an organization called Mobility India. Mobility India (MI) was formed in South India in 1994 to provide rehabilitation services in rural, poverty-stricken areas of India. The bulk of their projects center on providing low cost prosthetic devices to those who are normally unable to afford them. The underlying goal of this organization is to produce “an inclusive society where people with disabilities have equal rights and a good quality of life” (Mobility India).

MI has a large research and training center called “Millennium Building on Disability,” which is a modern disability accessible building where training with orthotics, prosthetics, and rehabilitation can be received. These programs are used to train people in methods for prosthetic construction in order to give them the necessary tools to reach out into the community and provide for the less fortunate individuals who require prosthetic limbs. The students receiving this training are often from low income families in rural areas and urban slums. Once they have finished the training, they will work in their local area to help people with disabilities

Their current project is the development of a lower limb prosthetic which has been broken up into components. This device comes in a kit, making it easier to assemble in rural areas. The pylon has been made in several sizes to maximize the number of heights it can accommodate. Also, the varying pieces can be adjusted slightly to increase the comfort of the patient. Through the implementation of this system, MI is aiding the less fortunate amputees in various areas of India (Mobility India).

Handicap International

Handicap International (HI) is a global program which is providing amputees in third world countries with the means to walk again after a traumatic misfortune. This organization

has been providing for impoverished victims of accidents who are in need of rehabilitation services at a low cost since 1982. Currently, they have 240 programs in nearly sixty different countries.

HI uses prosthetic devices and rehabilitation to put people who have been injured back on the road towards independent living. HI recognizes that their program cannot be implemented the same in every environment and in turn work hard to adapt each project to the local capabilities. Whatever technology is used for the project, HI provides prostheses, orthoses, and other orthopedic devices needed to successfully aid the local people. The training is provided by HI through local health structures to ensure that the system is sustainable once HI is no longer active in that area; orthopedic centers are created in this way. To ensure the best services possible, training is also provided for people to become well versed in physical therapy, occupational therapy, and speech therapy. Once they are educated, they are then able to assist the patients with the necessary therapy to adjust to their new prosthetic or orthotic device.

Beyond prosthetic devices, in the case of an emergency or natural disaster, HI will give assistance and aid to the affected people in the form of home redevelopment, education, supplies, and other activities. They are also proactively working to prevent the use of landmines. Further, they are continually campaigning for disability inclusion in all areas including basic rights and accessibility (Handicap International, 2007).

Helping Hands for Haiti

Helping Hands for Haiti (HHH) is an organization that is providing quality rehabilitation services for the physically disabled in Haiti. Their underlying goal is to give the people of Haiti the tools necessary to implement the production and distribution of prosthetic devices in their local area on their own. HHH accomplish this goal by offering rehabilitation education, clinical treatments, disability prevention projects, and public awareness of disabilities and proper rehabilitation. With a heightened awareness of how to care for the disabled people, Helping Hands for Haiti foresees the treatment of the disabled people in Haiti to change in a positive way through more respect and general care. No one with financial difficulties will ever be

turned away; HHH will make sure that their services are equally available for anyone who needs them (Helping Hands for Haiti, 2007).

Bhagwan Mahaveer Viklang Sahayata Samiti (BMVSS)

Bhagwan Mahaveer Viklang Sahayata Samiti (BMVSS) was established in India in 1975 as a non-profit organization dedicated to helping the physically challenged who could not afford the technology they needed to account for their disability. BMVSS has fitted the largest number of artificial limbs to the handicapped in the world. They have provided these artificial limbs, calipers, crutches, wheel chairs, tricycles, and many other handicapped appliances for no cost whatsoever. BMVSS provides the training, facilities, and devices necessary to aid those in need. They provide everything from prosthetic limbs to hearing aids and shoes. They offer a broad range of programs for people with disabilities and they are leaving a lasting impact on developing countries throughout the world. Their most well known prosthetic device is the Jaiper foot (BMVSS, 2007).

Prosthetics Outreach Foundation

Prosthetics Outreach Foundation (POF) is working around the world to provide disadvantaged amputees and others suffering from disabilities the tools they need to restore their mobility. Recognizing that there are many tragic injuries throughout the world, particularly in countries which have been war torn, POF has dedicated their time to restoring the victims' mobility and independence. Their main outreach areas are currently Vietnam, Bangladesh, and Sierra Leone. Within the last fifteen years, POF has helped more than 13,000 children and adults regain their independence through providing them with the devices they need to be mobile again (POF 2007).

Their main activities involve clinical outreach to amputees, orthopedic surgical assistance, and local prosthetic and orthotic manufacturing training in remote areas of the world. The underlying goal of these projects is to provide these low income societies with the

tools and training they need to continue to provide aid for disabled persons without the continuous help of POF (POF 2007).

An example of one of the POF projects is being implemented in Vietnam. The materials used in all of their projects are locally found resources to ensure that the artificial limbs stay low cost and easy to continue to fabricate in the future without dependence on POF to provide the materials. The U.S. Agency for International Development (USAID) has given aid to POF to catalyze the programs in different countries. In each country, an area specific manufacturing process and prosthetic device are developed. For example, in Vietnam, a foam foot which had previously been used in other countries was deteriorating due to the humid climate. POF developed a water resistant rubber foot instead to be manufactured and distributed around Vietnam (POF 2007).

Appendix D: Circular Shank Parameter Combinations

Table 23: Circular Shank Parameter Combinations

Shank Length	Diameter (mm)	Rib Length (mm)
360 mm (380 mm, including plate)	48.5	0
	48.5	10
	48.5	20
	53.5	0
	53.5	10
	53.5	20
	58.5	0
	58.5	10
	58.5	20
	63.5	0
	63.5	10
	63.5	20

Appendix E: Analytical Stress Calculations Procedure

To provide more validity to our computer modeling and finite element analysis, stress calculations have been performed by hand and compared to the COSMOSWorks data output values. This analysis was performed on a monolimb that has a diameter of 53.5 mm, a shank length of 360 mm, a material thickness of 5 mm, and a rib length of 0 mm. The stresses that were found to contribute to the normal stresses in the u direction, σ_f , are the axial normal stresses which are the product of the load in the u direction, the bending stresses caused by the load in the u direction, and the bending stresses caused by the load in the u direction. Each of these stresses were calculated separately and then added together, which was an appropriate approach due to the principle of superposition. Once this stress value was calculated by hand, the model was run in COSMOSWorks and the point where the stresses had been calculated was probed in the model to determine the stress value output by the computer analysis.

First, the normal stresses were found by first determining the axial reactionary load to the offset load in the f direction. Once this value was found through a static analysis, the area was calculated using the following equation.

$$A = \frac{\pi}{4} (D^2 - d^2)$$

Once the area had been found, the reactionary force and the calculated area were input into the equation below to solve for the normal compressive stresses.

$$\sigma_{normal} = \frac{R_u}{A}$$

There are also bending stresses that occur from the load in the u direction and these were calculated through the following steps. The overall equation for bending is included below.

$$\sigma_{bu} = \frac{M_f c}{I_f}$$

First, the moment was calculated by multiplying the load by the moment arm.

$$M_f = F l_f$$

Next, the second moment of area was calculated through the following equation:

$$I_f = \frac{\pi}{64}(D^4 - d^4)$$

Finally, the “c” value in the equation represents the distance of the point where the stresses are being measured from the neutral axis. The stress is being calculated at the outer diameter, making the value .02675, which is the outer radius of the shank. Finally, each of these components were combined into the original bending stress equation.

The next bending stresses which were found to contribute to the normal stresses in the u direction at the chosen point were caused by the f load. The same steps were followed as described above; however, the numbers were altered to correspond to the f load. The updated equation has been included below.

$$\sigma_{bf} = \frac{M_f c}{I_f}$$

Finally, each of these components were added together to determine the total normal stresses present at the point 10 mm above the top of the plate and on the frontal side of the shank.

$$\sigma_{u \text{ total}} = \sigma_{\text{normal}} + \sigma_{bu} + \sigma_{bf}$$

This calculated stress value was then compared to the value found at this point in COSMOSWorks.

Appendix F: Analytical Stress Calculation Results

Following the procedure detailed above, the normal stresses in the u direction were calculated to verify the validity of the values output from COSMOSWorks. First, the normal stresses were investigated and after a static analysis on the monolimb with the u load being applied, the reactionary force was found to equal the u load. Therefore, the normal axial stresses would be the quotient of the reactionary force and the cross sectional area. The equation below details the steps taken to calculate these normal stresses.

$$-R_u = F_u = -3240.44 \text{ N}$$

$$\sigma_{normal} = \frac{R_y}{A}$$

The area of the cross section was calculated by the below equation.

$$A = \frac{\pi}{4} (D^2 - d^2) = 7.62 * 10^{-4} m^2$$

The quotient of these has been calculated as follows and the negative sign demonstrates that the normal stresses are compressive.

$$\sigma_{normal} = \frac{R_u}{A} = \frac{-3240.44 \text{ N}}{7.62 * 10^{-4} m^2} = -4.25 * 10^6 \frac{N}{m^2}$$

There are also bending stresses that occur from the load in the y direction and these were calculated through the following steps. The overall equation for bending is included below.

$$\sigma_{bu} = \frac{M_f c}{I_f}$$

First, the moment was calculated by multiplying the load by the moment arm.

$$M_f = F l_f = 3240.44 \text{ N} (.03075 \text{ m}) = 99.64 \text{ Nm}$$

Next, the second moment of area was calculated through the following equation:

$$I_f = \frac{\pi}{64} (D^4 - d^4) = \frac{\pi}{64} (.0535 m^4 - .0435 m^4) = 2.264 * 10^{-7} m^4$$

Finally, the “c” value in the equation represents the distance of the point where the stresses are being measured from the neutral axis. In this case, that value is .02675 m. When each of these components was combined into the original bending stress equation, the following value was obtained:

$$\sigma_{bu} = \frac{M_f c}{I_f} = \frac{(99.64 \text{ Nm})(.02675 \text{ m})}{2.264 * 10^{-7} \text{ m}^4} = 1.173 * 10^7 \frac{\text{N}}{\text{m}^2}$$

The next bending stresses which contribute to the normal stresses in the y direction at the chosen point are caused by the z load. The same steps were followed, but with numbers which correspond to the z load. The process has been included below.

$$\sigma_{bf} = \frac{M_f c}{I_f}$$

The moment arm was calculated, using the same equation as above, but using the z load component.

$$M_f = Fl_f = -648.09 \text{ N} (.03 \text{ m}) = -19.44 \text{ Nm}$$

The second moment of area remains the same.

$$\sigma_{bf} = \frac{M_f c}{I_f} = \frac{(-19.44 \text{ Nm})(.02675 \text{ m})}{2.264 * 10^{-7} \text{ m}^4} = -2.3 * 10^6 \frac{\text{N}}{\text{m}^2}$$

Each of these components was added together to determine the total normal stresses present at the point 10 mm above the top of the plate and on the frontal side of the shank.

$$\sigma_{u \text{ total}} = -4.25 * 10^6 \frac{\text{N}}{\text{m}^2} + \left(1.173 * 10^7 \frac{\text{N}}{\text{m}^2}\right) + \left(-2.3 * 10^6 \frac{\text{N}}{\text{m}^2}\right) = 5.18 * 10^6 \frac{\text{N}}{\text{m}^2}$$

This point on the model was probed in COSMOSWorks to be $5.36 * 10^6 \frac{\text{N}}{\text{m}^2}$ and can be visually seen in the figure below, Figure 46. This stress value contributes to a 3.47% error when compared with the calculated value. With such a low percentage of error present between the hand calculations and the value calculated in COSMOSWorks, the COSMOSWorks values have been determined to be accurate enough to continue with the investigation.

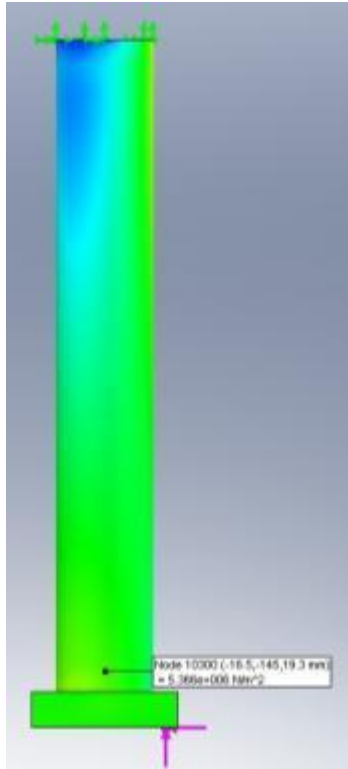


Figure 46: U Normal Stresses

Appendix G: von Mises Stress Contour Plots

Loading Condition I: Circular Shank: 53.5 mm Outer Diameter

The stress plots, shown below as **Error! Reference source not found.** visually displays the stress distributions throughout the shank with each of the set of parameters for this outer diameter: with no rib, a 10 mm rib, and a 20 mm rib, displayed respectively from left to right. In the figure below, the contour plots have been displayed next to each other to better compare the differences between the three shanks with the same outer diameter and differing rib lengths. It is important to note the similarities between these stress plots, particularly throughout the pattern of the stress distributions throughout each shank. There is a maximum area of stress 180 degrees from the load location, which is displayed as a red area and the stresses lessens as they get further away from this point.

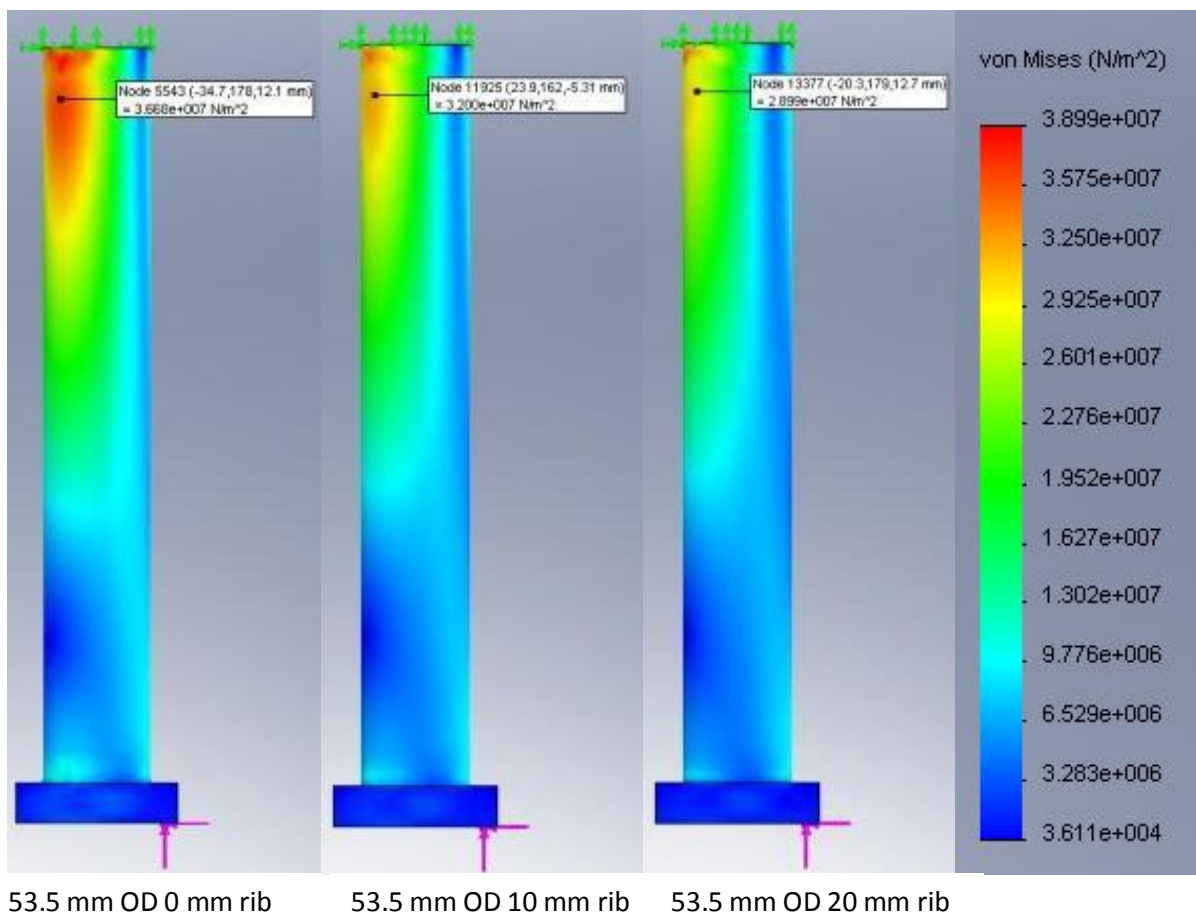


Figure 47: 53.5 mm OD von Mises Stress Contour Plots

Looking at the three contour plots, the stresses found at the specified point decrease as the length of the rib increases, as shown in the table below, Table 14.

Table 24: 53.5 mm OD von Mises Stress Values (Loading Condition I)

Loading Condition	0 mm rib length	10 mm rib length	20 mm rib length
I (Heel Strike)	$3.666 \times 10^7 \text{ N/m}^2$	$3.200 \times 10^7 \text{ N/m}^2$	$2.889 \times 10^7 \text{ N/m}^2$
Yield Strength	$3.07 \times 10^7 \text{ N/m}^2$		

For this shank diameter, the 20 mm rib length model is the only one whose stress value lies below the Yield Strength.

Circular Shank: 58.5 mm Outer Diameter

In the below contour plots, **Error! Reference source not found.**, an area where maximum stresses are present can be seen on the anterior region of the shank, as shown in the front views from COSMOSWorks.

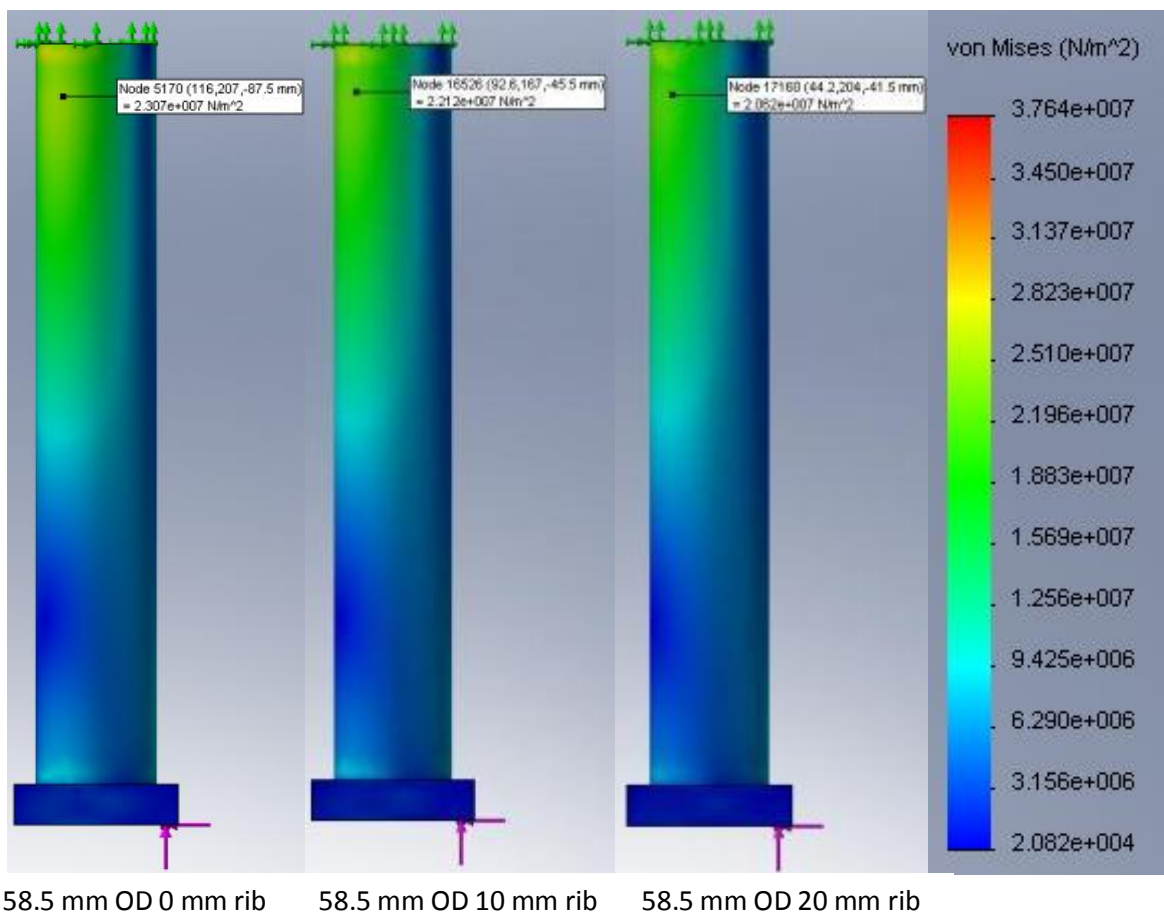


Figure 48: 58.5 mm OD von Mises Stress Contour Plots (Loading Condition I)

The values of these stresses are low enough to fall below the Yield Strength in the models with 10 mm and 20 mm rib lengths; however, the stress value is 5% higher than the Yield Strength in the model with a 0 mm rib length.

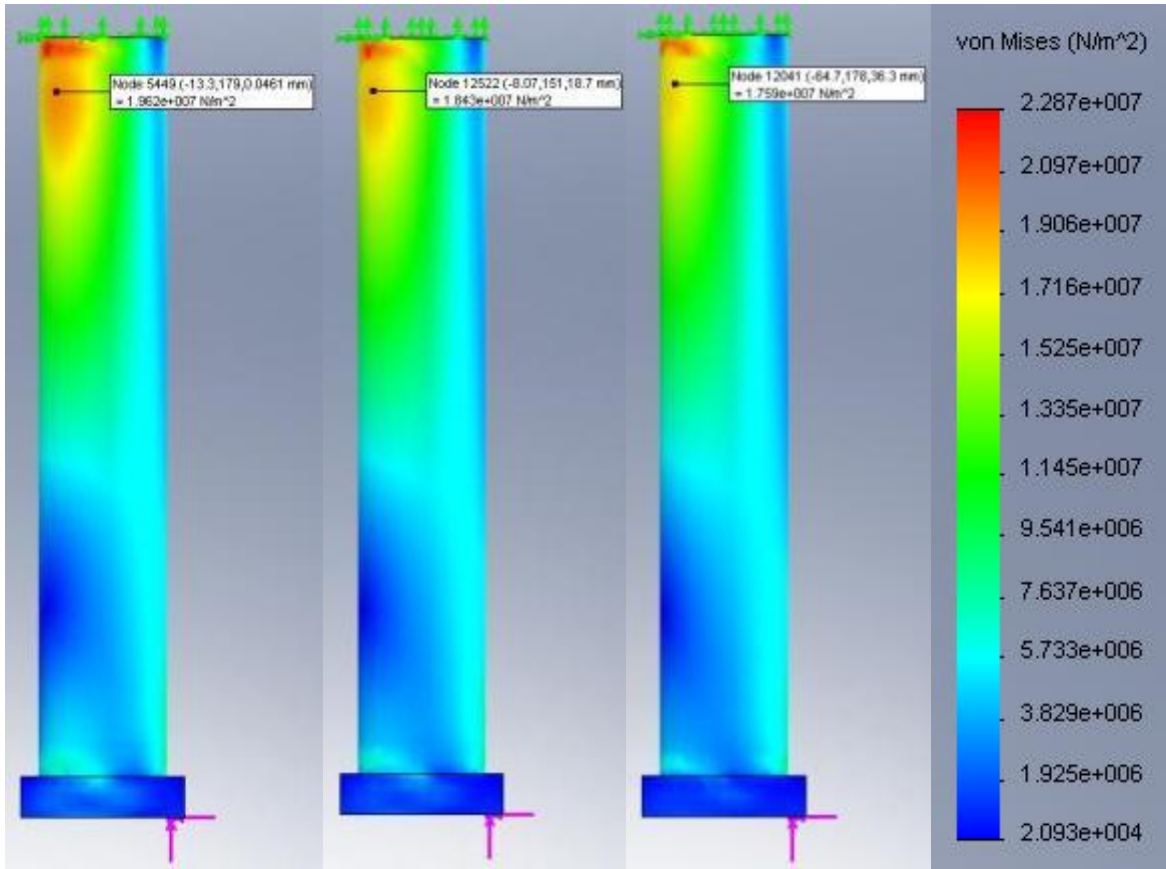
Loading Condition	0 mm rib length	10 mm rib length	20 mm rib length
I (Heel Strike)	$3.215 \cdot 10^7 \text{ N/m}^2$	$2.212 \cdot 10^7 \text{ N/m}^2$	$2.062 \cdot 10^7 \text{ N/m}^2$
Yield Strength	$3.07 \cdot 10^7 \text{ N/m}^2$		

Circular Shank: 63.5 mm Outer Diameter

The contour plots for the 63.5 mm OD have been included below as **Error! Reference source not found..** The overall stress distribution follows a similar trend to that of the 53.5 mm OD with an area of maximum stresses lying 180 degrees from the load location and the stress values decreasing as the distance from this area increases. The maximum stresses are all at least 36% lower than the Yield Strength, demonstrating that they pass the von Mises stress failure criteria by successfully withstanding the applied loads. The stress values also decrease as the rib length increases. These values can be better seen through **Error! Reference source not found..**

Table 25: 63.5 mm OD von Mises Stress Values (Loading Condition I)

Loading Condition	0 mm rib length	10 mm rib length	20 mm rib length
I (Heel Strike)	$1.962 \cdot 10^7 \text{ N/m}^2$	$1.843 \cdot 10^7 \text{ N/m}^2$	$1.759 \cdot 10^7 \text{ N/m}^2$
Yield Strength	$3.07 \cdot 10^7 \text{ N/m}^2$		



63.5 mm OD 0 mm rib 63.5 mm OD 10 mm rib 63.5 mm OD 20 mm rib

Figure 49: 63.5 mm OD von Mises Contour Plots (Loading Condition I)

Circular Shank: 53.5 mm Outer Diameter

The von Mises stress contour plots for shanks with a 53.5 mm OD and rib lengths of 0 mm, 10 mm, and 20 mm have been included respectively below for visual comparison of the stress distributions.

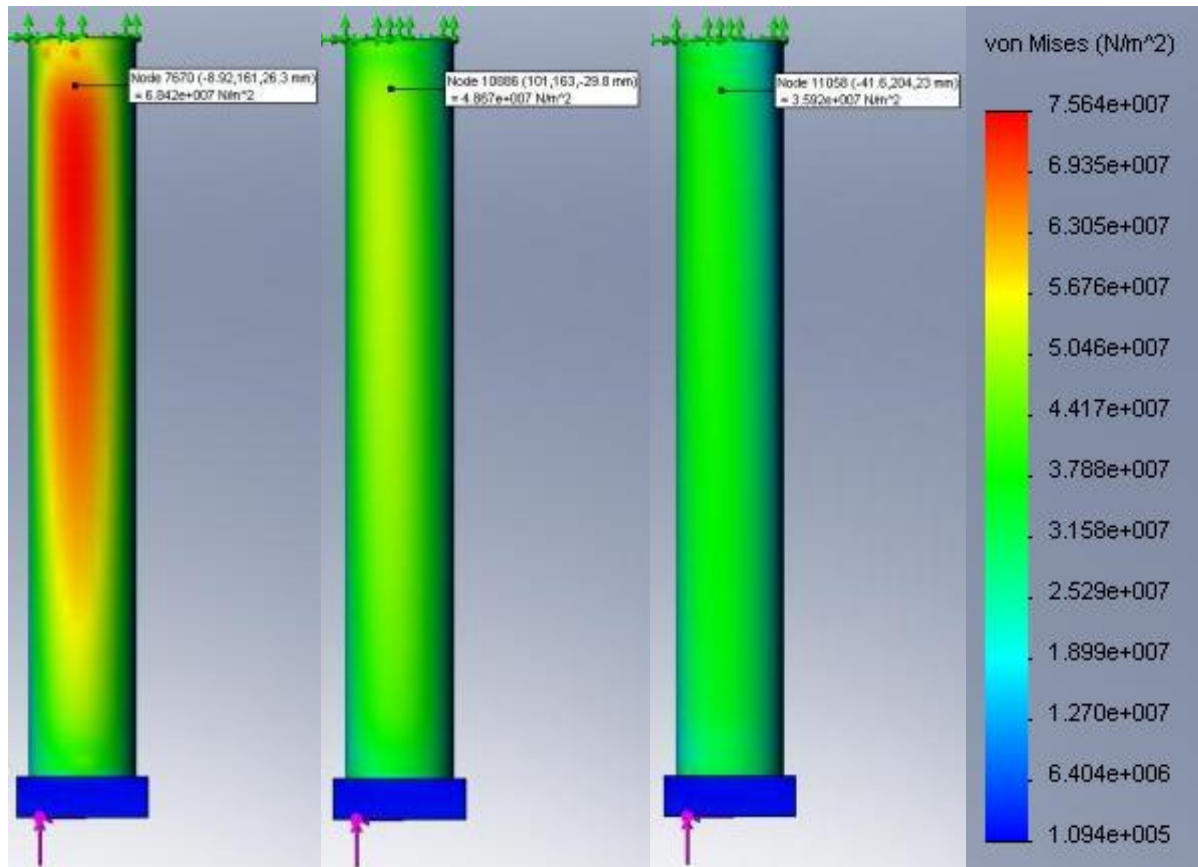


Figure 50: 53.5 mm OD von Mises Contour Plots (Loading Condition I)

The area where maximum stresses are located spans the majority of the frontal region of the shank in the model a 0 mm rib. This area significantly decreases as the rib increases. Also, the von Mises stresses are all above the Yield Strength. A visual depiction of the 53.5 mm OD, 0 mm rib has been included below through an isometric ISO Clipping figure from COSMOSWorks, **Error! Reference source not found.** This feature has only displayed the areas where the von Mises stresses are higher than the Yield Strength, which are on the outer diameter of the anterior and posterior portions of the shank. The deformation caused by the

loading can also be seen through this feature and it can be observed that there are significant levels of deformation present in this model.

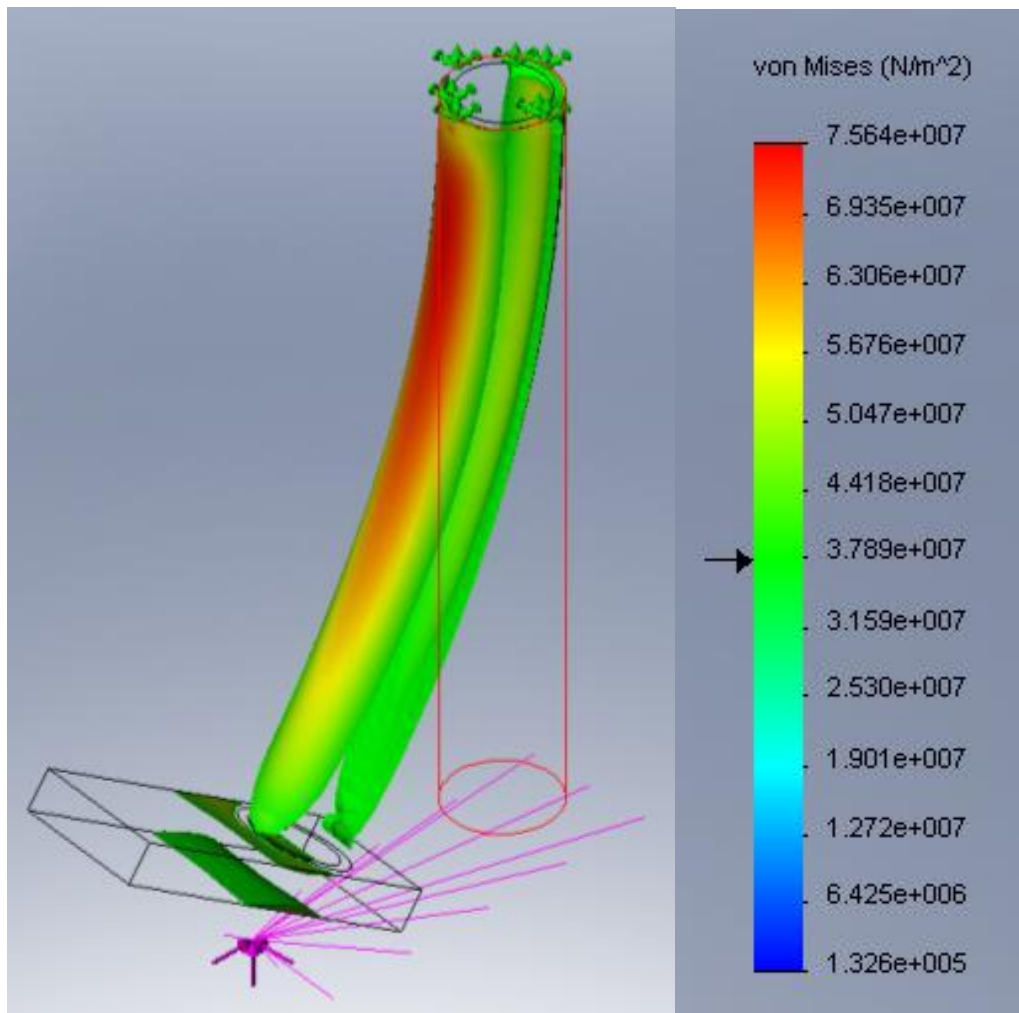


Figure 51:53.5 mm OD 0 mm Rib ISO Clipping (Loading Condition II)

For each of these models, the von Mises stresses are up to 122% higher than the Yield Strength. These high stresses are most likely occurring because the load location is 122.25 mm offset in the f direction from the origin of the model. With such a large offset, the bending stresses increase substantially, causing higher overall stresses throughout the shank.

Table 26: 53.5 mm OD von Mises Stress Values (Loading Condition II)

Loading Condition	0 mm rib length	10 mm rib length	20 mm rib length
II (Toe Off)	$6.842 \cdot 10^7 \text{ N/m}^2$	$4.867 \cdot 10^7 \text{ N/m}^2$	$3.592 \cdot 10^7 \text{ N/m}^2$
Yield Strength	$3.07 \cdot 10^7 \text{ N/m}^2$		

Loading Condition II:

Circular Shank: 58.5 mm Outer Diameter

In the below contour plots, **Error! Reference source not found.**, an area where maximum von Mises stresses are presented can easily be seen on the 0 mm rib model. Although this area is present in the 0 mm model, this area is not present in the models with a 10 mm and 20 mm rib length.

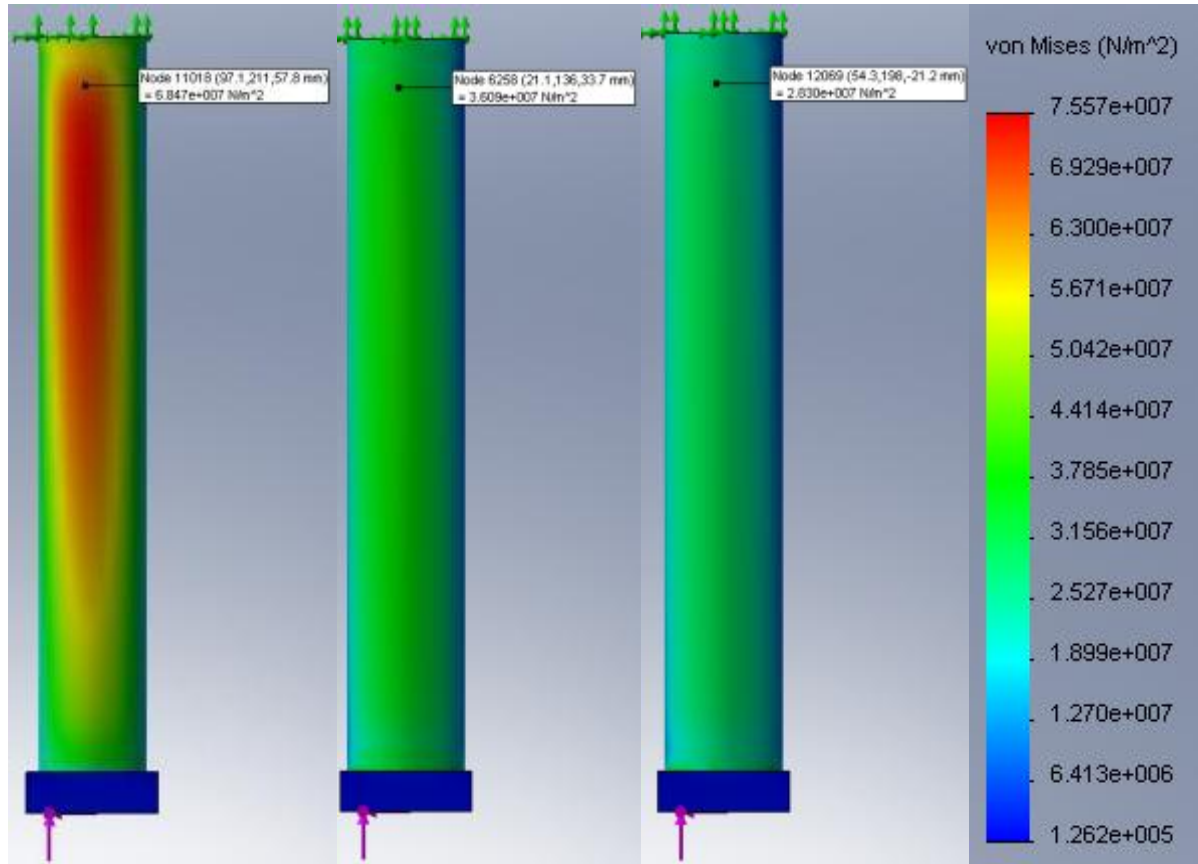


Figure 52: 58.5 mm OD von Mises Contour Plots (Loading Condition II)

Looking at the values of the probed points on the model in **Error! Reference source not found.**, the 20 mm rib length is the only model whose stress value lies below the Yield Strength. The model with a 10 mm rib length is 18% higher than the Yield Strength while the model with a 0 mm rib length is 123% higher than the Yield Strength, which is more than double the Yield Strength.

Table 27: 58.5 mm OD von Mises Stress Values (Loading Condition II)

Loading Condition	0 mm rib length	10 mm rib length	20 mm rib length
II (Toe Off)	$6.847 \times 10^7 \text{ N/m}^2$	$3.609 \times 10^7 \text{ N/m}^2$	$2.830 \times 10^7 \text{ N/m}^2$
Yield Strength	$3.07 \times 10^7 \text{ N/m}^2$		

Circular Shank: 63.5 mm Outer Diameter

The von Mises contour plots for the 63.5 mm diameter for loading condition II have been included below as **Error! Reference source not found..** These stress plots do not have a high stress concentration on the frontal region of the shank and the probed stress values are much lower than those of the previous models under loading condition II. The probed stress value lies above the Yield Strength in the shank without a rib; however, the trend of a decrease in stress values as the rib length increases is seen, and the stress value is lower than the Yield Strength for the models with 10 mm and 20 mm rib lengths.

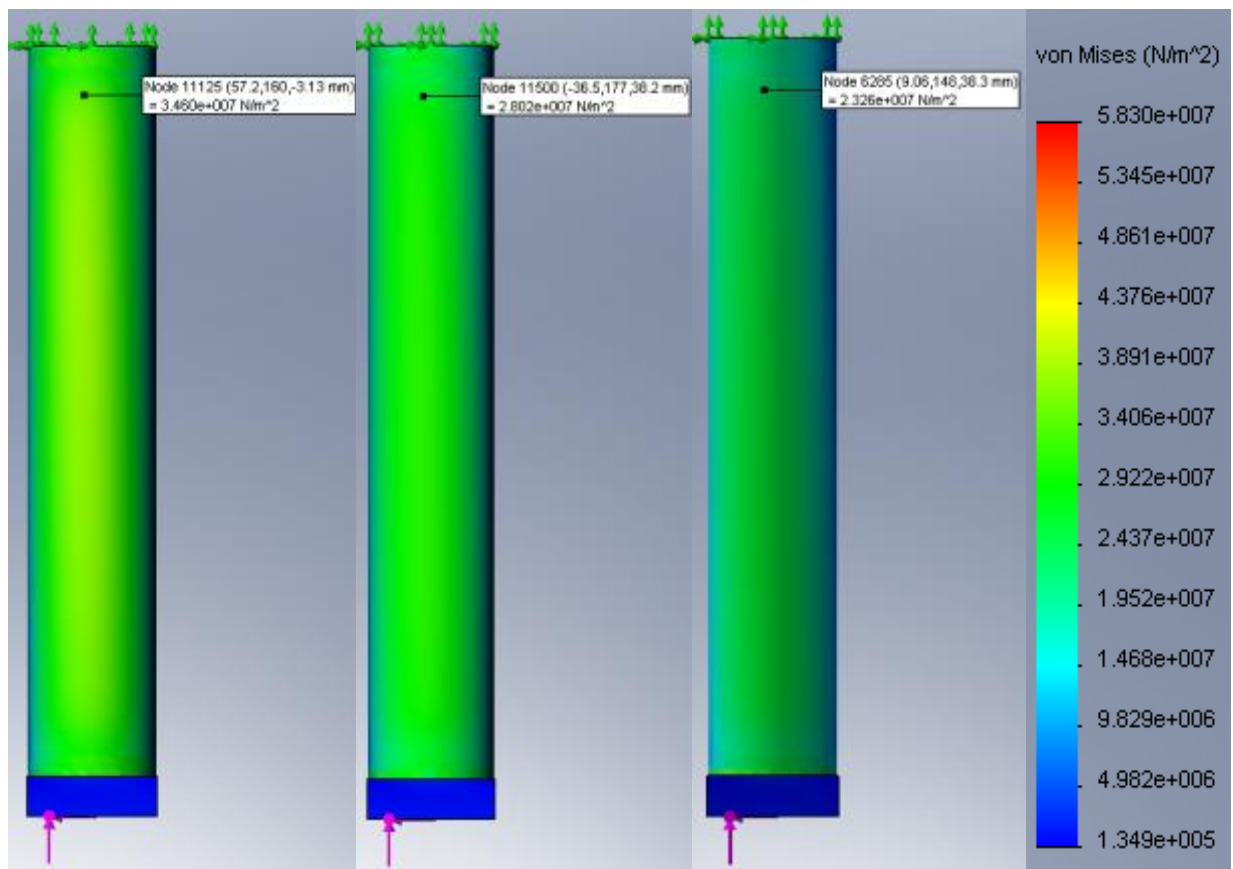


Figure 53: 63.5 mm OD von Mises Stress Contour Plots (Loading Condition II)

The stress values have been depicted again through a table below, **Error! Reference source not found..**

Table 28: 63.5 mm OD von Mises Stress Values (Loading Condition II)

Loading Condition	0 mm rib length	10 mm rib length	20 mm rib length
II (Toe Off)	$3.460 \cdot 10^7 \text{ N/m}^2$	$2.802 \cdot 10^7 \text{ N/m}^2$	$2.326 \cdot 10^7 \text{ N/m}^2$
Yield Strength	$3.07 \cdot 10^7 \text{ N/m}^2$		

Appendix H: Displacement Plots for Loading Condition I and Loading Condition II

Loading Condition I

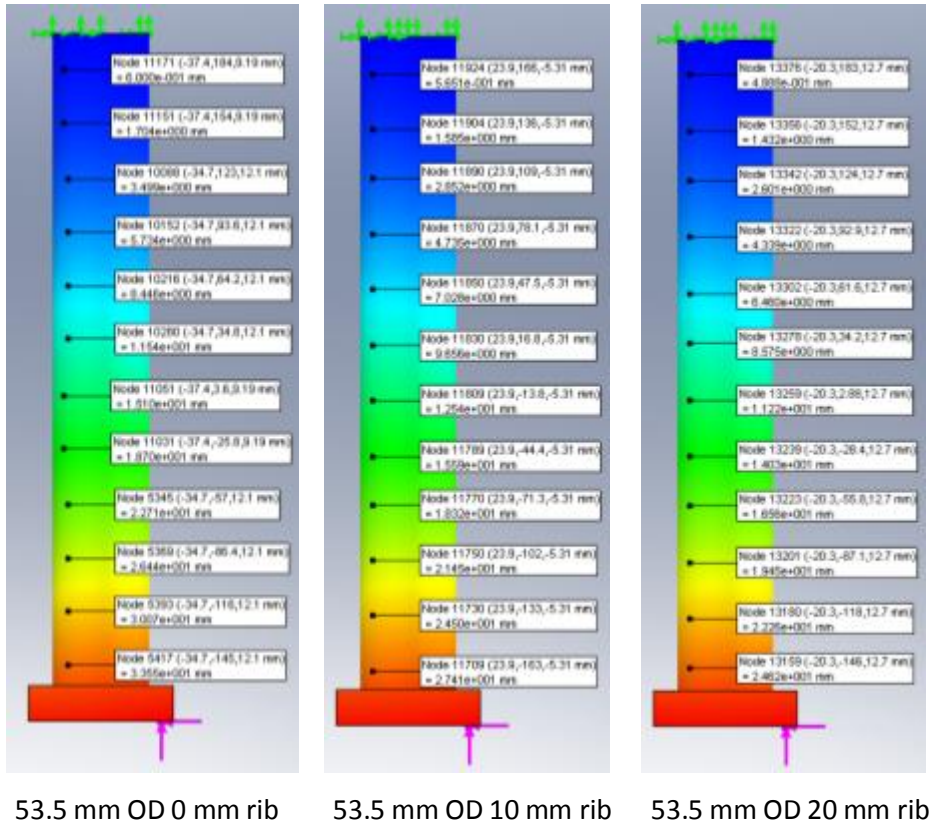
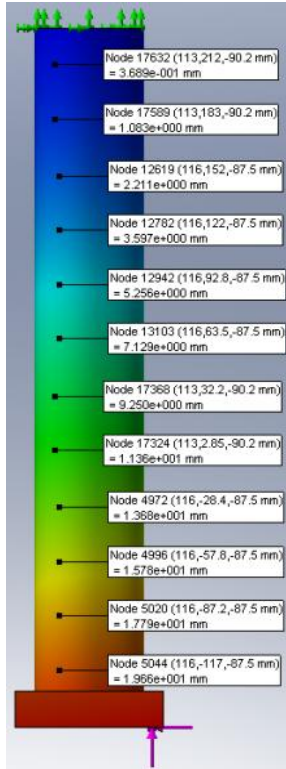
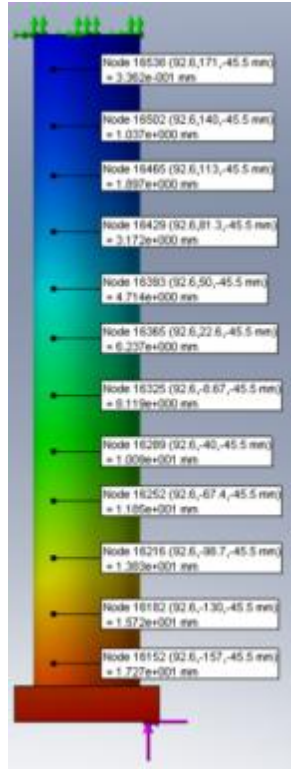


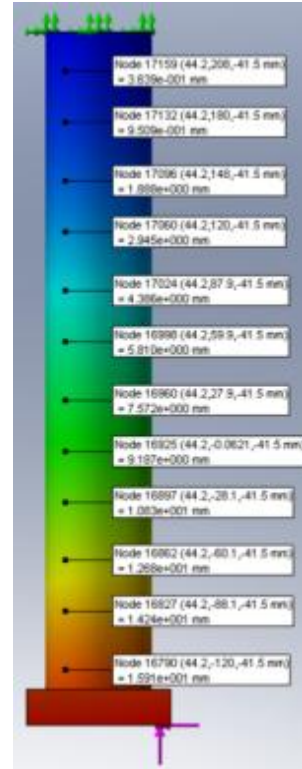
Figure 54: 53.5 mm OD Displacement Plots (Loading Condition I)



58.5 mm OD 0 mm rib

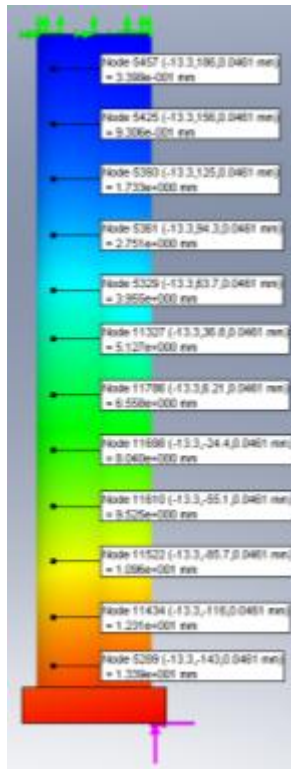


58.5 mm OD 10 mm rib

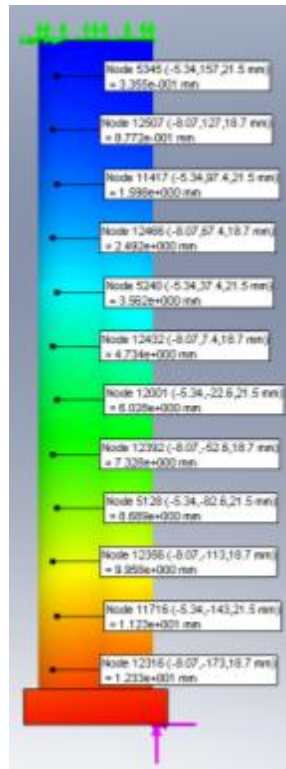


58.5 mm OD 20 mm rib

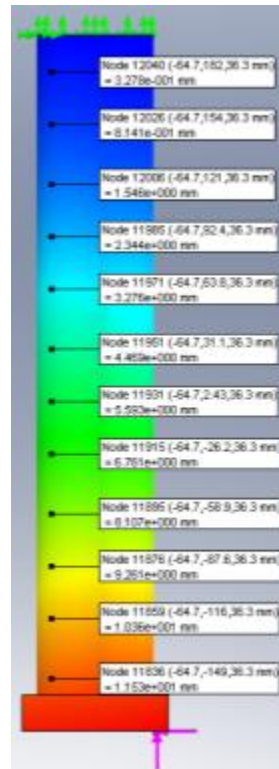
Figure 55: 58.5 mm OD Displacement Contour Plots (Loading Condition I)



63.5 mm OD 0 mm rib



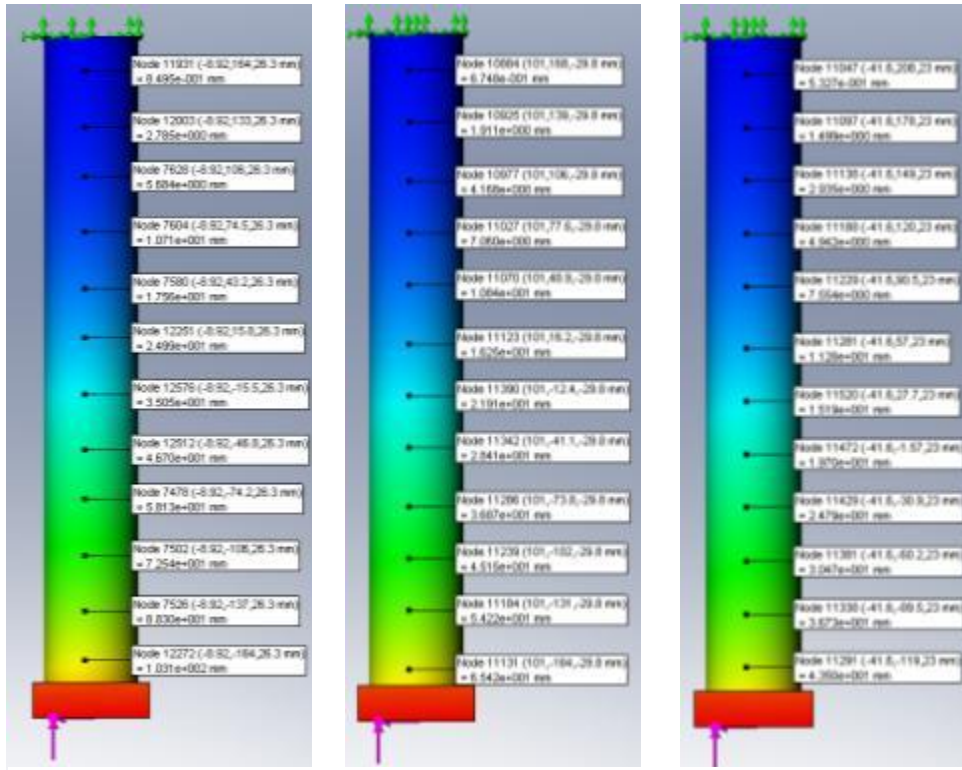
63.5 mm OD 10 mm rib



63.5 mm OD 20 mm rib

Figure 56: 63.5 mm OD Displacement Contour Plots (Loading Condition I)

Loading Condition II

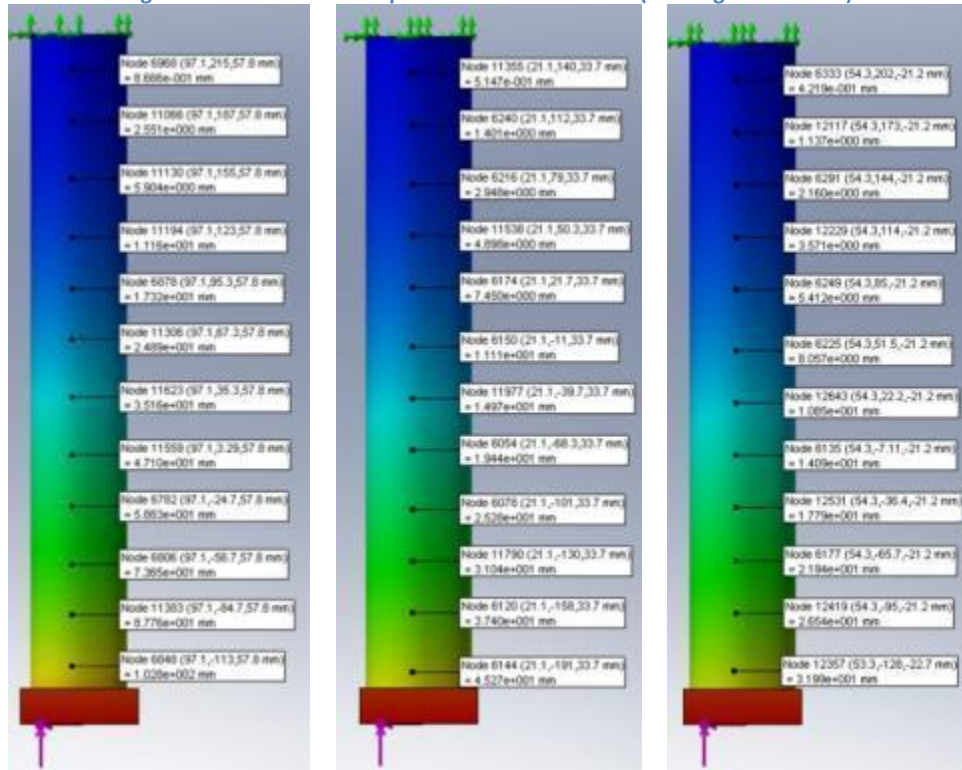


53.5 mm OD 0 mm rib

53.5 mm OD 10 mm rib

53.5 mm OD 20 mm rib

Figure 57: 53.5 mm OD Displacement Contour Plots (Loading Condition II)

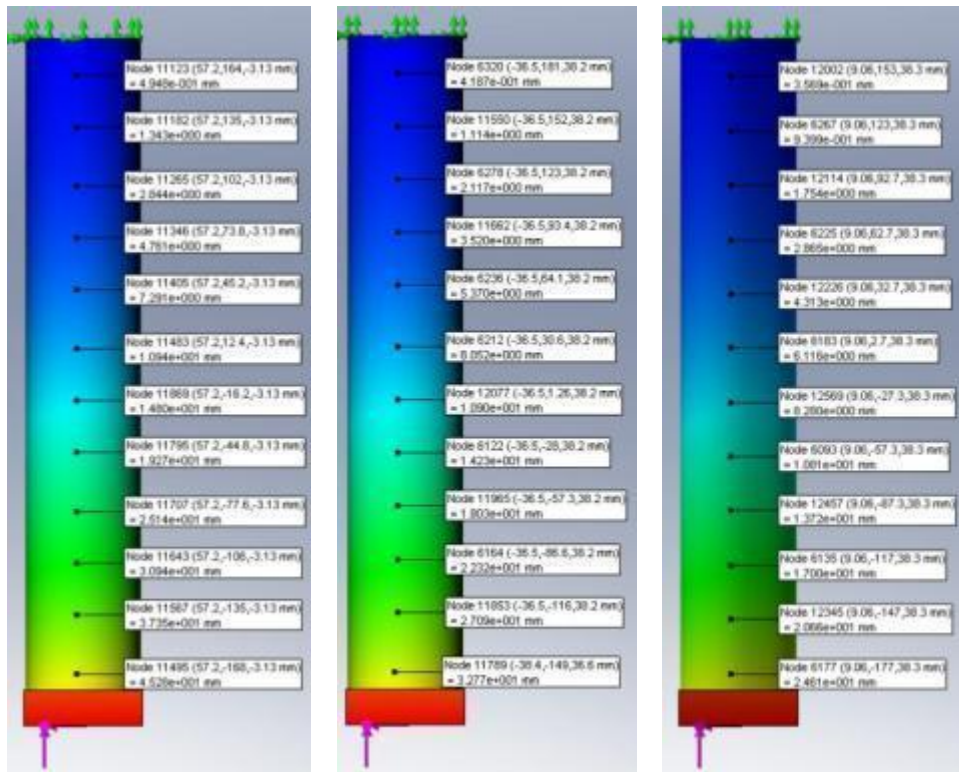


58.5 mm OD 0 mm rib

58.5 mm OD 10 mm rib

58.5 mm OD 20 mm rib

Figure 58: 58.5 mm OD Displacement Contour Plots (Loading Condition II)



63.5 mm OD 0 mm rib 63.5 mm OD 10 mm rib 63.5 mm OD 20 mm rib
 Figure 59: 63.5 mm OD Displacement Contour Plots (Loading Condition II)

Appendix I: In Plane Displacement Graphs

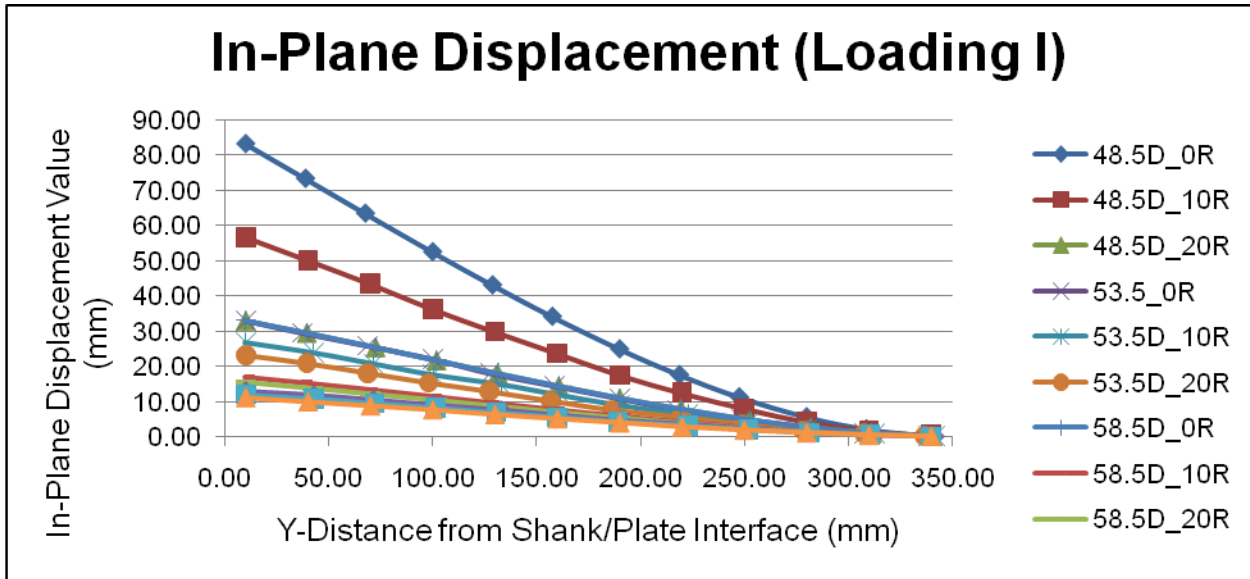


Figure 60: In-Plane Displacement (Loading Condition I)

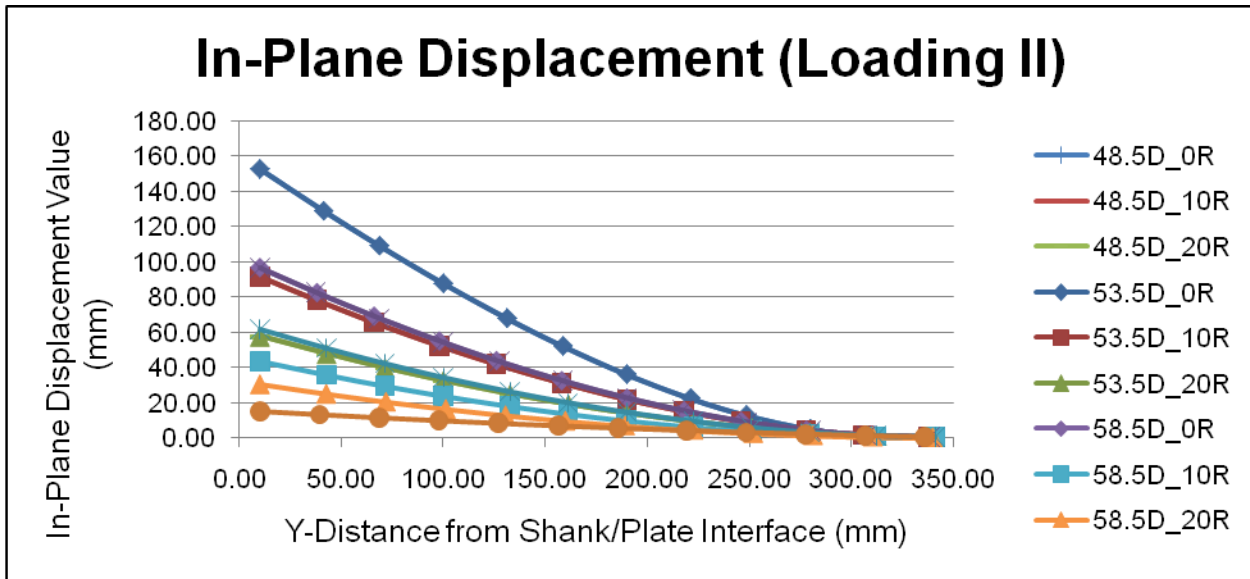


Figure 61: In-Plane Displacement (Loading Condition II)

Appendix J: Out of Plane Displacement Graphs

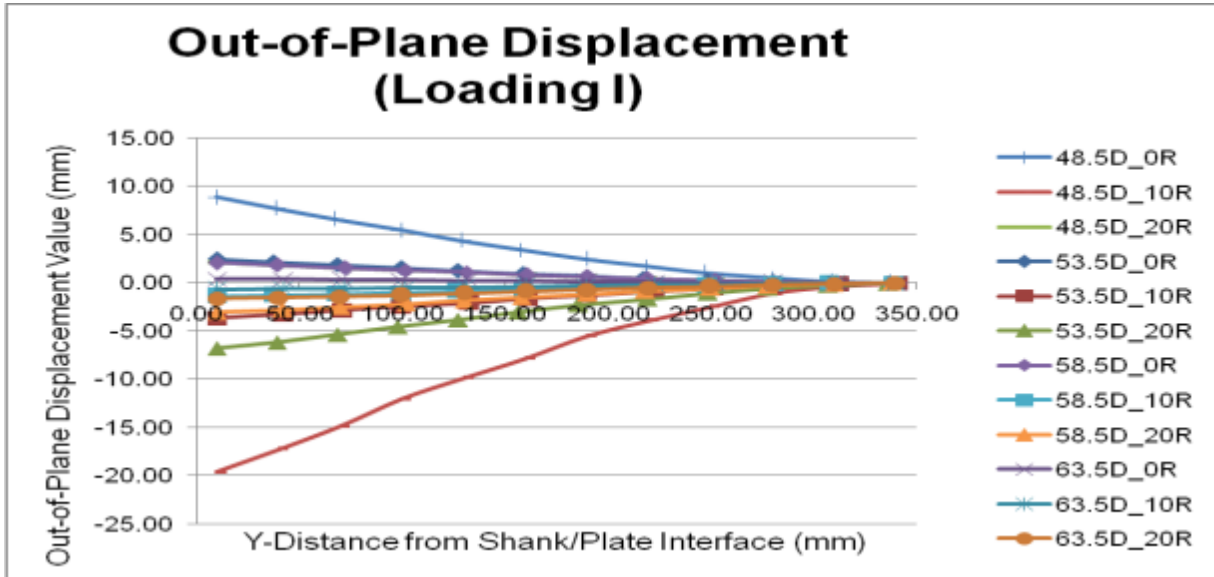


Figure 62: Displacement Trends for Loading Condition I

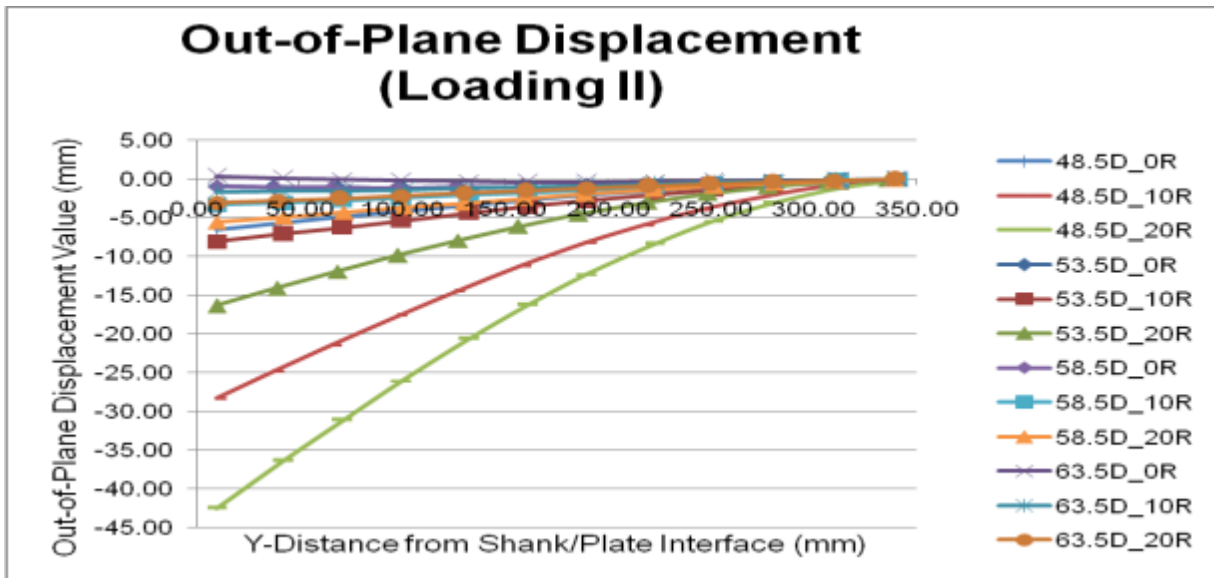


Figure 63: Out-of-Plane Displacement Trends for Loading Condition I